



**FACIAL RECONSTRUCTION FROM SKULL
USING FREE FORM DEFORMATION**

ARIYA NAMVONG

**DOCTOR OF PHILOSOPHY
IN
COMPUTATIONAL SCIENCE**

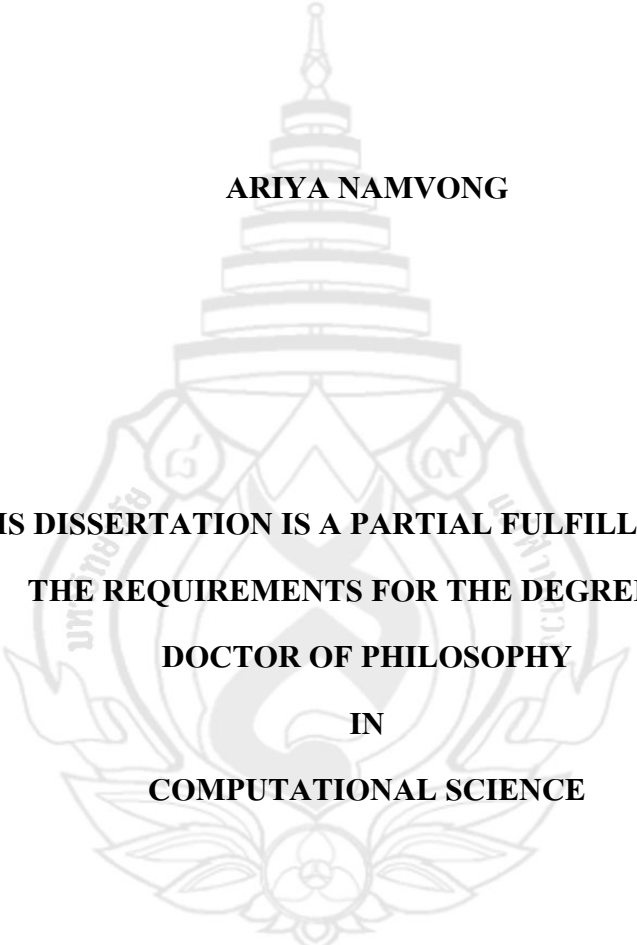
**SCHOOL OF SCIENCE
MAE FAH LUANG UNIVERSITY**

2011

©COPYRIGHT BY MAE FAH LUANG UNIVERSITY

**FACIAL RECONSTRUCTION FROM SKULL
USING FREE FORM DEFORMATION**

ARIYA NAMVONG



**THIS DISSERTATION IS A PARTIAL FULFILLMENT OF
THE REQUIREMENTS FOR THE DEGREE OF
DOCTOR OF PHILOSOPHY
IN
COMPUTATIONAL SCIENCE**

**SCHOOL OF SCIENCE
MAE FAH LUANG UNIVERSITY**

2011

©COPYRIGHT BY MAE FAH LUANG UNIVERSITY

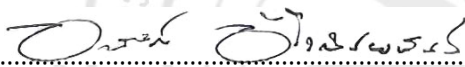
FACIAL RECONSTRUCTION FROM SKULL USING FREE FORM DEFORMATION

ARIYA NAMVONG

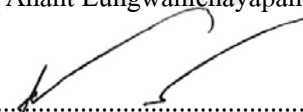
THIS DISSERTATION HAS BEEN APPROVED
TO BE A PARTIAL FULFILLMENT OF THE REQUIREMENTS
FOR THE DEGREE OF DOCTOR OF PHILOSOPHY
IN
COMPUTATIONAL SCIENCE

2011

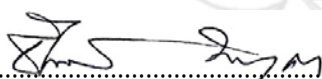
DISSERTATION COMMITTEE

.....CHAIRPERSON


(Dr. Anant Eungwanichayapant)

.....ADVISOR

(Dr. Rungrote Nilthong)

.....EXAMINER

(Dr. Theeradech Mookum)

.....EXTERNAL EXAMINER

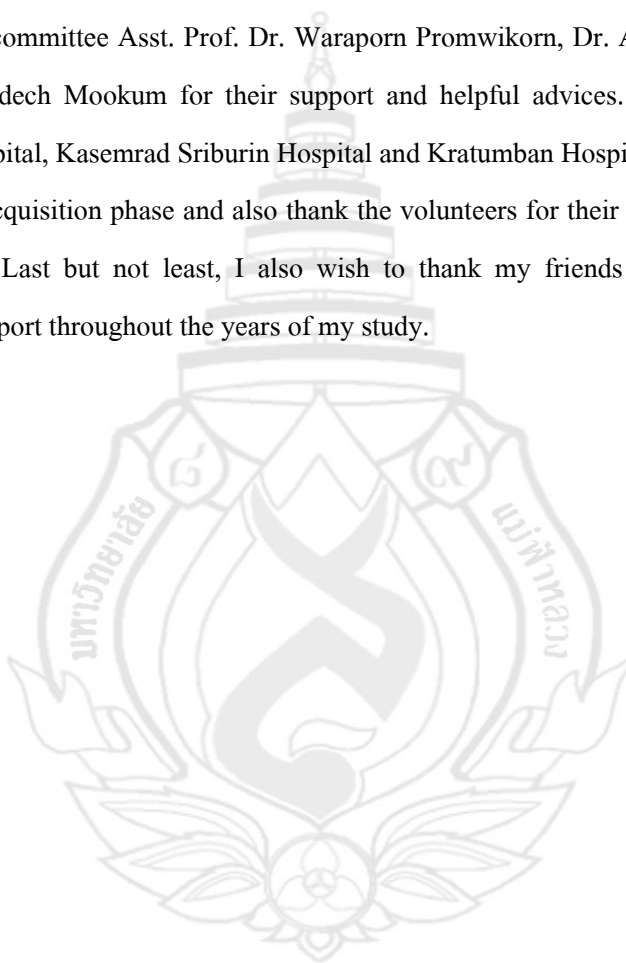
(Asst. Prof. Dr. Waraporn Promwikorn)

©COPYRIGHT BY MAE FAH LUANG UNIVERSITY

ACKNOWLEDGEMENTS

I am extremely grateful to my supervisor Dr. Rungrote Nilthong for his constant encouragement and invaluable help throughout the period of my study. I would also like to thank my examining committee Asst. Prof. Dr. Waraporn Promwikorn, Dr. Anant Eungwanichayapant and Dr. Theeradech Mookum for their support and helpful advices. I also thank the staff of Overbrook Hospital, Kasemrad Sriburin Hospital and Kratumban Hospital for precious help in the head CT data acquisition phase and also thank the volunteers for their dedications that make this work possible. Last but not least, I also wish to thank my friends and my family for their unwavering support throughout the years of my study.

Ariya Namvong



Dissertation Title	Facial Reconstruction from Skull Using Free Form Deformation
Author	Ariya Namvong
Degree	Doctor of Philosophy (Computational Science)
Advisor	Dr. Rungrote Nilthong

ABSTRACT

The purpose of facial reconstruction is to estimate the facial outlook from a discovered skull with the intention of providing a positive effect for deceased identification. At present, the reconstruction is performed by a forensic artist. This method is done manually using clay modeling. It is very subjective and not reproducible. Other drawbacks are that it is very time consumed, and hard to change and modify the model. Therefore computerizing the process is challenging and makes the reconstruction more scientific. This work proposed a novel method for computerized facial reconstruction through the use of Free Form Deformation. In the experiment, all heads in the head database were aligned to be same position, proportion and orientation as questioned skull using Iterative Closest Point algorithm which is a straightforward algorithm that minimizes the difference between two surfaces. Partial similarity between skulls in the database and questioned skull were assessed using Cylindrical Projection approach. Each part of skulls in the head database which was the best match to the corresponding part of questioned skull was selected as reference part. All reference parts were deformed according to questioned skull using Free Form Deformation. Deforming of soft tissue after the skull gave the desired face shape. The resulting faces from this experiment shows promising for forensic facial identification in the face pool test achieving approximately 45% success rate.

Keywords: Facial Reconstruction/Free Form Deformation/Cylindrical Projection/Iterative Closest Point/Partial Similarity

TABLE OF CONTENTS

	Page
ACKNOWLEDGEMENTS	(3)
ABSTRACT	(4)
LIST OF TABLES	(8)
LIST OF FIGURES	(9)
CHAPTER	
1 INTRODUCTION	1
1.1 Background	1
1.2 Objective	4
1.3 Scope	5
1.4 Methodology	6
2 THEORY AND LITERATURE REVIEW	7
2.1 Manual Clay Facial Reconstruction	7
2.2 Craniometric Landmarks	8
2.3 Computerizing the Manual Method	10
2.4 Computerized Facial Reconstruction	16
3 METHODOLOGY	25
3.1 Data Acquisition from CT Scanner	25
3.2 Craniometric Landmarks	26
3.3 Frankfurt Plane	27
3.4 Iterative Closest Point	28
3.5 Free Form Deformation	29

TABLE OF CONTENTS (continued)

	Page
CHAPTER	
3.6 Cylindrical Coordinate System	32
3.7 Cylindrical Projection	33
3.8 Nose Profile Estimation from Nasal Aperture	35
3.9 Skull Similarity in Parts	36
3.10 Facial Reconstruction Procedure	39
4 RESULTS AND DISCUSSION	41
4.1 Facial Reconstruction Results	41
4.2 Visual Evaluation	46
4.3 Discussion	49
5 CONCLUSION AND FUTURE WORK	51
5.1 Conclusions	51
5.2 Future Work	52
REFERENCES	53
APPENDICES	57
Appendix A Demonstration of Iterative Closest Point Performance	58
Appendix B FFD Formula Derivation	69
Appendix C Demonstration of Absolute Error Calculation Between Two Cylindrical Projection Surfaces	78

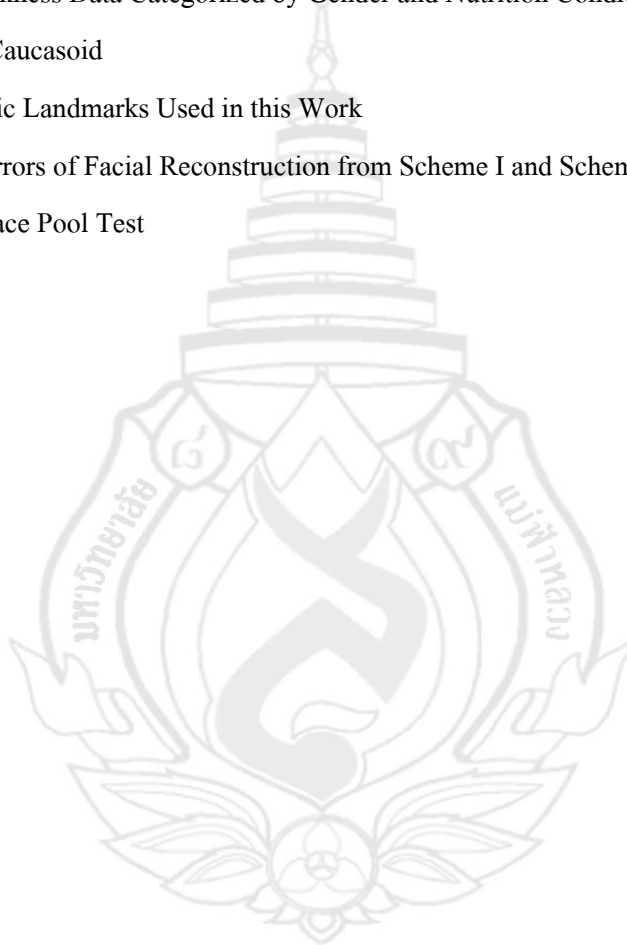
TABLE OF CONTENTS (continued)

	Page
Appendix D The Evaluation of Nose Profile Estimation from Nasal Aperture for Thai People	81
Appendix E Full Set of Face Pool Test Form	88
Appendix F Publications	100
CURRICULUM VITAE	122



LIST OF TABLES

Table	Page
2.1 Tissue Thickness Data Categorized by Gender and Nutrition Condition of American Caucasoid	9
3.1 Craniometric Landmarks Used in this Work	27
4.1 Absolute Errors of Facial Reconstruction from Scheme I and Scheme II	46
4.2 Result of Face Pool Test	49



LIST OF FIGURES

Figure	Page
1.1 A Snapshot of the Beginning Stages of a Manual Reconstruction Using the Tissue Thickness Method	3
1.2 The Basic Overview of Facial Reconstruction from Skull Using Free Form Deformation	4
2.1 Manual Clay Facial Reconstruction	8
2.2 Craniometric Landmarks from the Work of Rhine	9
2.3 Unknown Skull Used in the Work of Archer	11
2.4 The Predefined Face Template of the Unknown Skull Used in the Work of Archer Which was Created from Imagination of an Artist	12
2.5 Craniometric Landmarks According to the Work of Rhine Used in the Work of Archer	12
2.6 Extended Landmarks Based on the Work of Rhine from the Work of Archer	13
2.7 The Reconstructed Face Created by Fitting the Face Template to the Extended Landmarks Using Hierarchical B-Spline Interpolation in the Work of Archer	13
2.8 The Reconstructed Faces Created by Fitting the Face Template to the Extended Landmarks Using Different Weight Type of Hierarchical B-Spline Interpolation in the Work of Bullock	14
2.9 The Photo of Test Person and Reconstructed Faces which were Manual Manipulated by the Forensic Science Experts from the Work of Andersson and Valfridsson	15
2.10 General Workflow of Computerized Craniofacial Reconstruction Techniques	16
2.11 Landmarks Correlation Between Discovered Skull and Reference Skull from the Work of Jones	18
2.12 Reconstructed Results from the Work of Jones	18

LIST OF FIGURES (continued)

Figure	Page
2.13 The Samples of Pairing Crest Lines from the Work of Subsol and Coworkers	19
2.14 Reconstructed Results from the Work of Subsol and Coworkers	20
2.15 Craniometric Landmarks Used in the Work of Abate and Coworkers	21
2.16 Reconstructed Face Using Free Form Deformation from the Work of Abate and Coworkers	21
2.17 Reconstructed Faces from the Work of Abate and Coworkers Rendering with Texture and Hair	22
2.18 Reference face, Target Face and Reconstructed Face from the Work of Kermi and Coworkers	22
2.19 Reference Skull, Reference Face and Questioned Skull Used in the Work of Jiang and Coworkers	23
2.20 Reconstructed Faces Using Three Different Methods From the Work of Jiang and Coworkers	24
3.1 3D Head Database Acquisition From CT Scanner	25
3.2 Illustration of Craniometric Landmarks Used in this Work	26
3.3 Illustration of Frankfurt Horizontal Plane and 3D Rotation	28
3.4 Deformation of the Object According to the Deformation of the Lattice	30
3.5 Deformation of Face According to the Deformation of the Incisor	31
3.6 Cylindrical Coordinate System and Cartesian Coordinate System	32
3.7 Projection of 3D Head Surface onto Cylindrical Plane which is the Flattened	33
3.8 Cylindrical Projections of Face and Skull.	34

LIST OF FIGURES (continued)

Figure	Page
3.9 Absolute Errors of Cylindrical Projection Surfaces.	34
3.10 Nose Profile Estimation from Nasal Aperture.	35
3.11 Absolute Errors of Cylindrical Projection Surfaces for Scheme I.	37
3.12 Absolute Errors of Cylindrical Projection Surfaces for Scheme II.	38
3.13 Illustration of Masseter Muscle Which Originates at Zygomatic Bone and Terminates at Mandibular Bone	38
3.14 Facial Reconstruction Scheme I	39
3.15 Facial Reconstruction Scheme II	40
4.1 Scheme I Facial Reconstruction of Subjects 1 - 5.	42
4.2 Scheme I Facial Reconstruction of Subjects 6 -11.	43
4.3 Scheme II Facial Reconstruction of Subjects 1 - 5.	44
4.4 Scheme II facial Reconstruction of Subjects 6 - 11.	45
4.5 Example of the Face Pool Test. Top Image is the Reconstructed Face to be Identified with the Faces from the Face Pool.	48

CHAPTER 1

INTRODUCTION

1.1 Background

In the popular television programs especially CSI and Bones, people might impress the criminal investigation of CSI agent Gil Grissom or forensic anthropologist Temperance Brennan. They could easily reconstruct the face from the skull found in the crime scene. The reconstructed face looked exactly the same as the face of the victim in the FBI face database system that could accurately identify the victim. This process seemed very useful as it could help to rule out numerous possibilities to only one identity. With the support of the facial reconstruction and facial recognition system they finally solved the case, jailed the murderer. It is popular but somewhat unrealistic. In the real world, facial reconstruction from skull is rather used when other evidence is absent or severely damaged. This method would be considered at last when all other attempts are failed, according to its unreliable. Prag and Neave (1997) stated that it has an average success rate of 50% when it is used for identification purpose. Maraj (2007) stated that facial reconstruction plays a significant role in the identification of skeleton remains but it is inadmissible in court proceedings as a sole means of body identification.

We have to accept the fact that there are many ways in which soft tissue may cover the same skull leading to different facial outlook. The purpose of facial reconstruction is not to produce exact likeness of the person during life, but to provide some positive effects for human identification. The obtained face will not exactly be the same as face of person during life but it may be similar enough to stimulate someone's recognition. Echeverria (2003) suggested that for this technique to work effectively, it is necessary that the reconstruction is seen by someone who has known the subject and welcome to cooperate with the investigation. Facial reconstruction is performed in the hope that it may stimulate recognition, and consequently narrows the field of

identification, allowing other legally accepted identification tests, such as radiographic or dental/medical records comparisons, DNA analysis, or techniques to establish positive identification (Vanezis, 2007). There are several reasons why identification is essential. For every unidentified deceased person, there might be someone who cared about. Family members should have known what happened to their loved one. Most of the time, an unidentified body is found, crime remains unsolved and the murderer may be still walking around.

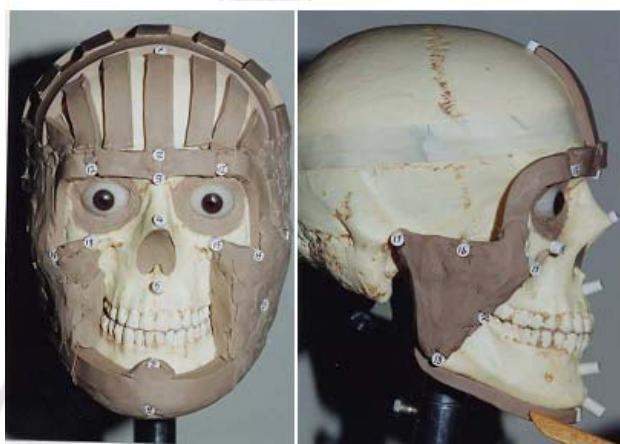
Knight (1991) had outlined a number of reasons why identification is essential:

1. Ethical and humanitarian need, especially information for surviving relatives.
2. The facts of the death need to be ascertained for official, statistical and legal purposes.
3. Administrative and ceremonial purpose for burial or cremation.
4. To discharge legal claims and obligation regarding for example, property, estate and debts.
5. To prove claims for life insurance contracts, survivors' pensions and other financial matters.
6. To allow legal proceedings to proceed with firm knowledge of the identification of the deceased.
7. To facilitate enquiries into criminal or suspicious deaths.

Facial reconstruction has also been used to reproduce the faces of ancient human remains, mostly of mummies. In these cases, the reconstruction is made only for the purpose of creating an accurate image of this person, rather than to make a match with some known individual (Echeverria, 2003).

An old technique which is still in use and constantly evolving is the manual clay facial reconstruction also known as sculptural technique. This method uses average skin thickness data at the skull landmarks. A snapshot of the beginning stages of a reconstruction using the tissue thickness method is shown in Figure 1.1. Taylor (2001) named this operation as a technical phase. From tissue thickness at the skull landmarks, the remaining open spaces are interpolated to form the features of the face. Taylor (2001) named this operation as an artistic phase. Echeverria (2003) supported the term artistic phase and states that there is no defined method to do the interpolation, so it is done according to the discretion of the artist, and thus, the resulting face is very subjective and not reproducible. Khatod (2004) stated that the traditional clay facial reconstruction method requires expertise in the

field of anatomy, forensic science and art. The process is very time consuming and when a victim is not identified, a second face reconstruction may be attempted with slightly different features. Since the original skull is needed, the first reconstructed face needs to be taken apart in order to restart the process. Since there are no exact rules for the traditional manual facial reconstruction therefore computerizing the process is challenging and makes the reconstruction more scientific. The advantages of the computerized method over the manual clay reconstruction are speed, rapid editing capability, and production of images can be stored and repeated at any time if required (Vanezis, 2007).



From Taylor, K. T. (2001). **Forensic Art and Illustration**. Florida: CRC.

Figure 1.1 A Snapshot of the Beginning Stages of a Manual Reconstruction Using the Tissue Thickness Method.

This work introduced a novel approach to computerized facial reconstruction through the use of Free Form Deformation method. This approach differed from other researches that tried to interpolate all face features from small set of tissue thickness data. Stephan, Taylor (2001) stated that the relationships between skull and the external appearance of the face are complicated by muscle, fat and vasculature. The relationship between connective tissue and skull is not completely known at this time. The assumption behind this new approach is change in the facial soft tissue responds to the change in the skull. The reconstruction is obtained by deforming the

craniometric landmarks of known skull into unknown skull. Forcing soft tissue of the known skull to the unknown skull with the associated deformation gives a desired shape of the soft tissue for the unknown skull. The basic overview of this approach is shown in Figure 1.2.

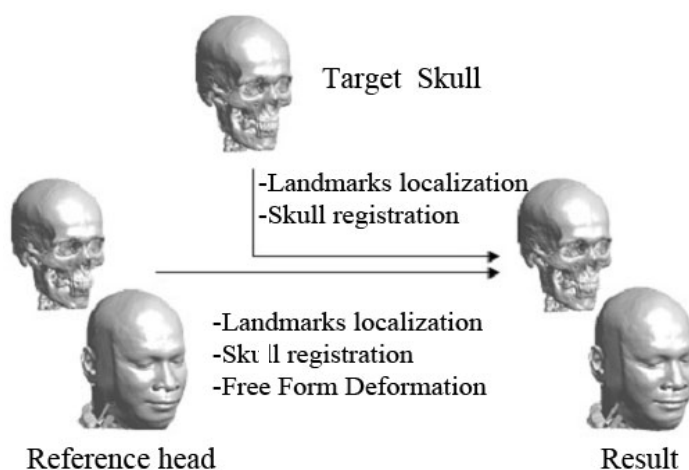


Figure 1.2 The Basic Overview of Facial Reconstruction from Skull Using Free Form Deformation

The remainder of this paper was organized as follows: in Chapter 2, we reviewed the theories and researches that were related to this work. Chapter 3 described our facial reconstruction method. Chapter 4 presented the experimental results. The conclusion for this work was presented in Chapter 5.

1.2 Objective

The objective of this work is to develop a method for computerized facial reconstruction from skull through the use of Free Form Deformation method that can be used as supporting system for the criminal investigation to rule out numerous possibilities to some identities when other identification methods are failed. The purpose of this facial reconstruction method is not to reproduce the exact face as the person when he/she is alive. The plausible face may be the right term to define the result from this approach. We expected that the result of this work will be useful as the supporting system for criminal investigation, disastrous devastation remains identification, and ancient human remains facial reconstruction. The objectives of this work are listed as follows:

1.2.1 To collect the 3D head database from CT scanner

1.2.2 To develop the numerical facial and skull similarity measurement method using Cylindrical Projection.

1.2.3 To develop the partial similarity measurement method for skull comparison.

1.2.4 To develop the computerized facial reconstruction method using Free Form Deformation.

1.2.5 To explore the possibility of using computerized facial reconstruction as a supporting tool for forensic identification from skull.

1.3 Scope

At present, facial reconstruction is performed manually by a forensic artist. This work proposed a novel approach to computerize the reconstruction. The head database used in this work was acquired from CT scanner. Due to the limitation of access this kind of data, this work was performed using only 11 heads in the head database. All volunteers are Thai male with the age range of 25-55 years. We expected that the result of this work will be useful as the supporting system for forensic facial identification in Thailand. The scopes and limitations of this work are listed as follows:

1.3.1 The 3D head models derived from CT scan images with 1 mm resolution are used in this research.

1.3.2 The head database used in this work containing 11 heads.

1.3.3 The target group of this facial reconstruction is Thai male 25-55 years old with normal nutrition condition and not too much emaciated or obese.

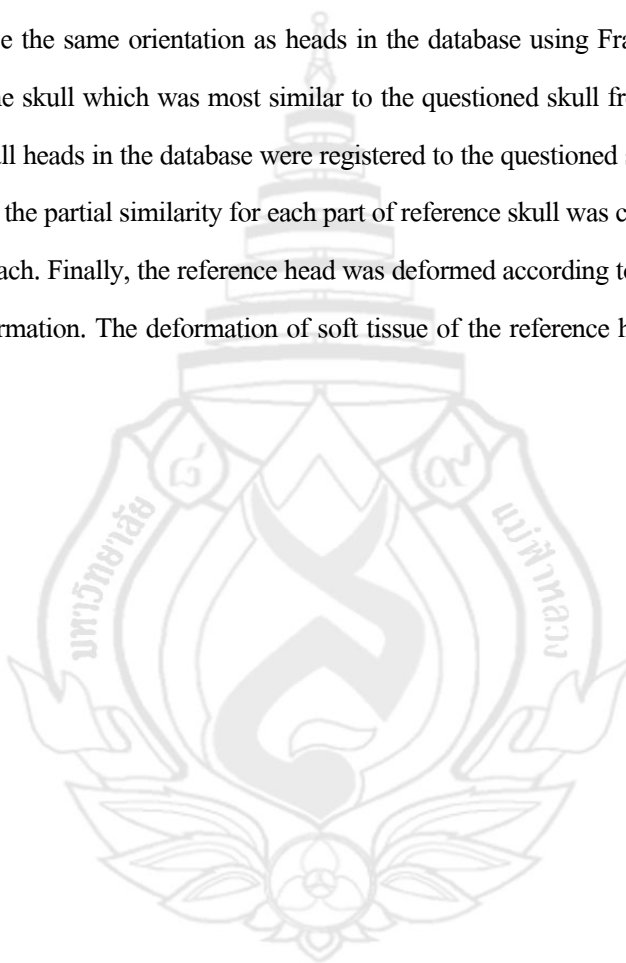
1.3.4 The normal expression of reference heads and questioned heads are required.

1.3.5 Manual craniometric landmarks localization is required.

1.3.6 Ears reconstruction and hair simulation are not included in this research.

1.4 Methodology

In order to produce this work, we studied available researches and previous works done in the field of facial reconstruction from skull and then developed our new approach later. Our methodology can be summarized as follows: First, the 3D head database was derived from CT scan images. Second, craniometric landmarks of questioned skull was needed to manual localization. Then questioned skull was aligned to be the same orientation as heads in the database using Frankfurt plane. After that, in order to select the skull which was most similar to the questioned skull from the head database to be reference head, all heads in the database were registered to the questioned skull using Iterative Closest Point. After that, the partial similarity for each part of reference skull was considered using Cylindrical Projection approach. Finally, the reference head was deformed according to the questioned skull using Free Form Deformation. The deformation of soft tissue of the reference head gave the desired facial shape.



CHAPTER 2

THEORY AND LITERATURE REVIEW

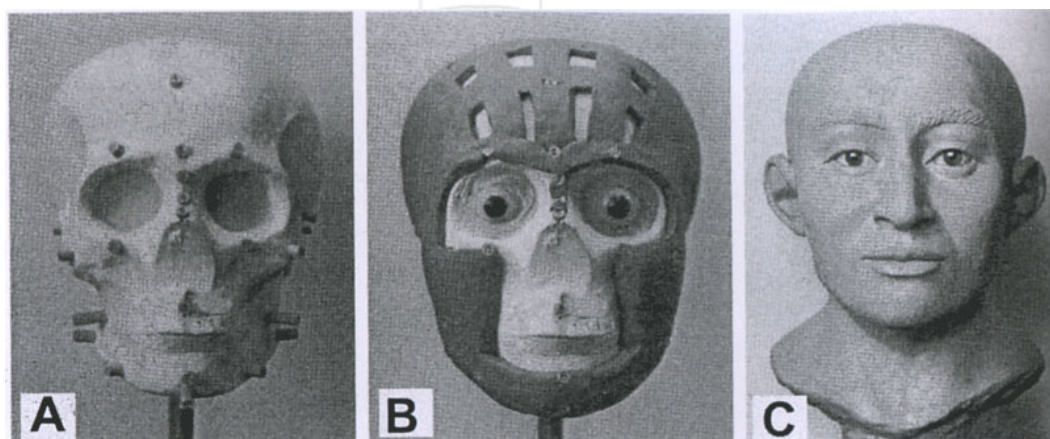
This chapter reviewed the methods related to facial reconstruction. The idea of manual facial reconstruction was briefly discussed first and then the researches involving in computerized facial reconstruction were reviewed. The remainder of this chapter was organized as follows: manual clay facial reconstruction, craniometric landmark, computerizing the manual method and computerized facial reconstruction.

2.1 Manual Clay Facial Reconstruction

Wilkinson (2004) had conceptual explanation of how facial reconstruction has been performed manually. From Figure 2.1A, the skull was set on a stand. The appropriate set of tissue thickness data was selected and cylinders of vinyl eraser were cut to the appropriate thickness and glued to the surface of the skull. Using modeling clay, these markers were connected by strips (see Figure 2.1B) to create a rough contour map of the surface of the face. From Figure 2.1C, the remaining open spaces were filled to form the face. Taylor (2001) divided the reconstruction method into two phases: the technical phase and the artistic phase. The technical phase involves information collection, skull preparation, tissue depth application and facial contour production. The artistic phase involves the sculpture of the facial features and finishing of the head.

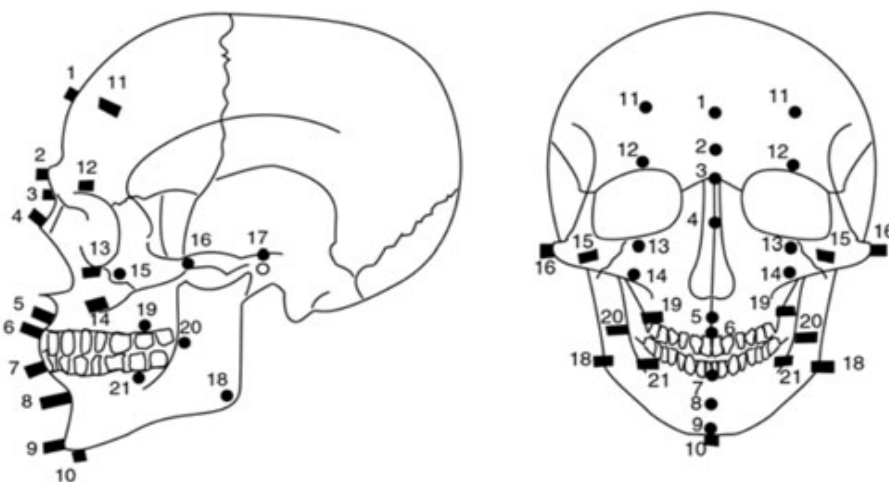
2.2 Craniometric Landmarks

The key information of manual clay facial reconstruction is the tissue thickness data. This data presents the tissue thickness at the craniometric landmarks. There are many sets of tissue thickness varied by many researchers. One of the most traditional data sets consists of 21 landmarks as shown in Figure 2.2. These data categorized tissue thickness by gender and nutrition condition. Tissue thickness data of the American Caucasoid are in Table 2.1. These depth data have been taken from dead bodies.



From Wilkinson, C. (2004). **Forensic facial reconstruction**. Cambridge: Cambridge University.

Figure 2.1 Manual Clay Facial Reconstruction. (A) Tissue Depth Markers Attached to the Surface of the Skull (B) Plasticine Strips Join the Tissue Depth Markers (C) Facial Features Modeled Between the Plasticine Strips



From Rhine, J. S., Moore, C. E. & Westin, J. T. (Eds.). (1982). **Facial reproduction: Tables of facial tissue thickness of american caucasoid in forensic anthropology**. New Mexico: Maxell Museum of Anthropology, University of New Mexico.

Figure 2.2 Craniometric Landmarks from the Work of Rhine

Table 2.1 Tissue Thickness Data Categorized by Gender and Nutrition Condition of American Caucasoid

Measurement	Emaciated (mm)		Normal (mm)		Obese (mm)	
	Male	Female	Male	Female	Male	Female
	(N=3)	(N=3)	(N=67)	(N=19)	(N=8)	(N=3)
Midline						
1. Supraglabella	2.50	2.50	4.25	3.50	5.50	4.25
2. Glabella	3.00	4.00	5.25	4.75	7.50	7.50
3. Nasion	4.25	5.25	6.50	5.50	7.50	7.00
4. End of Nasals	3.00	2.25	3.00	2.75	3.50	4.25
5. Mid Philtrum	7.75	5.00	10.00	8.50	11.00	9.00
6. Upper Lip Margin	7.25	6.25	9.75	8.50	11.00	11.00
7. Lower Lip Margin	8.25	8.50	11.00	10.00	12.75	12.25
8. Chin-Lip Fold	10.00	9.25	10.75	9.50	12.25	13.75
9. Mental Eminence	8.25	8.50	11.25	10.00	14.00	14.25
10. Beneath Chin	5.0	3.75	7.25	5.75	10.75	9.00

Table 2.1 (Continues)

Measurement	Emaciated (mm)		Normal (mm)		Obese (mm)	
	Male	Female	Male	Female	Male	Female
	(N=3)	(N=3)	(N=67)	(N=19)	(N=8)	(N=3)
Bilateral						
11. Frontal Eminence	3.25	2.75	4.25	3.50	5.50	5.00
12. Supraorbital	6.50	5.25	8.25	6.75	10.25	10.00
13. Suborbital	4.50	4.00	5.75	5.75	8.25	8.50
14. Inferior Malar	8.50	7.00	13.50	12.50	15.25	14.00
15. Lateral Orbit	6.75	6.00	9.75	10.50	13.75	13.25
16. Zygomatic Arch, midway	3.50	3.50	7.00	7.00	11.75	9.50
17. Supraglenoid	5.00	4.25	8.25	7.75	11.25	8.25
18. Gonion	6.50	5.00	11.00	9.75	17.50	17.50
19. Supra M2	8.50	12.00	18.50	17.75	25.00	23.75
20. Occlusal Line	9.25	11.00	17.75	17.00	23.50	20.25
21. Sub M2	7.00	8.50	15.25	15.25	19.75	18.75

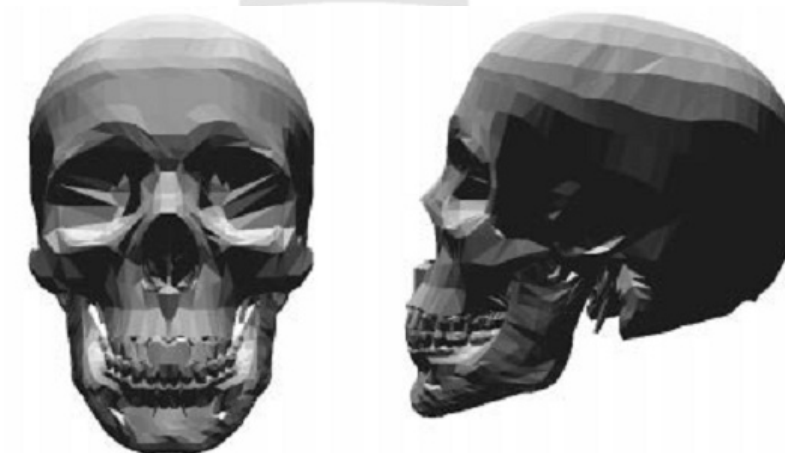
From Rhine, J. S., Moore, C. E. & Westin, J. T. (Eds.). (1982). **Facial reproduction: Tables of facial tissue thickness of american caucasoid in forensic anthropology.** New Mexico: Maxell Museum of Anthropology, University of New Mexico.

2.3 Computerizing the Manual Method

As mentioned in previous section, the number of facial tissue thickness data is relatively small compared to remaining open space. The artist has to interpolate the remaining from the surrounding points. There is no defined method to do the interpolation, so it is done according to the discretion of the artist, and thus, the resulting face is very subjective and not reproducible (Echeverria, 2003). Thus, it is hard to computerize the process. There are some researches trying to computerize the manual method. However, this scheme suffered the need for human interaction

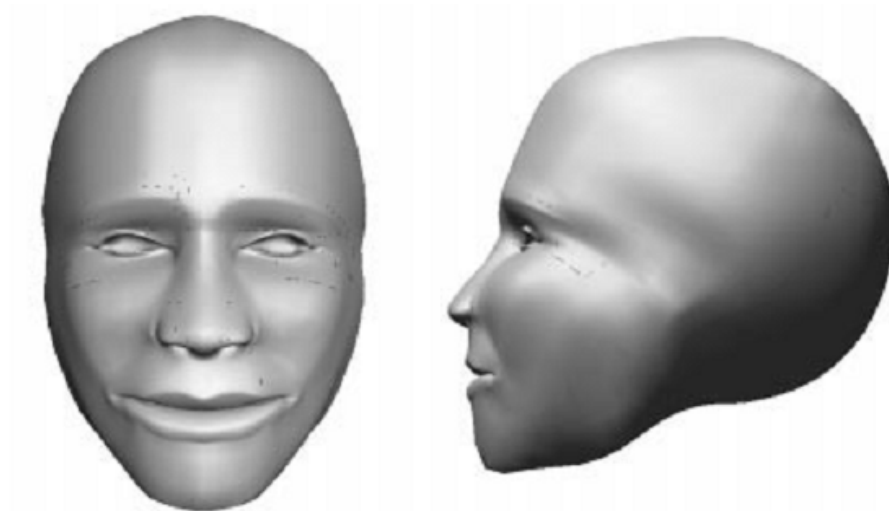
in every phase; preprocessing, processing and postprocessing. This scheme also required other tricks to carry out.

Archer (1997) attempted to reconstruct the face of the unknown skull (see Figure 2.3). The skull is that of a male, most likely Caucasoid. The original facial appearance of the individual from whom the model was obtained is unknown. The predefined face template of the unknown skull was created from imagination of an artist (see Figure 2.4). The skull landmarks are located after Rhine's landmarks (see Figure 2.5). The extended landmarks were located (see Figure 2.6). The reconstructed face was created by fitting the face template to the extended landmarks using hierarchical B-spline interpolation (see Figure 2.7). The accuracy of this result cannot be evaluated because no one knows the real face of the unknown skull.



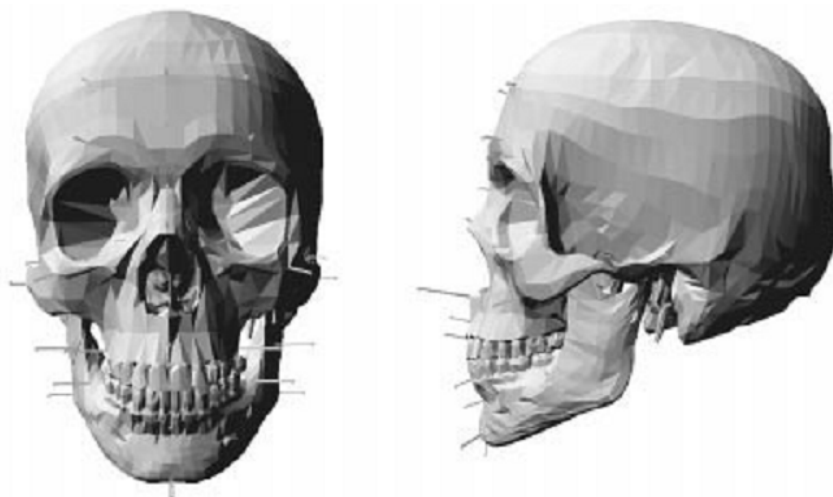
From Archer, K. M. (1997). **Craniofacial reconstruction using hierarchical B-Spline interpolation.** Master's Thesis. University of British, Columbia.

Figure 2.3 Unknown Skull Used in the Work of Archer



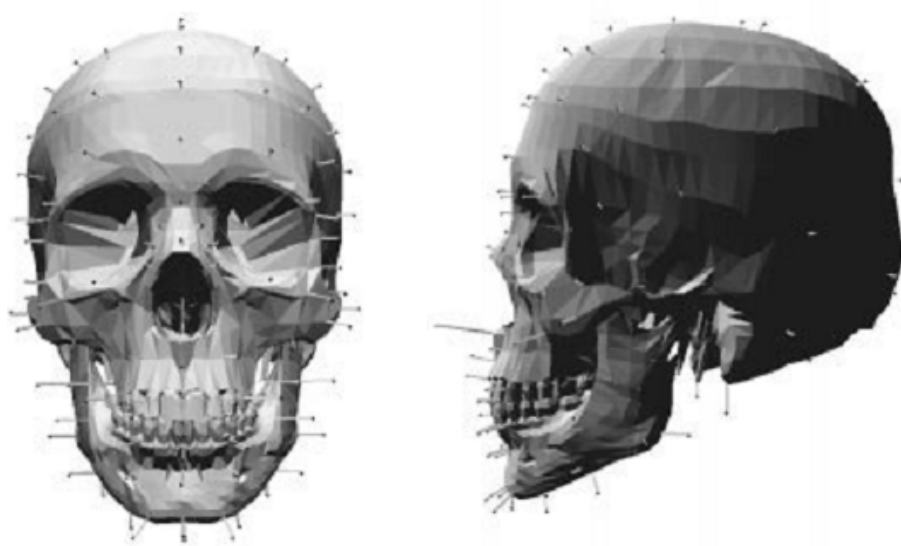
From Archer, K. M. (1997). **Craniofacial reconstruction using hierarchical B-Spline interpolation.**
Master's Thesis. University of British, Columbia.

Figure 2.4 The Predefined Face Template of the Unknown Skull Used in the Work of Archer
which was Created from Imagination of an Artist.



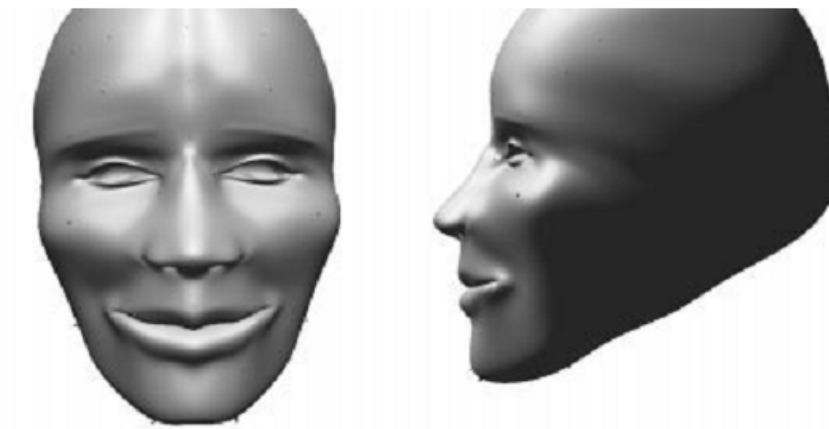
From Archer, K. M. (1997). **Craniofacial reconstruction using hierarchical B-Spline interpolation.**
Master's Thesis. University of British, Columbia.

Figure 2.5 Craniometric Landmarks According to the Work of Rhine Used in the Work of Archer



From Archer, K. M. (1997). **Craniofacial reconstruction using hierarchical B-Spline interpolation.** Master's Thesis. University of British, Columbia.

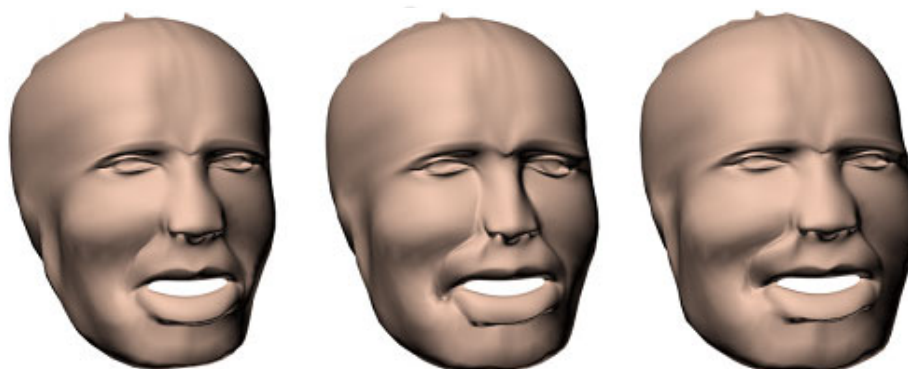
Figure 2.6 Extended Landmarks Based on the Work of Rhine from the Work of Archer



From Archer, K. M. (1997). **Craniofacial reconstruction using hierarchical B-Spline interpolation.** Master's Thesis. University of British, Columbia.

Figure 2.7 The Reconstructed Face created by Fitting the Face Template to the Extended Landmarks Using Hierarchical B-Spline Interpolation in the Work of Archer

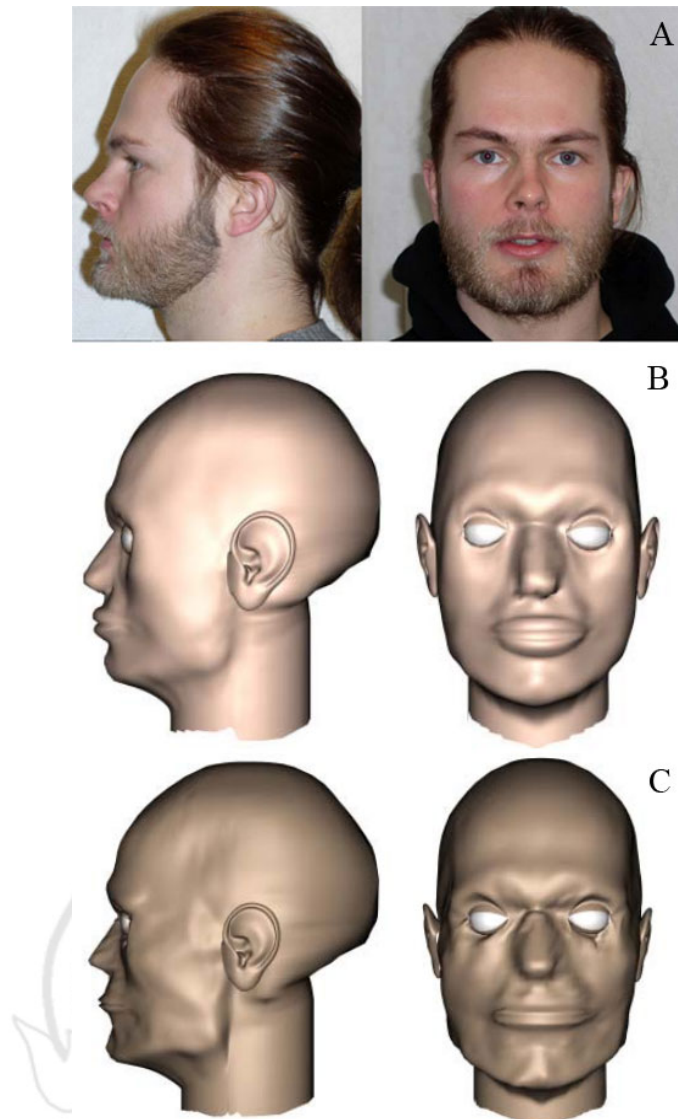
Bullock (1999) proposed the method which is an extension of work previously done by Archer. The reconstructed face results were generated using hierarchical B-spline fitting model with different weight type (see Figure 2.8). The accuracy of this method could not be evaluated because the original facial appearance of the individual from whom the model was obtained is unknown.



From Bullock, D. W. (1999). **Computer assisted 3D craniofacial reconstruction**. Master's Thesis. University of British, Columbia.

Figure 2.8 The Reconstructed Faces Created by Fitting the Face Template to the Extended Landmarks Using Different Weight Type of Hierarchical B-Spline Interpolation in the Work of Bullock

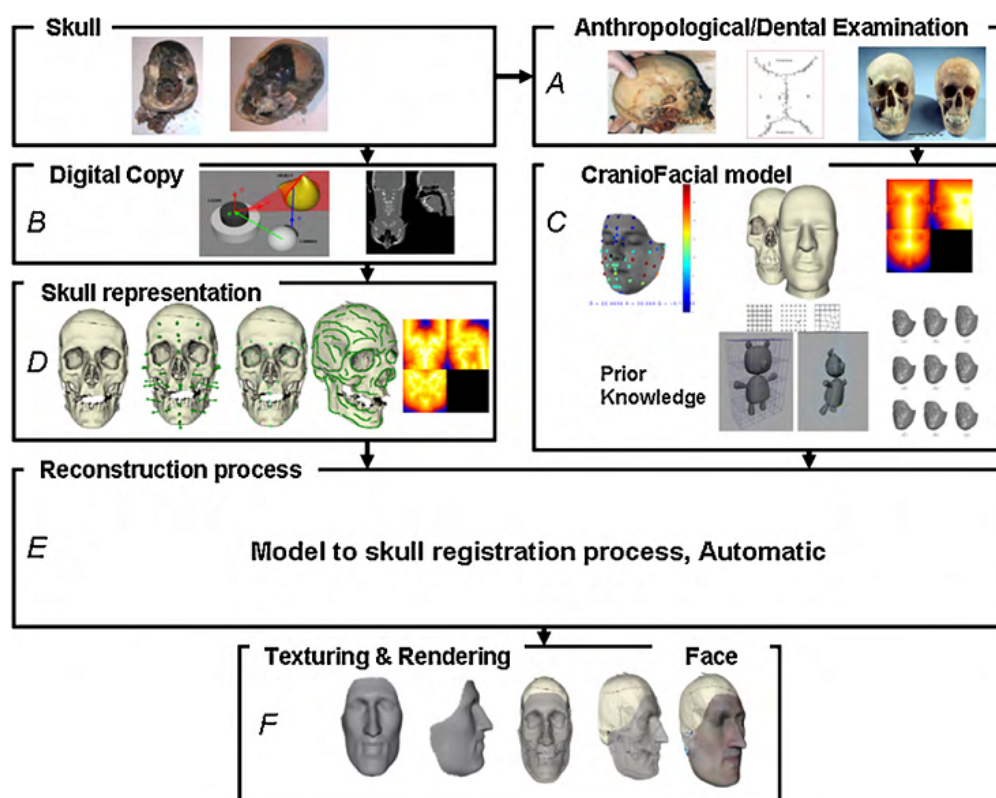
Andersson and Valfridsson (2005) utilized the graphical processing capabilities of 3D Studio Max software to reconstruct face of questioned skull. The Relax modifier was used to deal with surface creation and manipulation. The Paint deformation tool was used as a surface brush tool. First, the craniometric landmarks were manually located after Rhines. Then, applied the Relax modifier and Paint deformation tool to create preliminary face. Finally, the face was manually manipulated by forensic science experts, Winskog and Berge. The final reconstructed faces and photo of test person are in Figure 2.9 for visual evaluation purpose. The conclusion of this research is of believe that the forensic artist with prior experience of facial reconstruction will be able to use the software to perform a reconstruction in the future.



From Andersson, B. & Valfridsson, M. (2005). **Digital 3D facial reconstruction based on computed tomography.** Master's Thesis. Linkopings Universitet, Sweden.

Figure 2.9 The Photo of Test Person and Reconstructed Faces which were Manual Manipulated by the Forensic Science Experts from the Work of Andersson and Valfridsson. (A) Photo of Test Person (B) The Result of Winskog's Reconstruction (C) The Result of Berge's Reconstruction

2.4 Computerized Facial Reconstruction



From Claes, P., Vandermeulen, D., Greef, S. D., Willems, G., Clement, J. & Suetens, P. (2010). Computerized craniofacial reconstruction: Conceptual framework and review. **Forensic Science International**, 201(1-3), 138-145.

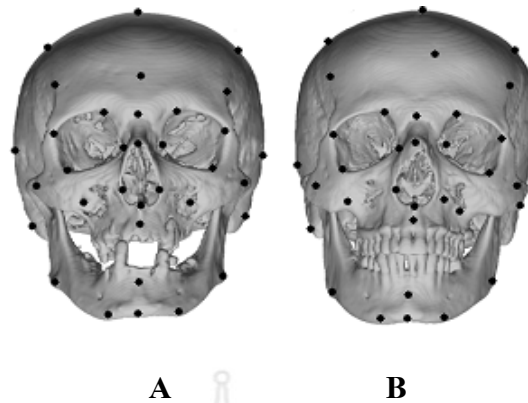
Figure 2.10 General Workflow of Computerized Craniofacial Reconstruction Techniques

The progress in medical imaging technologies during recent years has led to the development of alternative computer-based facial reconstruction methods (Claes et al., 2010). Instead of using small set of facial soft tissue thickness data and then interpolate the large remaining area, we can use whole facial soft tissue thickness data from 3D model derived from CT or MRI scanner and then approximate questioned face from reference face in face database. Current computerized facial reconstruction techniques all share the same workflow as shown in Figure

2.10. Figure 2.10A, the unknown skull is examined by anthropological and dental experts to determine properties like age, gender and race. Figure 2.10B, the unknown skull is digitized to get digital copy. Figure 2.10C, the core of process is craniofacial model which presents the relation between skull and face of heads in the database and also questioned head. Figure 2.10D, digital representation of skull is generated. Figure 2.10E, the reconstruction is obtained by appropriate processing relation between unknown skull and craniofacial model. Figure 2.10F, the final stage; the reconstructed face is given a skin color and texture.

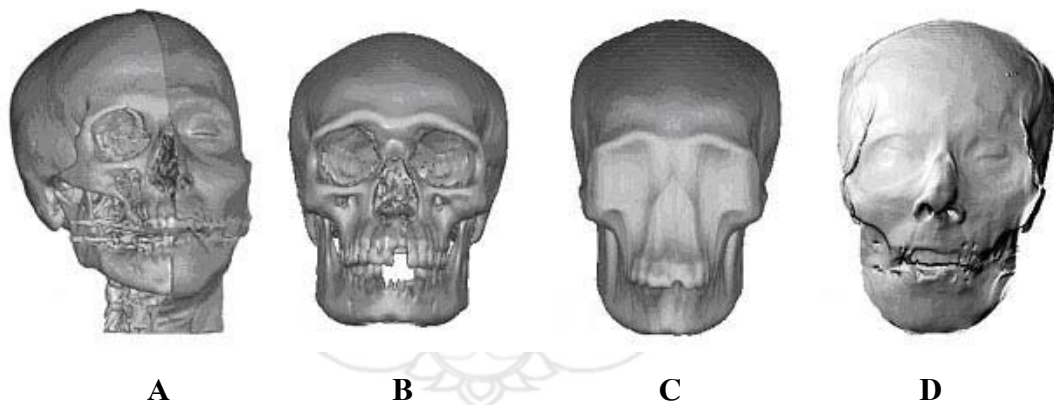
Jones (2001) presented the facial reconstruction from skull method as follows. A CT scanner was used to generate a 3D model of the discovered skull. A reference head that has the same gender, age and race is chosen. Using correlation techniques, a correspondence was created between the discovered skull and reference head as seen in Figure 2.11. The soft tissue from the reference head was then mapped onto the discovered skull using 2D warp of the 3D distance field technique as seen in Figure 2.12. Jones stated that this method needs to be improved to reconstruct more realistic result.

Subsol, Mafart, Lumey and Silvestre (2002) attempted to reconstruct a face of prehistoric Man called Tautavel Man from a face of Modern Man. This approach proposed the digital representation of skull shape by crest lines (see Figure 2.13). They expected that the relationship between unknown skull crest lines and known skull crest lines could be used to deform reference face to questioned face. The difficulty of this representation was that numerous and complex of crest lines of two skulls make it hard to find the correspondences between these features. Figure 2.13 shows samples of pairing (P1, Q1) and (P2, Q2). The deformation was computed by Thin-Plate Spline method. In Figure 2.14, the reconstructed face from this method and the reconstructed face from manual method are displayed for visual evaluation purpose.



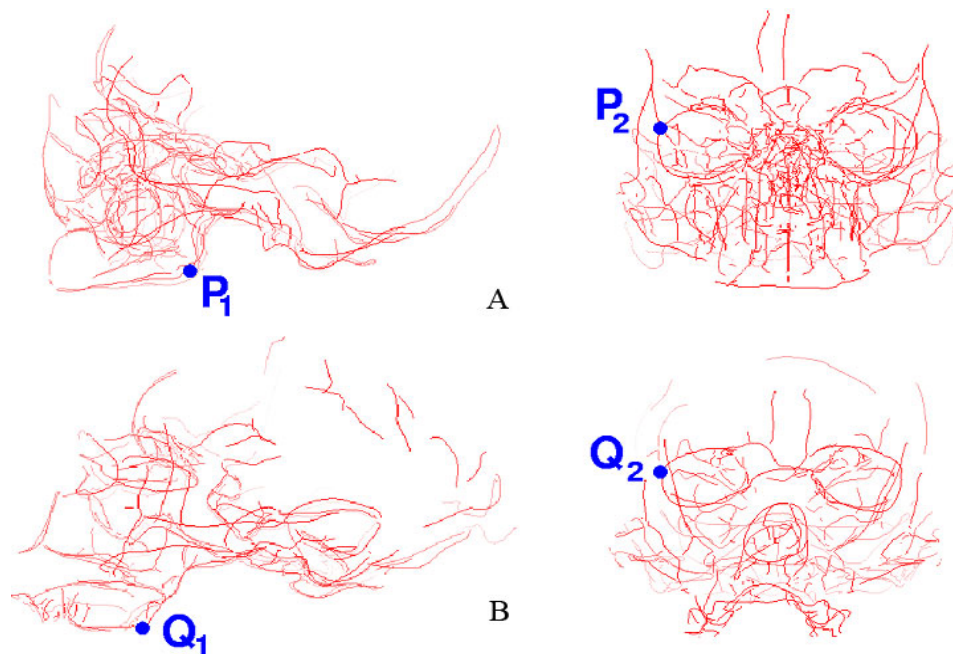
From Jones, M. W. (2001). Facial reconstruction using volumetric data, In **Proceedings of IEEE Vision, Modeling and Visualization** (pp. 135-142). Stuttgart: IEEE Press.

Figure 2.11 Landmarks Correlation Between Discovered Skull and Reference Skull from the Work of Jones. (A) Discovered Skull with Correlated Landmarks (B) Reference Skull with Correlated Landmarks



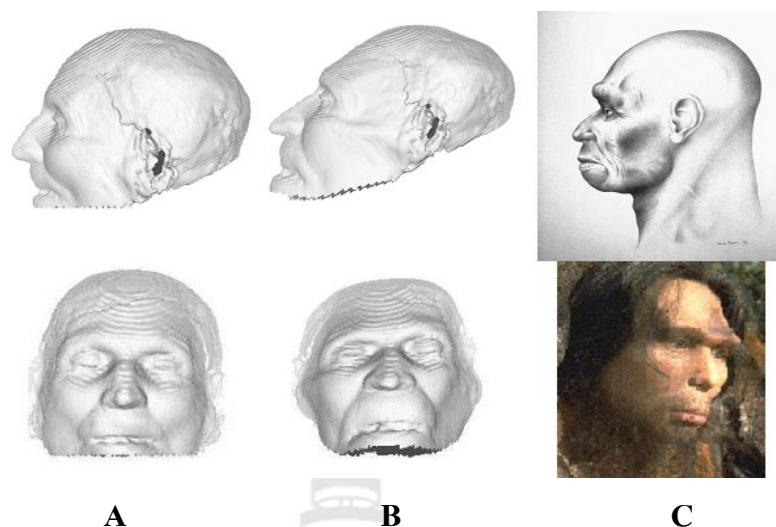
From Jones, M. W. (2001). Facial reconstruction using volumetric data, In **proceedings of IEEE Vision, Modeling and Visualization** (pp. 135-142). Stuttgart: IEEE Press.

Figure 2.12 Reconstructed Results from the Work of Jones. (A) Reference Skull with Reference Face (B) Discovered Skull (C) Discovered Skull After Filled hole (D) Reference Face Mapped onto Discovered Skull Using 2D Warp of the 3D Distance Field Technique



From Subsol, G., Mafart, B., Silvestre, A. & De Lumley, M. (2002). 3D image processing for the study of the evolution of the shape of the human skull. Presentation of the tools and preliminary results. In B. Mafart & H. Delingette (Eds.). **Three-dimensional imaging in paleoanthropology and prehistoric archaeology** (pp. 37-45), Acts of the XIVth UISPP Congress, University of Liège, Belgium, 2-8 September 2001. British Archaeological Record International Series 1049.

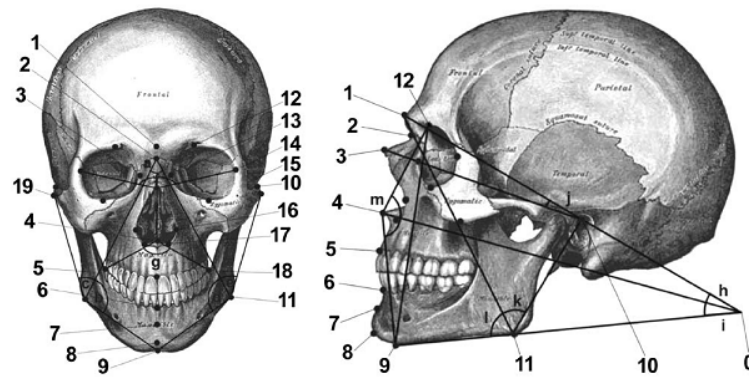
Figure 2.13 The Samples of Pairing Crest Lines from the Work of Subsol and Coworkers. (A) Crest Lines Extracted from Modern Man (B) Crest Lines Extracted from Tautavel Man (Q1 is a Pair of P1 and P2 is a Pair of Q2)



From Subsøl, G., Mafart, B., Silvestre, A. & De Lumley, M. (2002). 3D image processing for the study of the evolution of the shape of the human skull. Presentation of the tools and preliminary results. In B. Mafart & H. Delingette (Eds.). **Three-dimensional imaging in paleoanthropology and prehistoric archaeology** (pp. 37-45), Acts of the XIVth UISPP Congress, University of Liège, Belgium, 2–8 September 2001. British Archaeological Record International Series 1049.

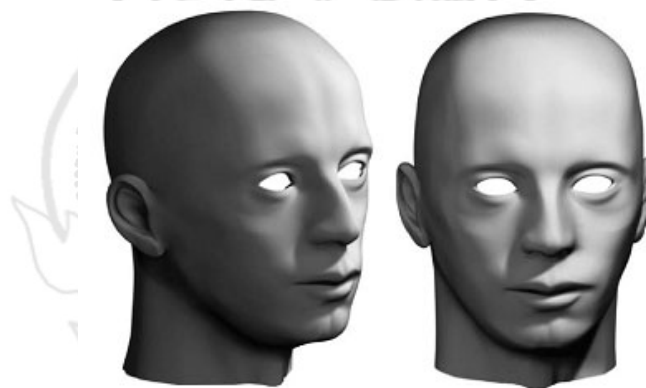
Figure 2.14 Reconstructed Results from the Work of Subsøl and Coworkers. (A) Reference Face (B) Reconstructed face Using Thin-Plate Spline Method (C) Picture and Sculpture from Manual Method for Visual Evaluation Purpose

Abate, Nappi, Ricciardi & Tortora (2004) attempted to reconstruct a face of ancient Pompei Man. This approach used 19 craniometric landmarks to represent skull shape (see Figure 2.15). The deformation process is computed by Free Form Deformation method. The result of this approach is displayed in Figure 2.16. Figure 2.17 is the resulting face with hair and texture. The accuracy of this method cannot be evaluated because the facial appearance of this ancient man is not presented.



From Abate, A. F., Nappi, M., Ricciardi, S. & Tortora, G. (2004). FACES: Facial reconstruction from ancient skulls using content based image retrieval. **Journal of Visual Languages & Computing**, 15(5), 373-389.

Figure 2.15 Craniometric Landmarks Used in the Work of Abate and Coworkers



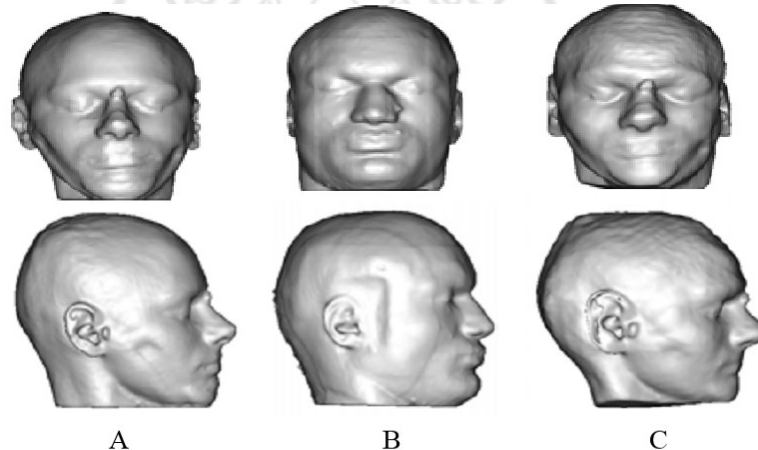
From Abate, A. F., Nappi, M., Ricciardi, S. & Tortora, G. (2004). FACES: Facial reconstruction from ancient skulls using content based image retrieval. **Journal of Visual Languages & Computing**, 15(5), 373-389.

Figure 2.16 Reconstructed Face Using Free Form Deformation from the Work of Abate and Coworkers



From Abate, A. F., Nappi, M., Ricciardi, S. & Tortora, G. (2004). FACES: Facial reconstruction from ancient skulls using content based image retrieval. **Journal of Visual Languages & Computing**, 15(5), 373-389.

Figure 2.17 Reconstructed Face from the work of Abate and Coworkers Rendering with Texture and Hair

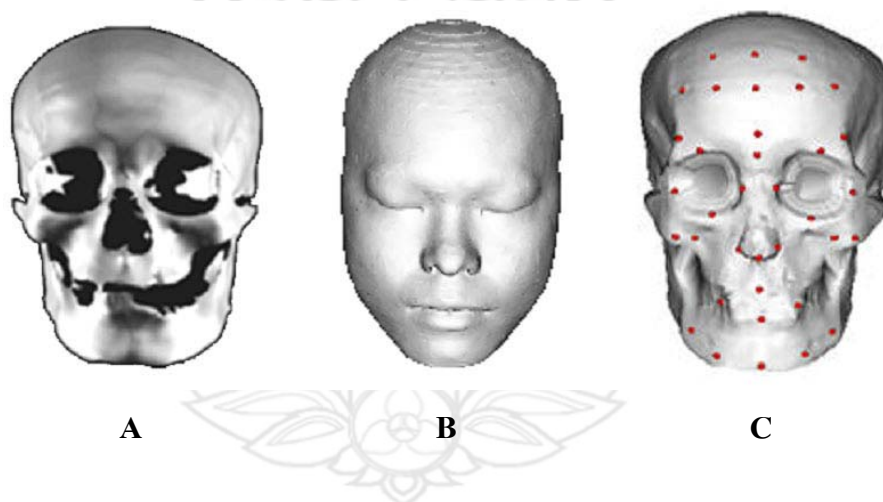


From Kermi, A., Laski, M. T. & Bloch, I. (2008). A three-dimensional computerized facial reconstruction using non-linear registration of a reference head. In **Proceedings of Intelligent Systems and Automation** (pp. 9-14). Maryland: American Institute of Physics.

Figure 2.18 Reference Face, Target Face and Reconstructed Face from the Work of Kermi and Coworkers. (A) Reference Face (B) Target Face (C) Reconstructed Face Using Free Form Deformation

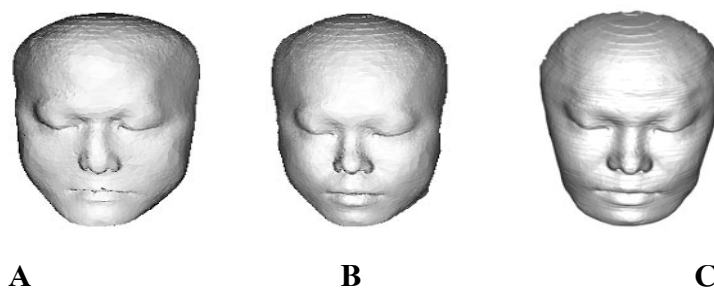
Kermi, Laski and Bloch (2008) also proposed a 3D facial reconstruction method that utilizes recent techniques of MRI medical imaging. The reference faces and questioned faces were segmented and acquired from MRI images. The facial reconstruction was obtained by calculating a volumetric transformation of the reference skull to questioned skull. Then applied the associated transformation to the reference face to approximate the questioned face. This approach also used Free Form Deformation as computational model to carry out throughout. The reconstructed face and the target face are in Figure 2.18 for visual evaluation purpose.

Jiang, Ma, Lin, Yu and Ye (2010) presented the facial reconstruction experiment using three different deformation methods. The reference skull, reference face and questioned skull with landmarks are displayed in Figure 2.19. The three different deformation methods are Radial Basis Functions Deformation, Moving Least Square Affine Deformation and Moving Least Square Rigid Deformation. The resulting faces are shown in Figure 2.20. For the evaluation issue, they mentioned that the photo of the dead is required.



From Jiang, L., Ma, X., Lin, Y., Yu, L. & Ye, Q. Y. (2010). Craniofacial reconstruction based on MLS deformation. *WSEAS Transactions on Computer*, 9(7), 758-767.

Figure 2.19 Reference Skull, Reference Face and Questioned Skull Used in the Work of Jiang and Coworkers. (A) Reference Skull (B) Reference Face (C) Questioned Skull with Landmarks



From Jiang, L., Ma, X., Lin, Y., Yu, L. & Ye, Q. Y. (2010). Craniofacial reconstruction based on MLS deformation. **WSEAS Transactions on Computer**, 9(7), 758-767.

Figure 2.20 Reconstructed Faces Using Three Different Methods from the Work of Jiang and Coworkers. (A) Radial Basis Functions Deformation (B) Moving Least Square Affine Deformation (C) Moving Least Square Rigid Deformation

In this chapter we reviewed the researches involving in facial reconstruction. For the last decade, several computerized facial reconstruction systems have been developed. Most of these systems reconstructed face from the unidentified skull or ancient skull which no one knows the real face. So, the evaluation is impossible. In our work, the questioned skulls are acquired from living persons by CT scanner. This kind of data provides both skulls and facial soft tissue volume. So, we can do visual evaluation later. To select reference head, past researches utilized only craniometric landmarks to compare skull similarity, while this work utilized skull surface which is more informative. In addition, past researches compared skull similarity in a whole while our work compare skull partially. Our work selects only the most similar part from reference skull to be reference part. In this work, the skull similarity was considered using Cylindrical Projection approach. For the reconstruction process, the reconstructed face was obtained by deforming the craniometric landmarks of known skull into unknown skull. Forcing soft tissue of the known skull to the unknown skull with the corresponded deformation gave the desired shape of the soft tissue for the unknown skull. The Free Form Deformation is known to be a powerful shape modification method that has been applied to geometric modeling. It is inspired to do a facial reconstruction. Abate et al (2004) and Kermi et al (2008) applied the theory of Free Form Deformation to do facial reconstruction but the details of the application did not presented. In this work, Free Form Deformation was also applied in our way for facial reconstruction.

CHAPTER 3

METHODOLOGY

This chapter presented the method for facial reconstruction through the use of volume deformation. Current volume deformation based facial reconstructions differed from others mainly by the selection of craniometric landmarks to be deforming points, selection of the skulls to be reference heads, registration and deformation methods. Our methodology can be summarized as follows: First, the 3D head database was derived from CT scan images. Second, craniometric landmarks of questioned skull were needed to manual localization. Then questioned skull was aligned to be the same orientation as heads in the database using Frankfurt plane. After that, in order to select the skull which was the most similar to the questioned skull from the head database to be reference head, all heads in the database were registered to the questioned skull using Iterative Closest Point. After that, the skull similarity was considered using Cylindrical Projection approach. Finally, the reference head was deformed according to the questioned skull using Free Form Deformation. The deformation of soft tissue of the reference head gave the desired facial shape.

3.1 Data Acquisition from CT Scanner

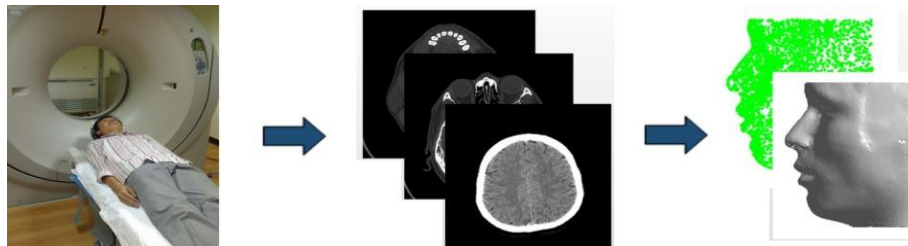


Figure 3.1 3D Head Database Acquisition from CT Scanner

The 3D data used in this paper were acquired from CT scanner (see Figure 3.1). The Cartesian coordinate was used to represent 3D data in the form of (x, y, z) or also known as point cloud. For the visualization purpose we used meshing, shading and shadowing.

3.2 Craniometric Landmarks

Craniometric landmarks are anatomical landmarks on the skull. For manual clay sculpturing method, average soft tissue thicknesses at the landmark points are used. From tissue thickness at the landmarks, the remaining open spaces are interpolated to form the features of the face. In this work, the reconstruction was obtained by deforming the craniometric landmarks of known skull into unknown skull gave the desired shape of the soft tissue for the unknown skull. The craniometric landmarks used in this work were modified from Rhine's landmarks. The illustration of craniometric landmarks used in this work is displayed in Figure 3.2. The lists of craniometric landmarks used in this work are in Table 3.1. In this work, craniometric landmarks of all heads in the head database have to be manually located after 3D head model was acquired.

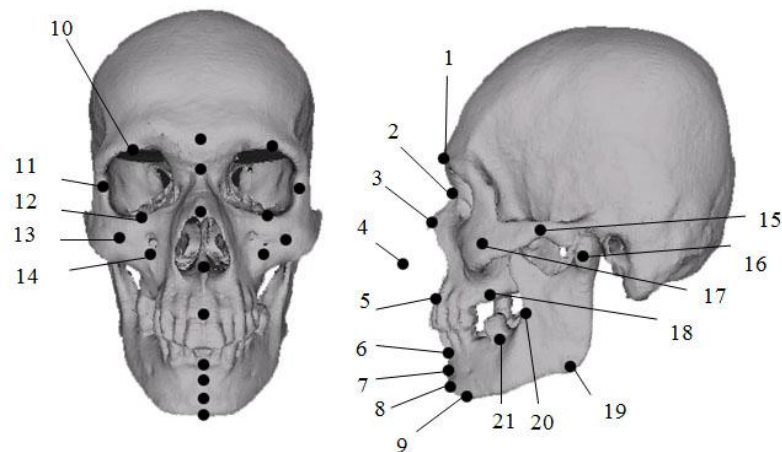


Figure 3.2 Illustration of Craniometric Landmarks Used in this Work

Table 3.1 List of Craniometric Landmarks Used in this Work.

#	Central Landmarks	#	Lateral Landmarks
1	Glabella	10	Supraorbital
2	Nasal	11	Outer orbital
3	End of nasal	12	Suborbital
4	Nose tip estimation	13	Zygoma
5	Upper lip margin	14	Inferior malar
6	Lower lip margin	15	Zygomatic arch
7	Chin-lip fold	16	Condyle
8	Mental eminence	17	Lateral orbit
9	Beneath chin	18	Supra M2
		19	Gonion
		20	Occlusal line
		21	Sub M2

3.3 Frankfurt Plane

The favorite standard orientation of skull used in forensic facial reconstruction is called Frankfurt plane. The position of Frankfurt plane is like someone looking straight ahead. The technical explanation of positioning the skull this way is to have the lowest point on the lower margin of the orbit aligning horizontally with the top edge of the external auditory meatus (Gibson, 2008). See Figure 3.3A for an illustration of this position. Figure 3.3B shows the 3D rotation procedure consisting of pitch, roll and yaw. Since the Frankfurt plane defined only how to control pitch, we have to define how to control roll and yaw our way. In this work, roll and yaw are controlled by the balance between left hand side landmarks and right hand side landmarks. In this work, all heads in the head database were aligned into this orientation. At this point, all skulls were aligned to be the same orientation using Frankfurt plane. Apart from orientation condition we have to deal with other conditions, position and proportion. All head in

the head database were aligned to be the same position by moving the center of craniometric landmarks to the origin point. At this point, all skulls in the head database were aligned to be the same orientation and position with the assumption that all skulls have not much different size. However, the results from this process are just in the initial conditions to be fed to the next process to further alignment call Iterative Closest Point which is the method that minimizes the difference between two surfaces. The process of Frankfurt plane alignment is much needed prior processing Iterative Closest Point algorithm to prevent the local minima phenomenon.

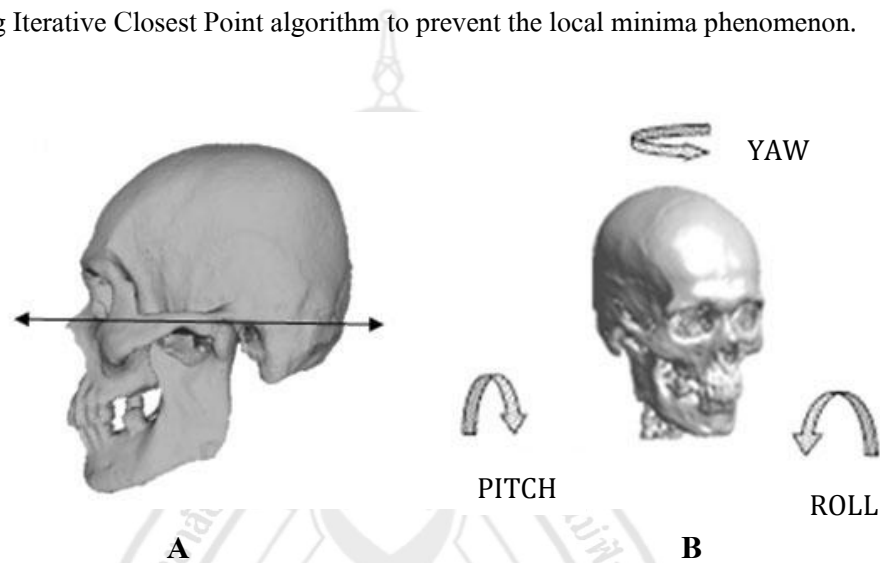


Figure 3.3 Illustration of Frankfurt Horizontal Plane and 3D Rotation. (A) Illustration of Frankfurt Plane (B) Illustration of 3D Rotation

3.4 Iterative Closest Point

In this work, questioned skull and reference skull were aligned to be the same position, proportion, and orientation using registration method called Iterative Closest Point also known as ICP which is a straightforward algorithm that minimizes the difference between two free form surfaces (Besl & McKay, 1992; Bae, 2006). The ICP algorithm to align reference skull to questioned skull is as follows:

The ICP Algorithm

3.4.1 Frankfurt plane gave the initial transformation

3.4.2 Iterative procedure to minimize the average distance of closest point pairs between reference skull and questioned skull

3.4.2.1 Calculate the distance between reference skull and questioned skull for the current iteration

3.4.2.2 Calculate the distance between reference skull and questioned skull for the simulation of transforming the reference skull as follows:

1. Move reference skull a small step in the following directions: up, down, left, right, front and back
2. Rotate reference skull a small angle step in the following directions: yaw clockwise, yaw counterclockwise, pitch clockwise, pitch counterclockwise, roll clockwise, and roll counterclockwise.
3. Scale reference skull up and down for a small step size

3.4.2.3 Transform reference skull after the simulation that gives the minimum distance which is less than the distance of current iteration

3.4.2.4 Terminate if there are no transformation that reduce the distance between reference skull and questioned skull

Please see Appendix A to clarify the idea of Iterative Closest Point algorithm. We simplified and demonstrated the 2D version of the algorithm performance.

3.5 Free Form Deformation

Free Form Deformation (FFD) was introduced by Sederberg and Parry (Sederberg, 2007; Sederberg & Parry, 1986; Song & Yang, 2005) is known to be a powerful shape modification method that has been applied to geometric modeling. This technique deforms an object by embedding it within a solid defined with a control lattice. A change of the lattice deforms the solid and hence the object as seen in Figure 3.4. FFD generally involves with 1D, 2D and also 3D data. We can compute a new location P' from an old location P after deforming control point from P_{ijk} to P'_{ijk} as follows:

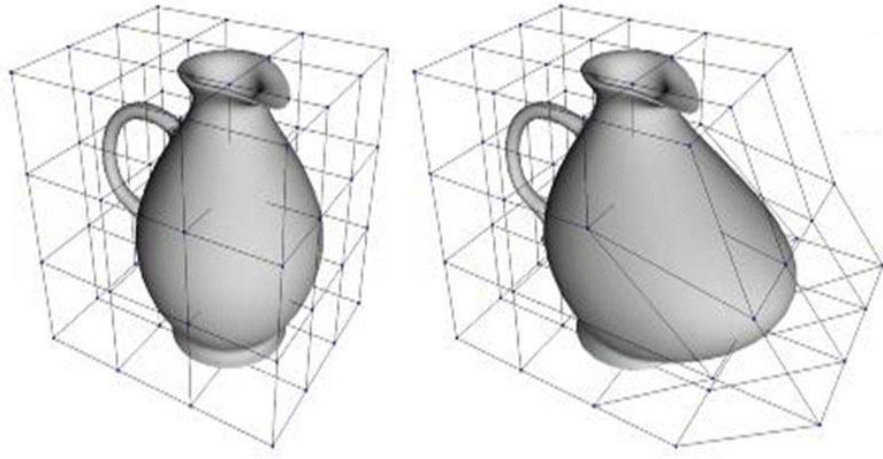
$$\text{1D FFD:} \quad P' = \sum_{i=0}^l B_i^l(t) P'_i \quad (3.1)$$

$$\text{2D FFD:} \quad P' = \sum_{i=0}^l \sum_{j=0}^m B_i^l(s) B_j^m(t) P'_{ij} \quad (3.2)$$

$$\text{3D FFD:} \quad P' = \sum_{i=0}^l \sum_{j=0}^m \sum_{k=0}^n B_i^l(s) B_j^m(t) B_k^n(u) P'_{ijk} \quad (3.3)$$

$$\text{Bernstein Polynomials:} \quad B_i^n(t) = \frac{n!}{(n-i)! i!} t^i (1-t)^{n-i} \quad (3.4)$$

Where point P' is the new location at (s', t', u') of an old point P at (s, t, u) after deforming control point P_{ijk} to P'_{ijk} , and l, m, n are the number of control points minus one in x, y, z axis. ($0 \leq s, t, u, s', t', u' \leq 1$). The derivation of this formula was presented in Appendix B.



From Barzel, R. (2003). **Computer graphics animation course notes**. France: Ecole Polytechnique.

Figure 3.4 Deformation of the Object According to the Deformation of the Lattice

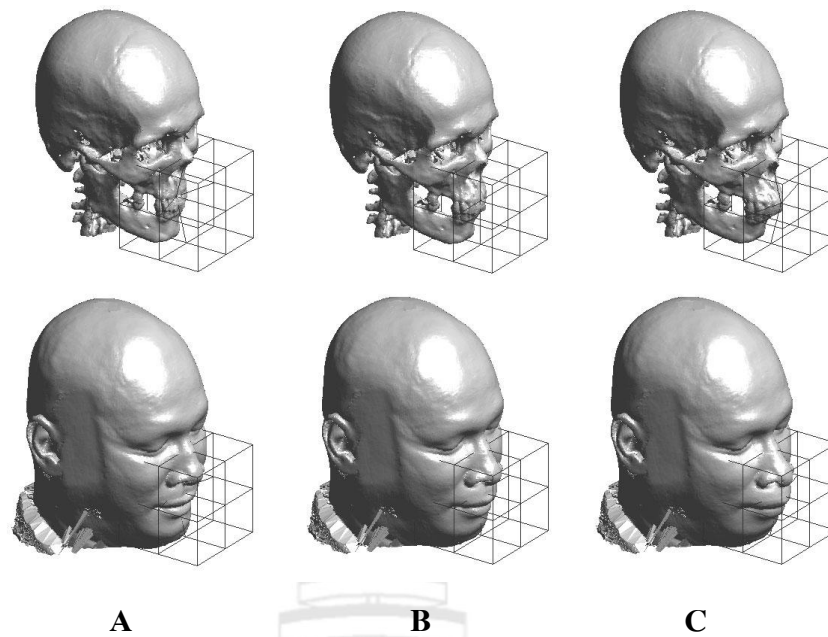


Figure 3.5 Deformation of Face According to the Deformation of the Incisor. (A) Moving the Incisor Inside (B) Original Head (C) Moving the Incisor Outside

In this work, we used FFD in the manner of local deformation by applying the local lattice to the craniometric landmarks. Figure 3.5 shows the deformation of face according to the deformation of incisor. In order to reconstruct the desired face we have to deform all landmarks of reference skull after landmarks of questioned skull.

3.6 Cylindrical Coordinate System

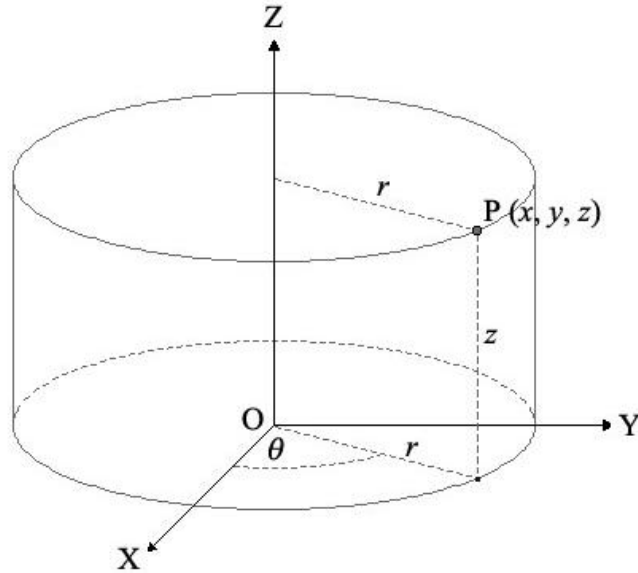


Figure 3.6 Cylindrical Coordinate System and Cartesian Coordinate System

Unlike traditional Cartesian coordinate system which specifies 3D point position by the distance from the three reference axis (x, y, z), Cylindrical coordinate system is a 3D coordinate system specifies point position by the distance from a chosen reference axis (r), the direction from the axis relative to a chosen reference direction (θ), and the distance from a chosen reference plane perpendicular to the axis (z) (see Figure 3.6). The origin of the system (O) is the point where all three distances can be given as zero. This is the intersection between the reference plane and the axis (Bradt, 2001). Cylindrical coordinates are useful when dealing with objects that have some rotational symmetry about the longitude axis or cylindrical-like shape. Cartesian coordinates (x, y, z) can be transformed into cylindrical coordinates (r, θ, z) as follows:

$$r = \sqrt{x^2 + y^2} \quad (3.5)$$

$$\theta = \begin{cases} 0, & \text{if } x = 0 \text{ and } y = 0 \\ \arcsin\left(\frac{y}{r}\right), & \text{if } x \geq 0 \\ -\arcsin\left(\frac{y}{r}\right) + \pi, & \text{if } x < 0 \end{cases} \quad (3.6)$$

3.7 Cylindrical Projection

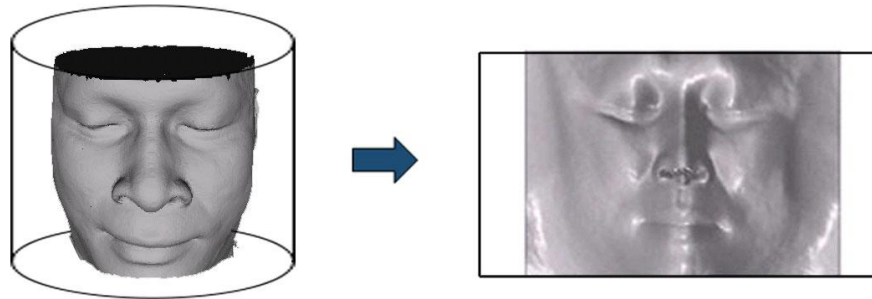


Figure 3.7 Projection of 3D Head Surface onto Cylindrical Plane which is then Flattened

Cylindrical projection can be thought of as a process or as the output of the process. The purpose of the cylindrical projection is to represent a 3D surface as 2D image-like which is convenient to do image processing task later. First step of cylindrical projection is projecting radial coordinate r onto cylindrical plane which is then flattened. After flatten the cylindrical plane, the output is then turn to the form of 2D image-like representation. This 2D image is defined such that the horizontal axis corresponds to angular coordinates θ , the vertical axis corresponds to the height coordinate z and the intensity of each pixel is set to the radial coordinate r (Tu, Hartley & Lorensen, 2005) (see Figure 3.7). The advantage of cylindrical projection is the convenient to compute absolute error between two 3D surfaces which can be directly computed from the different of the intensity from each corresponded pixel.

In this work, to compare skull and face, the 3D head models were transformed onto the plane using a cylindrical projection. Figure 3.8 shows the cylindrical projection of skull and face. Figure 3.9 shows the absolute errors of cylindrical projection surfaces. In Figure 3.9, upper row shows the comparison between two skulls, lower row shows the comparison between two faces. The demonstration of absolute error calculation between two cylindrical projection surfaces was presented in Appendix C.

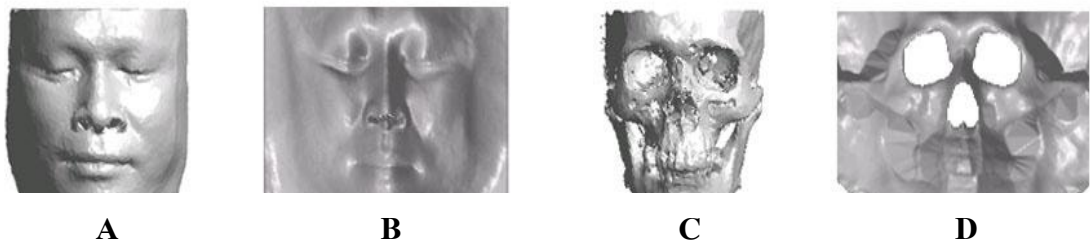


Figure 3.8 Cylindrical Projections of Face and Skull. (A) Face Before Cylindrical Projection (B) Face After Cylindrical Projection (C) Skull Before Cylindrical Projection (D) Skull After Cylindrical Projection

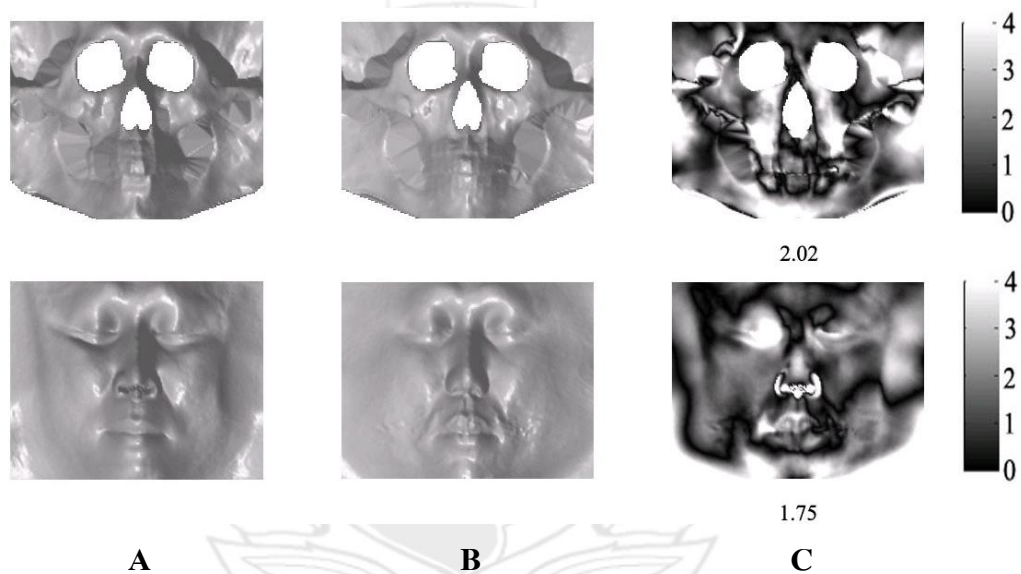


Figure 3.9 Absolute Errors of Cylindrical Projection Surfaces. Upper Row: The Comparison Between Two Skulls, Lower Row: The Comparison Between Two Faces (A) Target Head (B) Reference Head (C) Absolute Errors Surface when Compare Reference Head to Target Head. Errors are Measured in mm.

3.8 Nose Profile Estimation from Nasal Aperture

In order to compare the two cylindrical projection surfaces of skull at the nasal part, we have to estimate the nasal profile due to there is less information from nasal aperture. Figure 3.10 shows the nose profile estimation method modified from the work of Prokobec and Ubelaker (2002). Line A dissects the nasion and prosthion. Line B is parallel to line A and intersects the foremost point on the nasal bone. For each point of nasal aperture, the distance d from line B to the nasal aperture are calculated and mirrored to form the nasal profile estimation. Because the purpose of this work is to reconstruct the face of Thai people but this method was originally designed for Caucasoid people, so we have to know whether this method can be use for Thai people. Please see Appendix D for the evaluation of this method for Thai people.

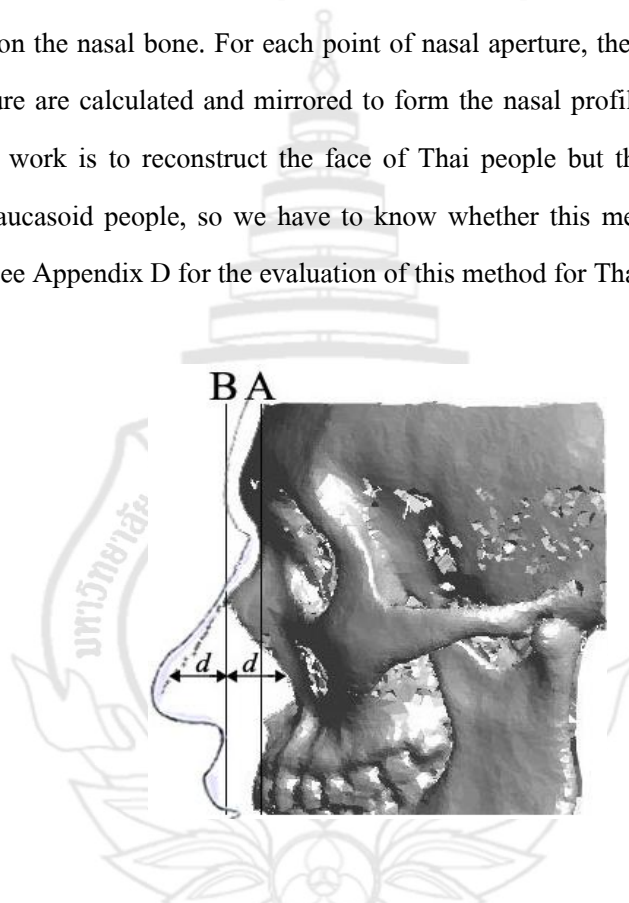
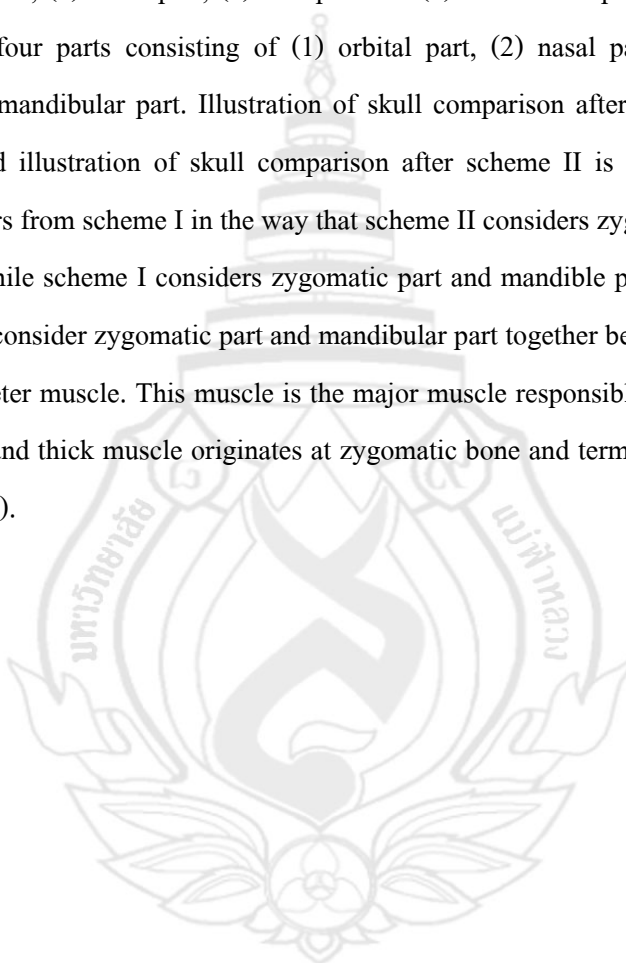


Figure 3.10 Nose Profile Estimation from Nasal Aperture: Line A Dissects the Nasion and Prosthion. Line B is Parallel to Line A and Intersects the Foremost Point on the Nasal Bone. For Each Point of Nasal Aperture, the Distance from Line B to the Nasal Aperture are Calculated and Mirrored to form the Nasal Profile Estimation.

3.9 Skull Similarity in Parts

Differ from past researches which considering skull similarity in a whole, this work, skull similarity was considered partially. In this work, there are two schemes of how to section the skull for comparing purpose. Scheme I, skull is sectioned into five parts consisting of (1) orbital part, (2) zygomatic part, (3) nasal part, (4) oral part and (5) mandibular part. Scheme II, the skull is sectioned into four parts consisting of (1) orbital part, (2) nasal part, (3) oral part and (4) zygomatic and mandibular part. Illustration of skull comparison after scheme I is displayed in Figure 3.11 and illustration of skull comparison after scheme II is displayed in Figure 3.12. Scheme II differs from scheme I in the way that scheme II considers zygomatic part and mandible part together while scheme I considers zygomatic part and mandible part separately. The reason why scheme II consider zygomatic part and mandibular part together because these two bones are linked by masseter muscle. This muscle is the major muscle responsible for facial appearance. It is a very large and thick muscle originates at zygomatic bone and terminates at mandibular bone (see Figure 3.13).



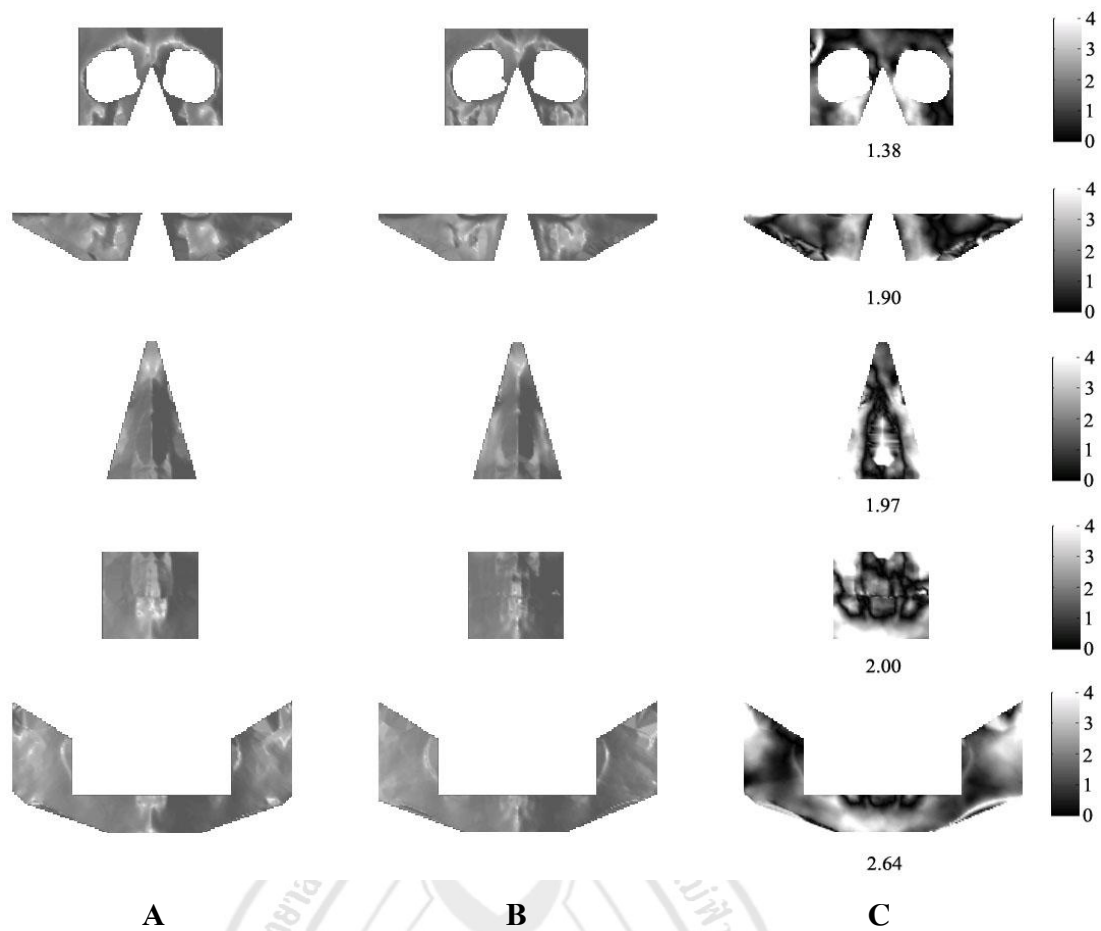


Figure 3.11 Absolute Errors of Cylindrical Projection Surfaces for Scheme I: First Row: Orbital Part, Second Row: Zygomatic Part, Third Row: Nasal Part, Fourth Row: Oral Part, Fifth Row: Mandible Part. (A) Target Skull (B) Reference Skull (C) Absolute Error Surfaces when Compare Reference Skull to Target Skull. Errors are Measured in mm.

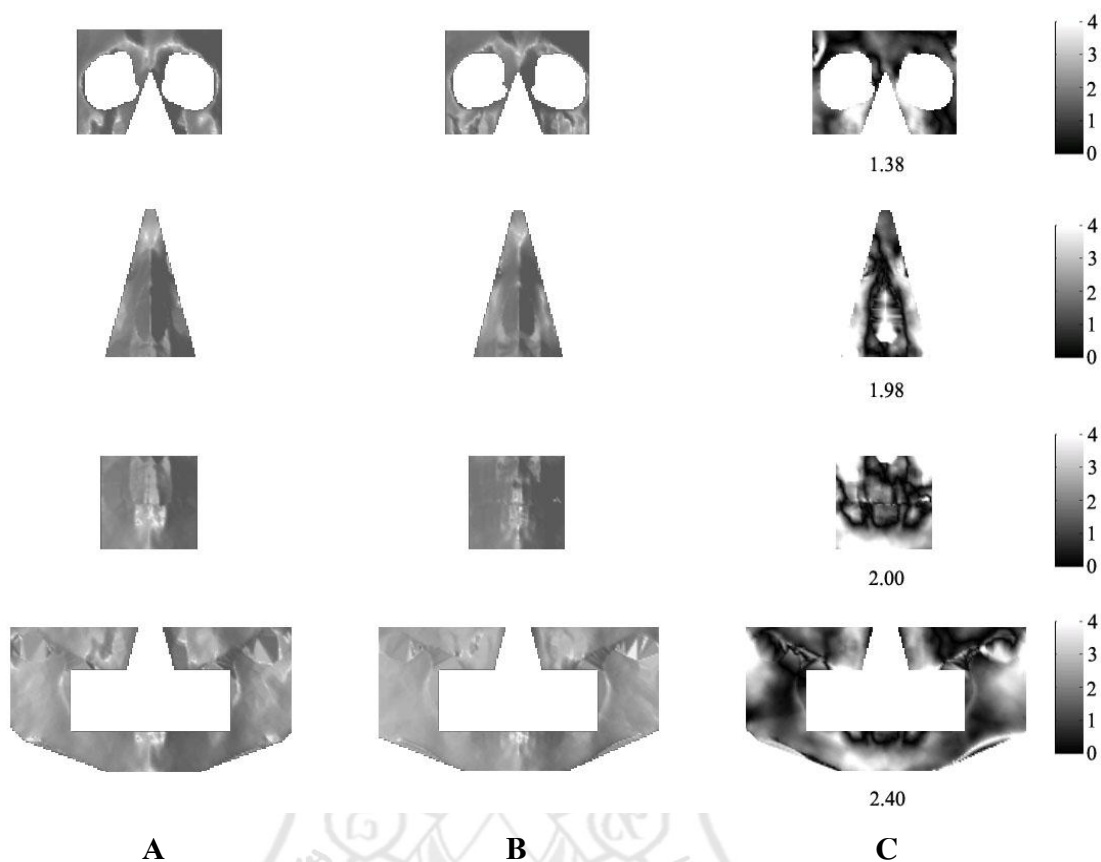


Figure 3.12 Absolute Errors of Cylindrical Projection Surfaces for Scheme II: First Row: Orbital Part, Second Row: Nasal Part, Third Row: Oral Part, Fourth Row: Zygomatic and Mandible Part. (A) Target Skull. (B) Reference Skull. (C) Absolute Error Surfaces when Compare Reference Skull to Target Skull. Errors are Measured in mm.

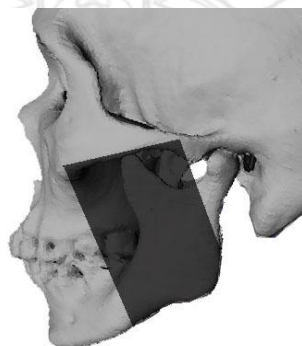


Figure 3.13 Illustration of Masseter Muscle which Originates at Zygomatic Bone and Terminates at Mandibular Bone.

3.10 Facial Reconstruction Procedure

Figure 3.14 and Figure 3.15 show the facial reconstruction procedure. Figure 3.14 shows facial reconstruction scheme I and Figure 3.15 shows facial reconstruction scheme II. There are 11 three dimensional head models in the head database. Each of them is selected as questioned skull and the remaining heads are used as reference heads. First of all, the questioned skull is compared to all skulls in head database each part separately. Next step, the best match for each part is selected as reference part. Then all of the reference parts are deformed according to the questioned skull. Finally, the deformed parts are combined to reconstruct the desired face.

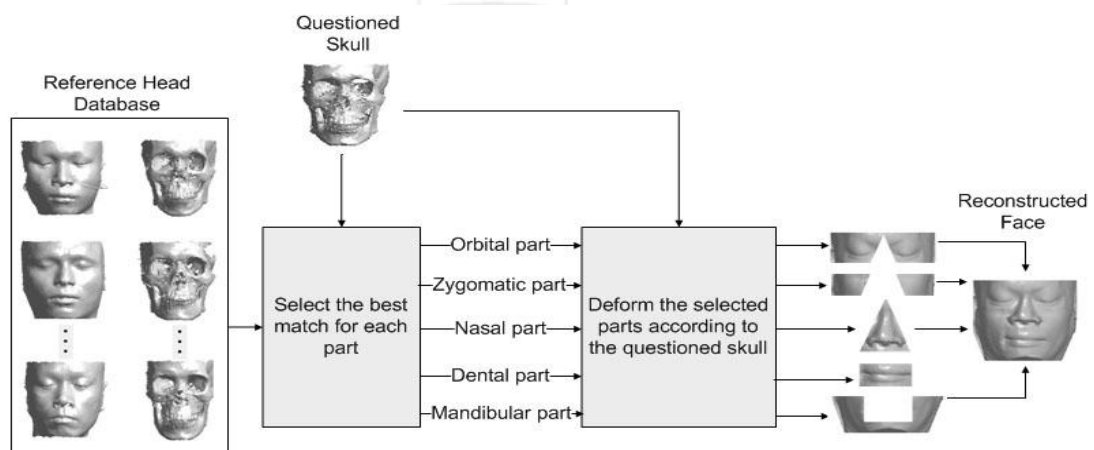


Figure 3.14 Facial Reconstruction Scheme I

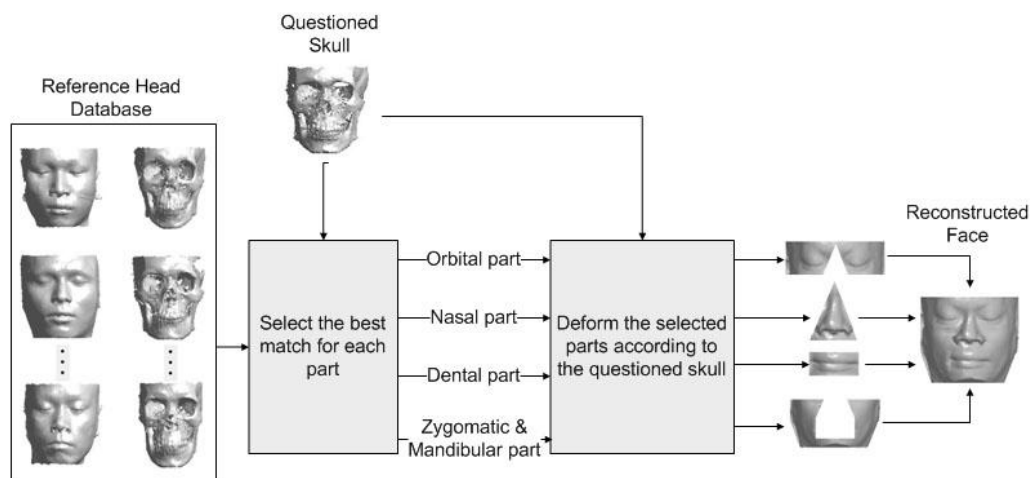


Figure 3.15 Facial Reconstruction Scheme II



CHAPTER 4

RESULTS AND DISCUSSION

This chapter presented the facial reconstruction results from face database through the use of facial reconstruction scheme I and facial reconstruction scheme II. There are 11 three dimensional head models in the head database. Each of them was selected as questioned skull and the remaining heads were used as candidates to be selected as reference heads.

4.1 Facial Reconstruction Results

Facial reconstruction results are displayed in Figure 4.1 to Figure 4.4. Figure 4.1 presents the scheme I facial reconstruction of subjects 1 – 5. Figure 4.2 presents the scheme I facial reconstruction of subjects 6 – 11. Figure 4.3 presents the scheme II facial reconstruction of subjects 1 – 5. Figure 4.4 presents the scheme II facial reconstruction of subjects 6 – 11. In Figure 4.1 to Figure 4.4, first column and second column demonstrate the target faces and reconstructed faces accordingly. These two columns are displayed for visual evaluation. Third column and fourth column present the cylindrical projection of target faces and reconstructed faces accordingly. The absolute error surfaces when compare reconstructed faces to target faces are calculated and display in fifth column. Errors are measured in mm.

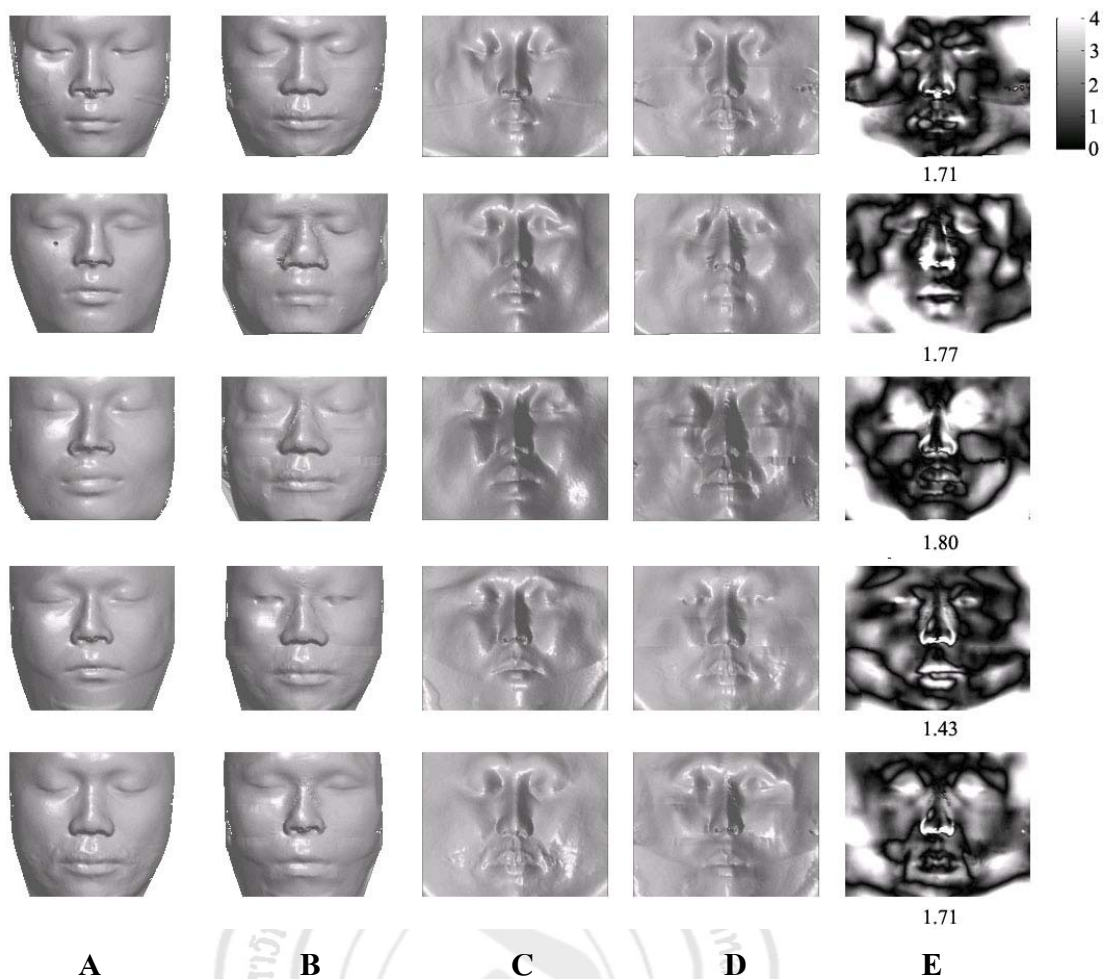


Figure 4.1 Scheme I Facial Reconstruction of Subjects 1 - 5. (A) Target Faces (B) Reconstructed Faces (C) Cylindrical Projection of Target Faces (D) Cylindrical Projection of Reconstructed Faces (E) Absolute Error Surfaces when Compare Reconstructed Faces to Target Faces. Errors are Measured in mm.

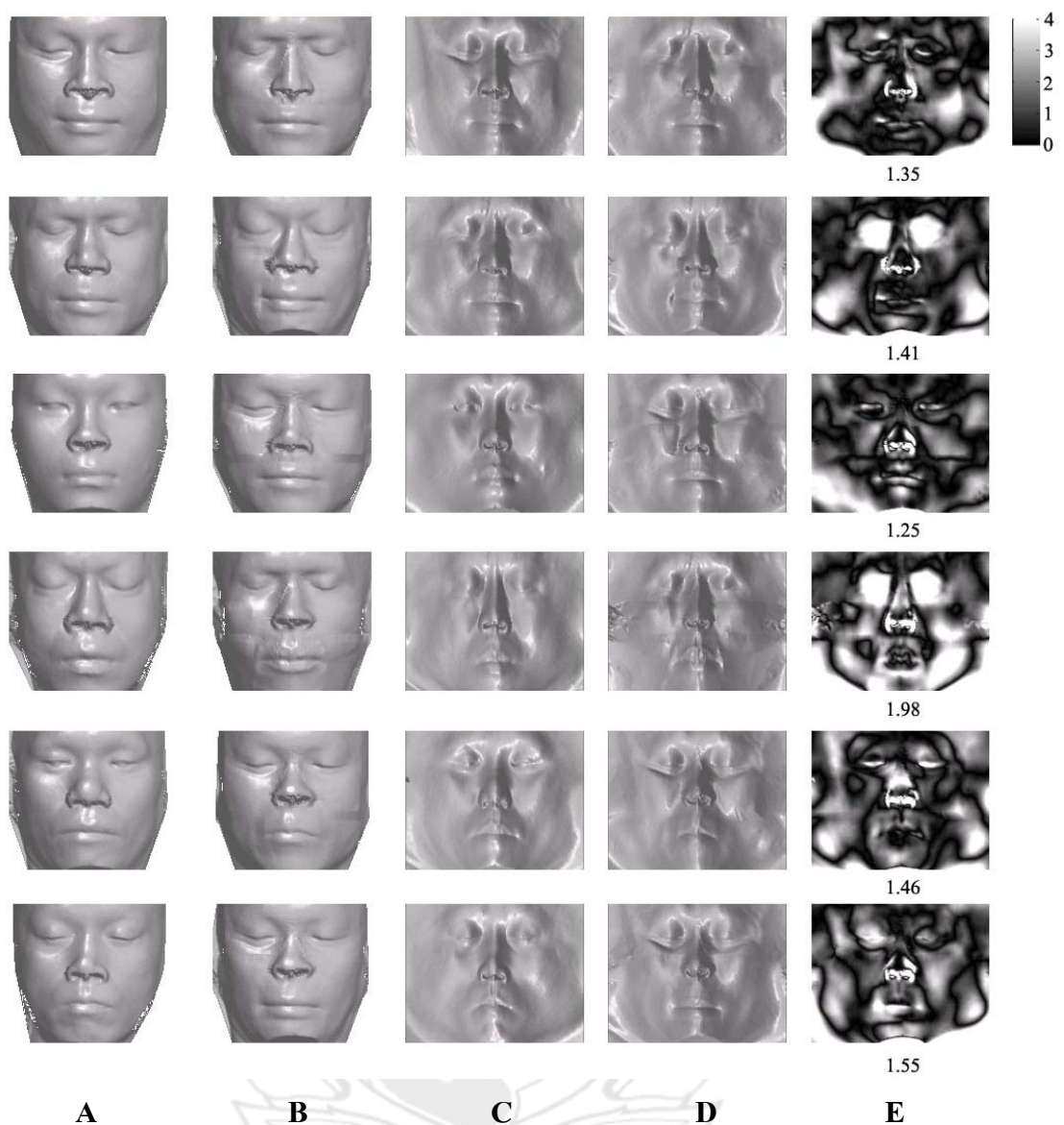


Figure 4.2 Scheme I Facial Reconstruction of Subjects 6 - 11. (A) Target Faces (B) Reconstructed Faces (C) Cylindrical Projection of Target Faces (D) Cylindrical Projection of Reconstructed Faces (E) Absolute Error Surfaces when Compare Reconstructed Faces to Target Faces. Errors are Measured in mm.

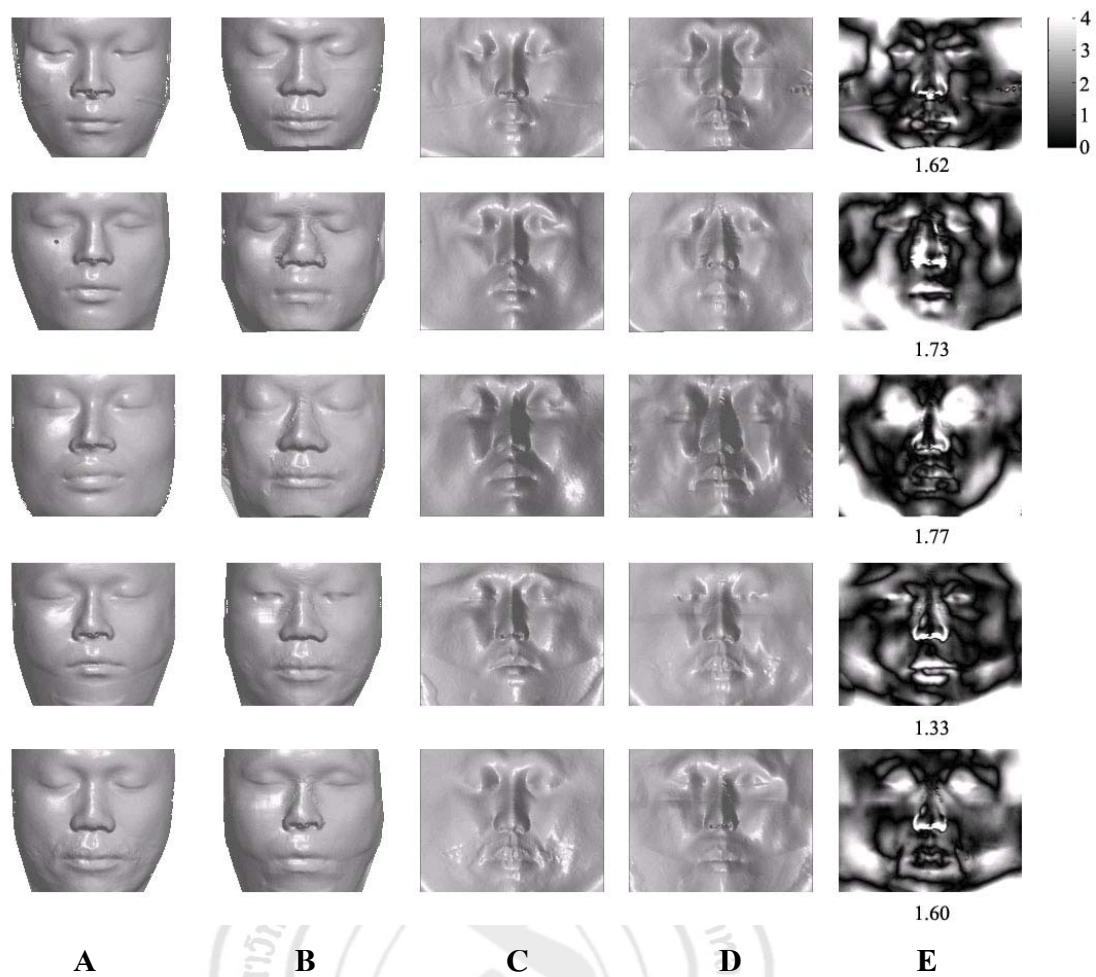


Figure 4.3 Scheme II Facial Reconstruction of Subjects 1 - 5. (A) Target Faces (B) Reconstructed Faces (C) Cylindrical Projection of Target Faces (D) Cylindrical Projection of Reconstructed Faces (E) Absolute Error Surfaces when Compare Reconstructed Faces to Target Faces. Errors are Measured in mm.

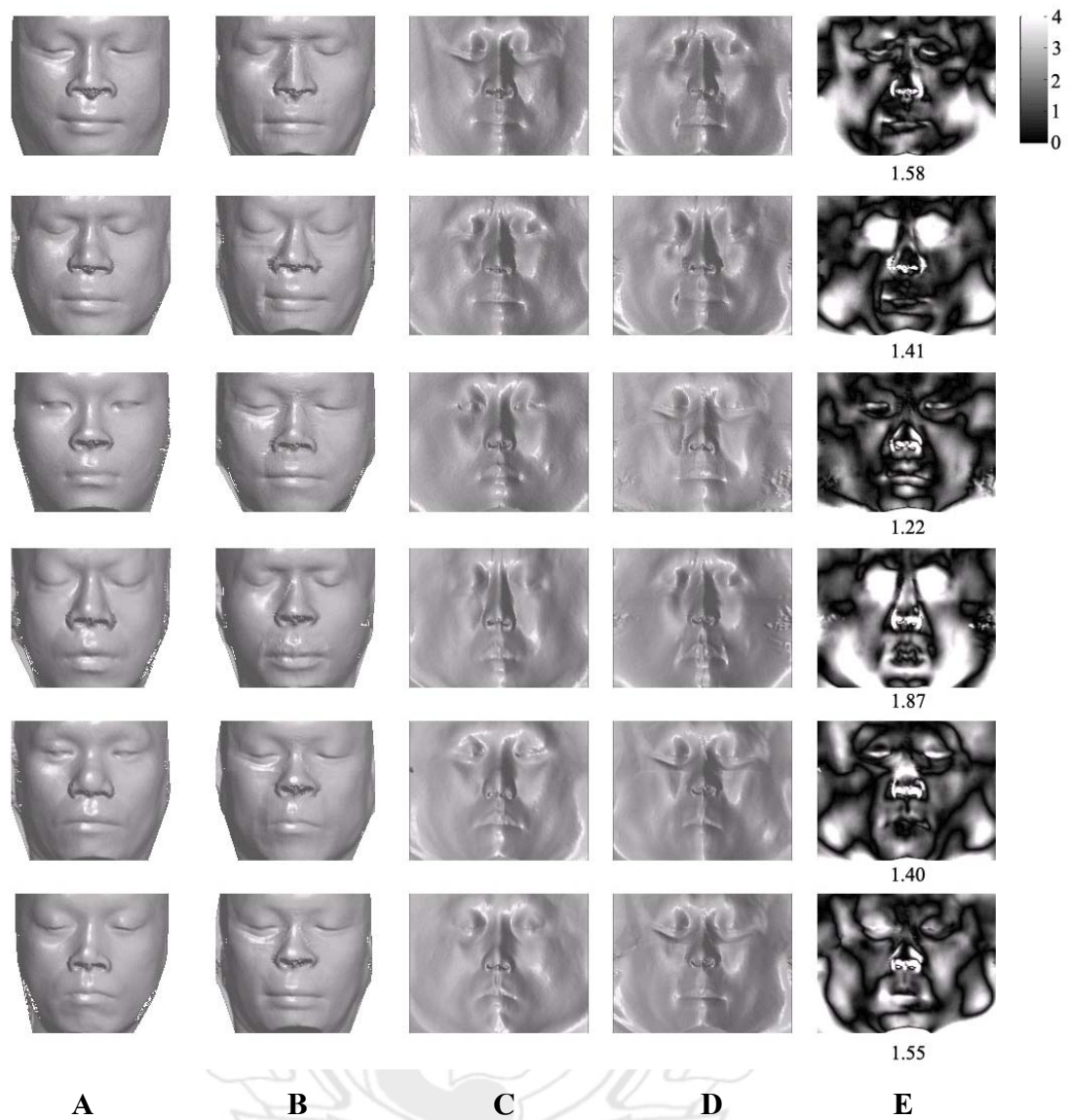


Figure 4.4 Scheme II Facial Reconstruction of Subjects 6 - 11. (A) Target Faces (B) Reconstructed Faces (C) Cylindrical Projection of Target Faces (D) Cylindrical Projection of Reconstructed Faces (E) Absolute Error Surfaces when Compare Reconstructed Faces to Target Faces. Errors are Measured in mm.

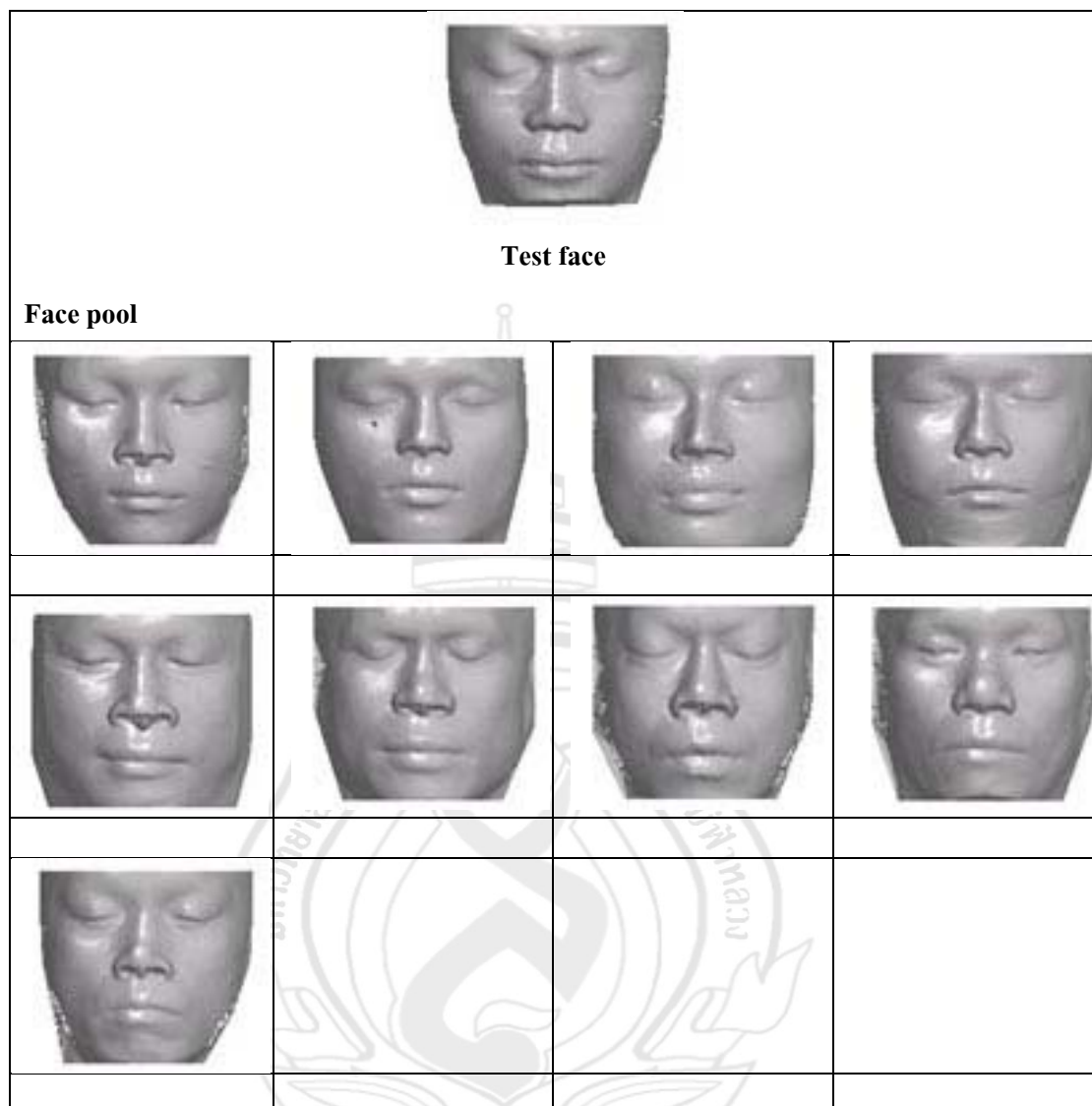
Table 4.1 Absolute Errors of Facial Reconstruction from Scheme I and Scheme II

Subject	Absolute Reconstruction from	Absolute Reconstruction
	Error from Scheme I	Error from Scheme II
1	1.71	1.62
2	1.77	1.73
3	1.80	1.77
4	1.43	1.33
5	1.71	1.60
6	1.35	1.58
7	1.41	1.41
8	1.25	1.22
9	1.98	1.87
10	1.46	1.40
11	1.55	1.55
Mean	1.58	1.55
Maximum	1.98	1.87
Minimum	1.25	1.22
Standard deviation	0.22	0.20

4.2 Visual Evaluation

In the previous section, the quantitative evaluation was performed using cylindrical projection approach. However, the goal of facial reconstruction is not reconstruction accuracy but rather recognition or identification success. As mentioned in the review of Claes et al. (2010), a more realistic and human subjective, identification process can be simulated by generating face pool test. An example of face pool test is shown in Figure 4.5. Top image is the reconstructed face to be identified with the faces from the face pool. The reconstructed faces in the face pool test were from Scheme II reconstruction. Face pool are a set of faces from the face database.

The reference faces of the reconstructed face were excluded from the face pool. The 19 human assessors were recruited from last year bachelor degree students in computer science at Rajamangala university of Technology Isan who registered to image processing course in second semester of academic year 2011. They were asked to indicate the best three match faces from the face pool. The ranks of recognition were indicated by the number 1, 2 and 3 accordingly. The result of face pool test is shown in Table 4.2. From Table 4.2, 1st rank recognizable presents the number of assessors who could correctly identify the target subjects from number 1. In the same manner, 2nd rank recognizable and 3rd rank recognizable present the number of assessors who could correctly identify the target subjects from number 2 and number 3 respectively. For example, considering reconstructed face number 9, the number 14 in the 1st rank recognizable presents that 14 assessors from all 19 assessors (approximately 74%) indicated number 1 in the subject number 9. The number 2 in the 2nd rank recognizable presents that 2 assessors from all 19 assessors (approximately 11%) indicated number 2 in the subject number 9. The number 1 in the 3rd rank recognizable presents that 1 assessor from all 19 assessors (approximately 5%) indicated number 3 in the subject number 9. And the number 2 in the cannot recognizable presents that 2 assessors from all 19 assessors (approximately 11%) did not indicated any number in the subject number 9. Please see the full set of face pool test in Appendix E.



Note. Instruction: Please look at the test face at the top and then consider the faces from face pool. Please select the best three match faces from the face pool. Please indicate the rank of the match by the number 1, 2 and 3 under the face in the face pool.

Figure 4.5 Example of the face pool test. Top image is the reconstructed face to be identified with the faces from the face pool.

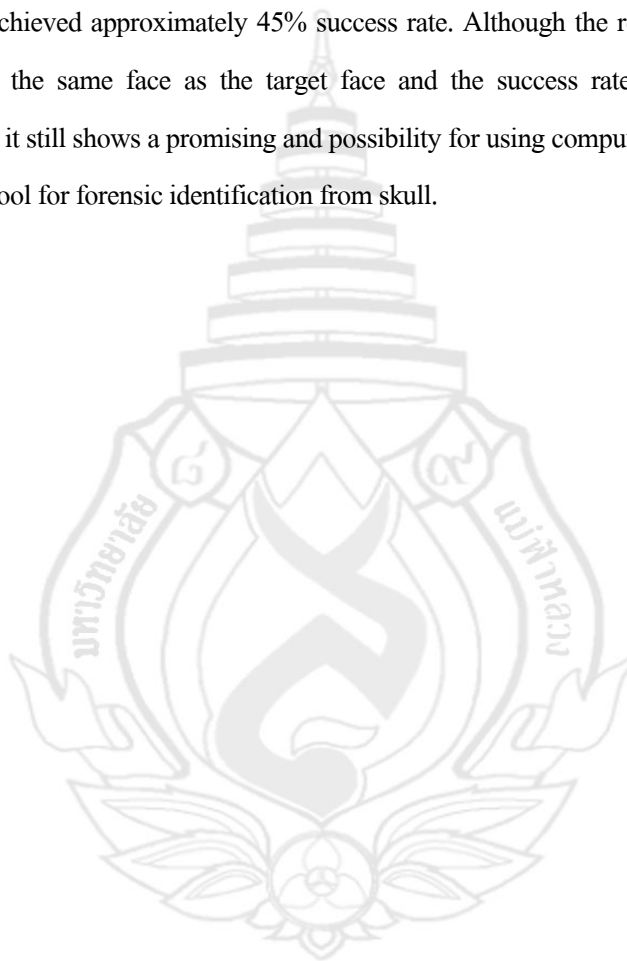
Table 4.2 Result of Face Pool Test

Reconstructed	1 st Rank	2 nd Rank	3 rd Rank	Cannot
Face	Recognizable	Recognizable	Recognizable	Recognizable
1	11 (58%)	4 (21%)	2 (11%)	2 (11%)
2	2 (11%)	2 (11%)	3 (16%)	12 (63%)
3	3 (16%)	2 (11%)	2 (11%)	12 (63%)
4	3 (16%)	7 (37%)	4 (21%)	5 (26%)
5	7 (37%)	3 (16%)	3 (16%)	6 (32%)
6	2 (11%)	2 (11%)	2 (11%)	13 (68%)
7	7 (37%)	4 (21%)	4 (21%)	4 (21%)
8	2 (11%)	3 (16%)	0 (0%)	14 (74%)
9	14 (74%)	2 (11%)	2 (11%)	1 (5%)
10	3 (16%)	5 (26%)	6 (32%)	5 (26%)
11	3 (16%)	6 (32%)	1 (5%)	9 (47%)

4.3 Discussion

From Table 4.1, when compare the results from scheme I and scheme II one by one, most of absolute errors from scheme II are less than absolute errors from scheme I except for subject 6. For subject 7 and 11, the absolute errors are equal because both Scheme I and II used the same reference parts for the reconstructions. When compare the results from scheme I and scheme II overall, the average of absolute errors from scheme I is 1.58 and the average of absolute errors from scheme II is 1.55. So, we can conclude that scheme II is slightly better than scheme I. However, the goal of facial reconstruction is not reconstruction accuracy but rather recognition or identification success. As mentioned in the review of Claes et al. (2010), a more realistic and human subjective, identification process can be simulated by generating face pool test. The result of face pool test is shown in Table 4.2. The reconstruction number 1 was considered success because more than a half of assessors could recognize this reconstruction to subject number 1 at first recognition. The reconstruction number 2 and

3 were considered fail because more than a half of assessors could not recognize the faces to the target subjects. The reconstruction number 4 was considered fail if we consider only first recognition because only about 16% of assessors could recognize the face at first recognition. But if we consider first recognition and second recognition together, the reconstruction number 4 can be considered success because more than a half of assessors could recognize the face to the target subject. Considering this way, we can conclude that the reconstruction number 1, 4, 5, 7 and 9 are considered success which achieved approximately 45% success rate. Although the result shows that we cannot produce exactly the same face as the target face and the success rate of identification was not considered high, it still shows a promising and possibility for using computerized facial reconstruction as a supporting tool for forensic identification from skull.



CHAPTER 5

CONCLUSIONS AND FUTURE WORK

5.1 Conclusions

A traditional manual facial reconstruction has been used for a long time in both forensic and archaeological fields. However, the progressive studies and medical imaging technology leads to the development of alternative computer-based facial reconstruction methods. We have to remark that there is no way to reproduce exactly the same face for discovered skull. Instead of using small set of facial soft tissue thickness data and then interpolate the large remaining area, we can use whole facial soft tissue thickness data from 3D head models derived from CT scanner and then interpolate questioned face from reference faces in the head database. This work presented possibility to use this scheme as a supporting tool for forensic facial reconstruction.

In comparison with past facial reconstruction research systems, our work presented a number of advantages. (1) Most of these previous systems reconstructed face from the unidentified skull or ancient skull which no one knows the real face. So, the evaluation is impossible. In our work, the questioned skulls were acquired from living persons by CT scanner. This kind of data provides both skulls and facial soft tissue volume. So, we can do visual evaluation later. (2) Most of these systems consider skull similarity in a whole, whereas our work considers skull similarity in parts. So, these previous works selected the reference head from overall similarity, while our work selected only the similar part from reference head which can exclude other parts that are not similar to questioned skull. (3) Most of these previous works considered skull similarity based on craniometric landmarks, while our work considered skull similarity from skull surface which is more informative and more reliable. (4) Some of these previous works did not present any kind of evaluation and some of these works presented only visual evaluation, while our work presented both visual evaluation using face pool test and numerical evaluation using cylindrical projection approach which is more informative.

This work proposed two schemes of facial reconstructions, categorized by how skull is sectioned and selected as references. Scheme I sectioned skull into 5 parts and scheme II sectioned skull into 4 parts. Scheme II differed from scheme I in the way that scheme II considered zygomatic part and mandible part together, while scheme I considered zygomatic part and mandible part separately. Three dimensional data of skulls and faces used in this work were all acquired by CT scanner. The reconstruction was obtained by deforming the craniometric landmarks of known skull into unknown skull. Forcing soft tissue of the known skull to the unknown skull with the corresponded deformation gave the desired shape of the soft tissue for the unknown skull. From the numerical evaluation, the results from scheme II were slightly better than scheme I. From the visual evaluation, this work achieves approximately 45% of recognition success rate. Although the result shows that we cannot produce exactly the same face as the target face and the success rate of identification was not considered high. The results showed promising for forensic facial reconstruction. However, the reconstruction efficiency was still limited due to the limitation of number of head in the head database.

5.2 Future Work

Preliminary results from our work presented the feasibility of this approach, although further investigations are required. (1) The head database needed to be increased to make this approach more useful in forensic facial identification. (2) The relationships between facial features and underneath skull should be more investigated separately (e.g. eyes, nose, mouth, cheek and chin). (3) Facial similarity measurement method for evaluation phase should be improved. We recommend machine learning approach. (4) Facial reconstruction according to nutrition and aging conditions is the one of interesting research topic. (5) In this work, we have to locate craniometric landmarks manually. So, automatic localization of craniometric landmarks is the one of future plan research.

REFERENCES



REFERENCES

- Abate, A. F., Nappi, M., Ricciardi, S. & Tortora, G. (2004). FACES: Facial reconstruction from ancient skulls using content based image retrieval. **Journal of Visual Languages & Computing**, 15(5), 373-389.
- Archer, K. M. (1997). **Craniofacial reconstruction using hierarchical B-Spline interpolation**. Master's Thesis. University of British, Columbia.
- Andersson, B. & Valfridsson, M. (2005). **Digital 3D facial reconstruction based on computed tomography**. Master's Thesis. Linkopings Universitet, Sweden.
- Bae, K. (2006). **Automated registration of unorganized point clouds from terrestrial laser scanners**. Doctoral Dissertation. Curtin University of Technology, Western, Australia.
- Barzel, R. (2003). **Computer graphics animation course notes**. France: Ecole Polytechnique.
- Besl, P. J. & McKay, N. D. (1992). A method for registration of 3-D shapes. **IEEE Transactions on Analysis and Machine Intelligence**, 14(2), 239-255.
- Bradt. (2001). **Mathematic supplement for physics**. Massachusetts: MIT Press.
- Bullock, D. W. (1999). **Computer assisted 3D craniofacial reconstruction**. Master's Thesis. University of British, Columbia.
- Claes, P., Vandermeulen, D., Greef, S. D., Willems, G., Clement, J. & Suetens, P. (2010). Computerized craniofacial reconstruction: Conceptual framework and review. **Forensic Science International**, 201(1-3), 138-145.
- Echeverria, G. (2003). **3D Facial reconstruction tissue depth measurement from MRI cans**. Master's Thesis. University of Sheffield.

- Gibson, L. (2008). **Forensic art essentials: A manual for law enforcement artists**. London: Academic Press.
- Jiang, L., Ma, X., Lin, Y., Yu, L. & Ye, Q. Y. (2010). Craniofacial reconstruction based on MLS deformation. **WSEAS Transactions on Computer**, 9(7), 758-767.
- Jones, M. W. (2001). Facial reconstruction using volumetric data. In **Proceedings of IEEE Vision, Modeling and Visualization** (pp. 135-142). Stuttgart: IEEE Press.
- Kermi, A., Laski, M. T. & Bloch, I. (2008). A three-dimensional computerized facial reconstruction using non-linear registration of a reference head. In **Proceedings of Intelligent Systems and Automation** (pp. 9-14). Maryland: American Institute of Physics.
- Khatod, H. N. (2004). **Towards automation of forensic facial reconstruction**. Master's Thesis. Louisiana State University.
- Knight, B. (1991). The establishment of identify of human remain. **Forensic Pathology**. New York: Oxford University Press.
- Maraj, S. J. (2007). **Facial reconstruction**. Master's Thesis. Touro College, New York.
- Prag, J. & Neave, R. A. H. (1997). **Making faces**. London: British Museum.
- Prokopec, M. & Ubelaker, D. H. (2002). Reconstructing the shape of the nose according to the skull. **Forensic Science Communications**, 4(1), na.
- Rhine, J. S., Moore, C. E. & Westin, J. T. (Eds.). (1982). **Facial reproduction: Tables of facial tissue thickness of american caucasoid in forensic anthropology**. New Mexico: Maxell Museum of Anthropology, University of New Mexico.
- Sederberg, T. W. (2007). **Computer aided geometric design course notes**. Utah: Department of Computer Science, Brigham Young University.

- Sederberg, T. W. & Parry, S. R. (1986). Free-form deformation of solid geometric models, **Computer Graphics**, **20**(4), 151-160.
- Song, W. & Yang, X. (2005). Free-form deformation with weighted T-spline. **The Journal of Visual Computer**, **21**(3), 139-151.
- Stephan, C. N., Taylor, R. G. & Taylor, J. A. (2008). Methods of facial approximation and skull-face superimposition, with special consideration of method development in australia. In M. Oxenham (Ed.), **Forensic approaches to death, disaster and abuse** (pp. 133-147). Queensland: Australian Academic.
- Subsol, G., Mafart, B., Silvestre, A. & De Lumley, M. (2002). 3D image processing for the study of the evolution of the shape of the human skull. Presentation of the tools and preliminary results. In B. Mafart & H. Delingette (Eds.) **Three-dimensional imaging in paleoanthropology and prehistoric archaeology** (pp. 37-45). Acts of the XIVth UISPP Congress, University of Lie`ge, Belgium, 2–8 September 2001. British Archaeological Record International Series 1049.
- Taylor, K. T. (2001). **Forensic art and illustration**. Florida: CRC.
- Tu, P., Hartley, R. I. & Lorensen, W. E. (2005). Computer-graphic facial reconstruction. In J. G. Clement & M. K. Marks (Eds.), **Face reconstructions using flesh deformation modes** (pp. 145-161). Oxford: Elsevier Academic.
- Vanezis, M. (2007). **Forensic facial reconstruction using 3-D computer graphics: Evaluation and improvement of Its reliability in identification**. Doctoral Dissertation. University of Glasgow, Scotland.
- Wilkinson, C. (2004). **Forensic facial reconstruction**. Cambridge: Cambridge University.

APPENDICES

APPENDIX A

DEMONSTRATION OF ITERATIVE CLOSEST POINT PERFORMANCE

In Chapter 3 we mentioned about using Iterative Closest Point (ICP) algorithm to align the skulls to be the same position, orientation, and proportion. The purpose of this section is to presents the progression of the algorithm to clarify the idea of the ICP algorithm. The demonstration was presented in 2D version of the ICP algorithm to simplify the understanding.

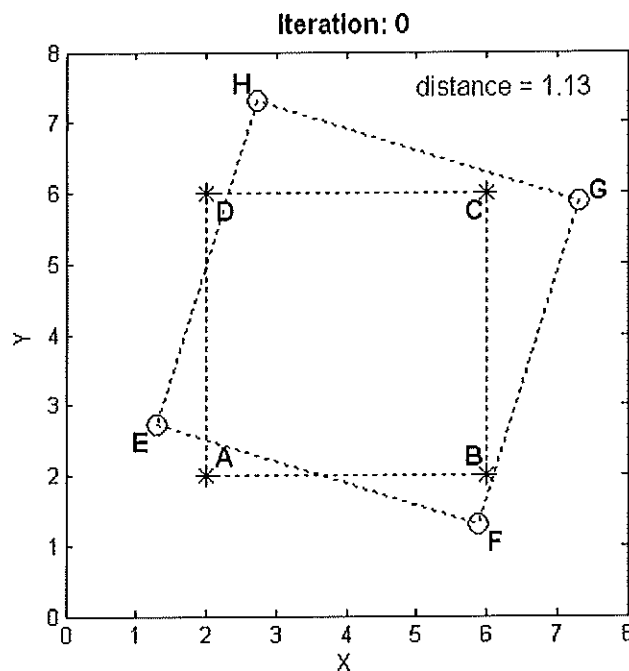


Figure A1 The Static Object with Asterisk-Marked at the Corner and the Moving Object with Circle-Marked at the Corner

To demonstrate the performance of the ICP algorithm, please see Figure A1, let the rectangle with asterisk-marked at the corners be the static object or target object and the rectangle with circle-marked at the corners be the moving object to be transformed to be the same position, orientation, and proportion as the target object using the ICP algorithm. In this section, the ICP algorithm from Chapter 3 was simplified from 3D approach to 2D approach to clarify the understanding. The ICP algorithm to align the moving object to the target object is as follows:

The ICP Algorithm

1. Initial transformation
2. Iterative procedure to minimize the average distance of closest point pairs between the target object and the moving object
 - 1) Calculate the distance between the target object and the moving object for the current iteration
 - 2) Calculate the distance between the target object and the moving object for the simulation of transforming the moving object as follows:
 - A. Move the object a small step in the following directions: up, down, left, and right
 - B. Rotate the object clockwise and counterclockwise for a small angle step
 - C. Scale the object up and down for a small step size
 - 3) Transform the object after the simulation that gives the minimum distance which is less than the distance of current iteration
 - 4) Terminate if there are no transformation that reduce the distance between the target object and the moving object

From the ICP algorithm, the initial transformation is presented in Figure A.1. From step 1, the distance between the target object and the moving object of this iteration or iteration 0 is 1.13. Definition of the distance between objects is the average value of the distance between closest point pairs from the objects. In this case, the closest point pairs between the objects are as follows: A and E, B and F, C and G, and H and I. The equation to calculate the distance between the objects is in equation (A.1).

$$\text{distance} = (\overline{AE} + \overline{BF} + \overline{CG} + \overline{DH})/4 \quad (\text{A.1})$$

From step 2, all candidate transformations of the moving object were simulated. The simulations of moving object to the right, to the left, up, and down are presented in Figure A2. The simulations of rotation object clockwise and counterclockwise are presented in Figure A3. The simulations of scaling object down and up are presented in Figure A4.

From step 3, transformed the moving object after the simulation that gives the minimum distance which is less than the distance of current iteration. From Figure A2 to A.4, we found that the simulation of rotation the object counterclockwise in Figure A3 gives the minimum distance of 0.9 which is less than current iteration distance of 1.13. Hence, the object was then counterclockwise rotated and the next iteration was processed. The progression of the ICP algorithm implementation from iteration 0 to 27 is presented in Figure A5. At the iteration 27, since, there are no transformation that reduces the distance between the target object and the moving object, then the processing was terminated in step 4.

From Figure A5, we can see the progression of the ICP algorithm implementation from iteration 0 to 27. The moving object was iteratively moved, rotated, and scaled with the intention of providing the best transformation that minimized the distance between the moving object and the target object. From Figure A6 and Table A1, we can see the progression of the distance from the distance of 1.13 at iteration 0 to the distance of 0.00 at the iteration 27. In this case, we can see the convergence of the progression but please note that in general case the pre-alignment processing is needed prior processing the ICP algorithm to prevent the local minima phenomenon.

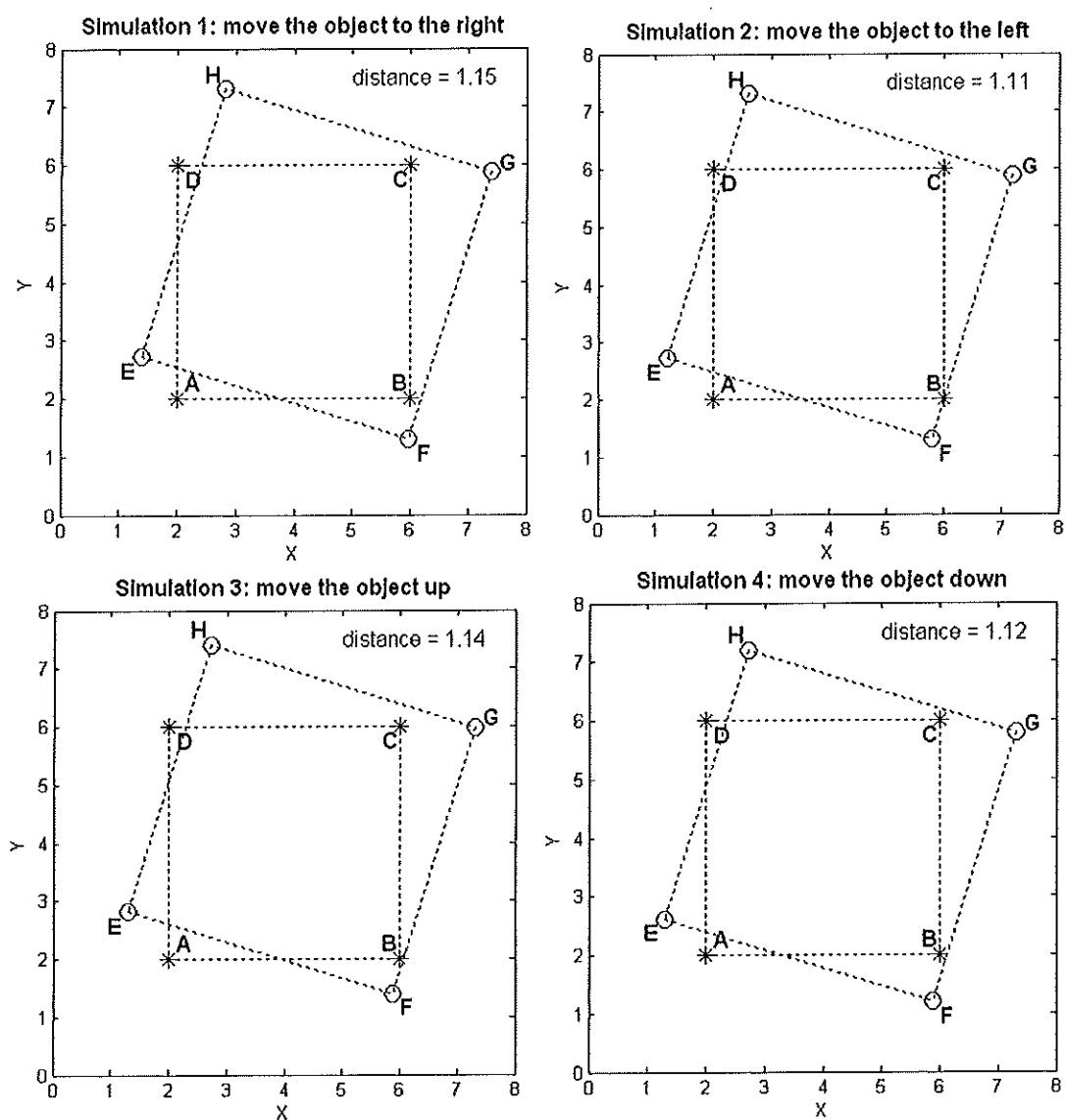


Figure A2 The Simulations of Moving Object to the Right, to the Left, up, and Down

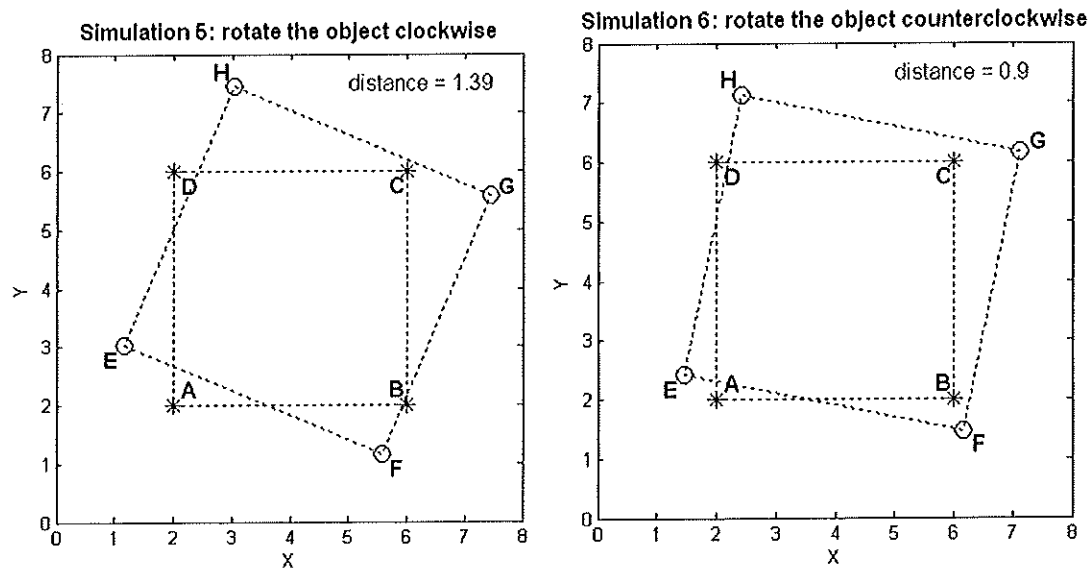


Figure A3 The Simulations of Rotation Object Clockwise and Counterclockwise

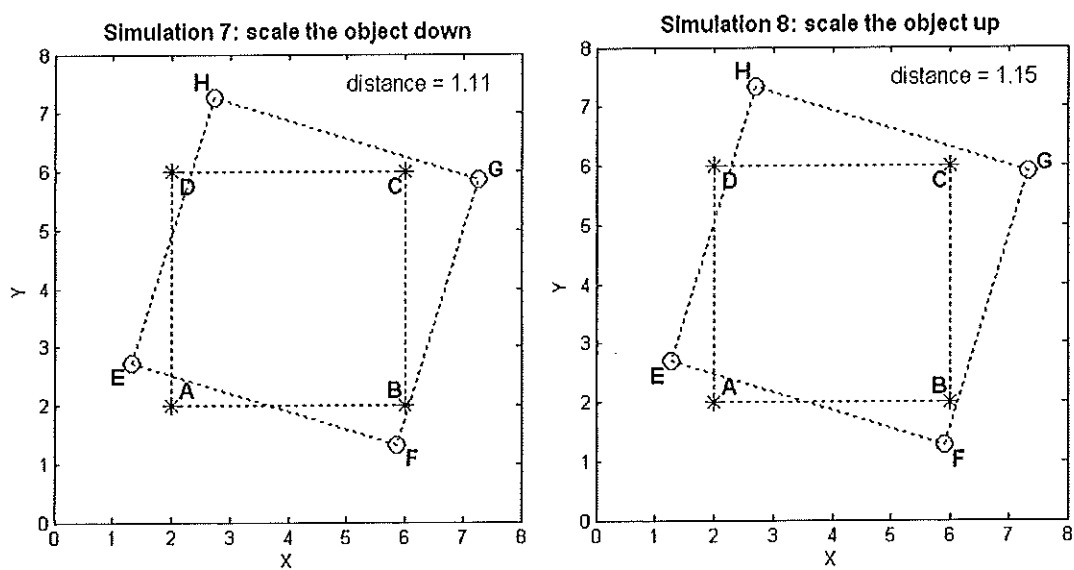


Figure A4 The Simulations of Scaling Object Down and Up.

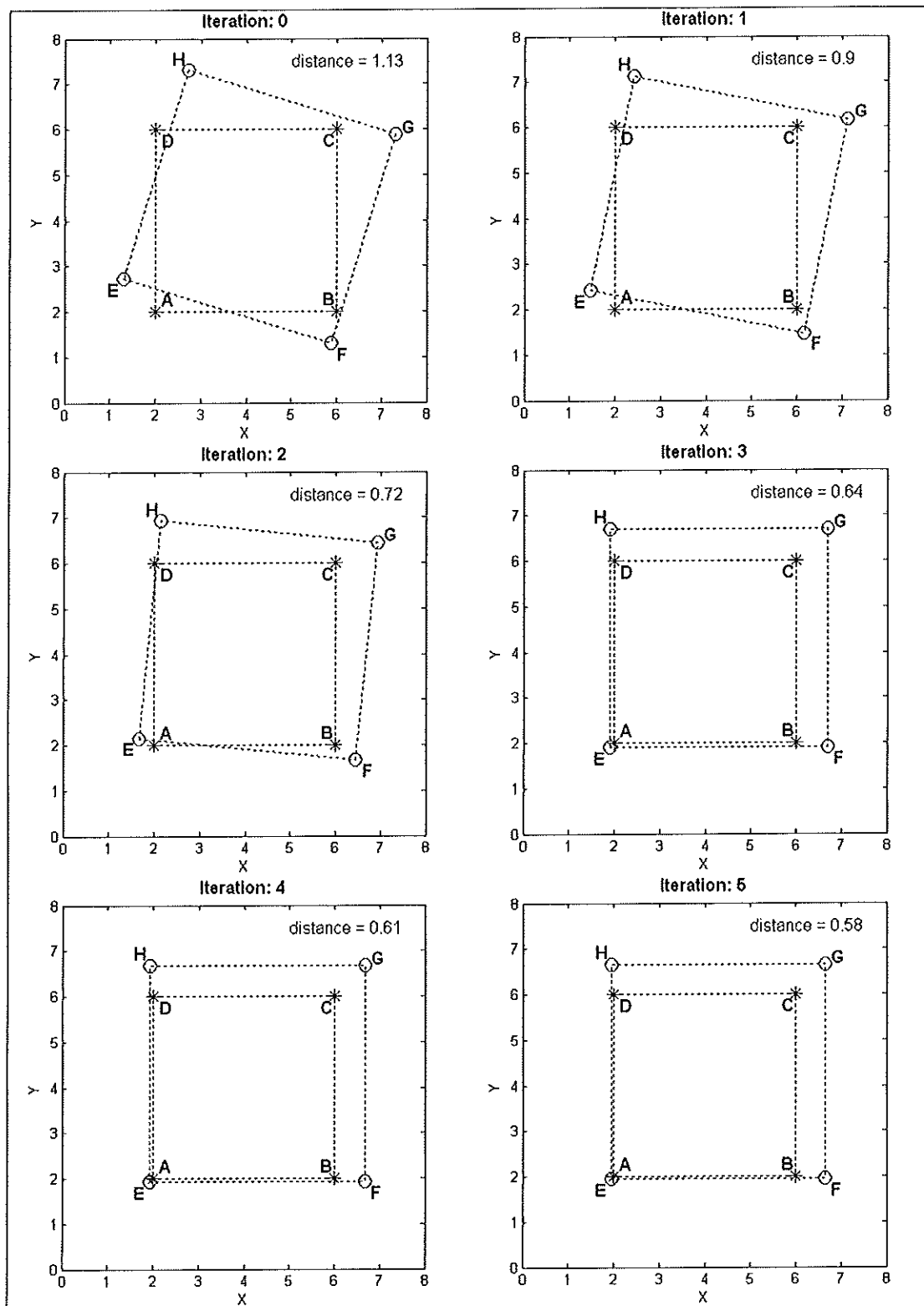


Figure A5 Progression of the ICP Algorithm Implementation from Iteration 0 to 27

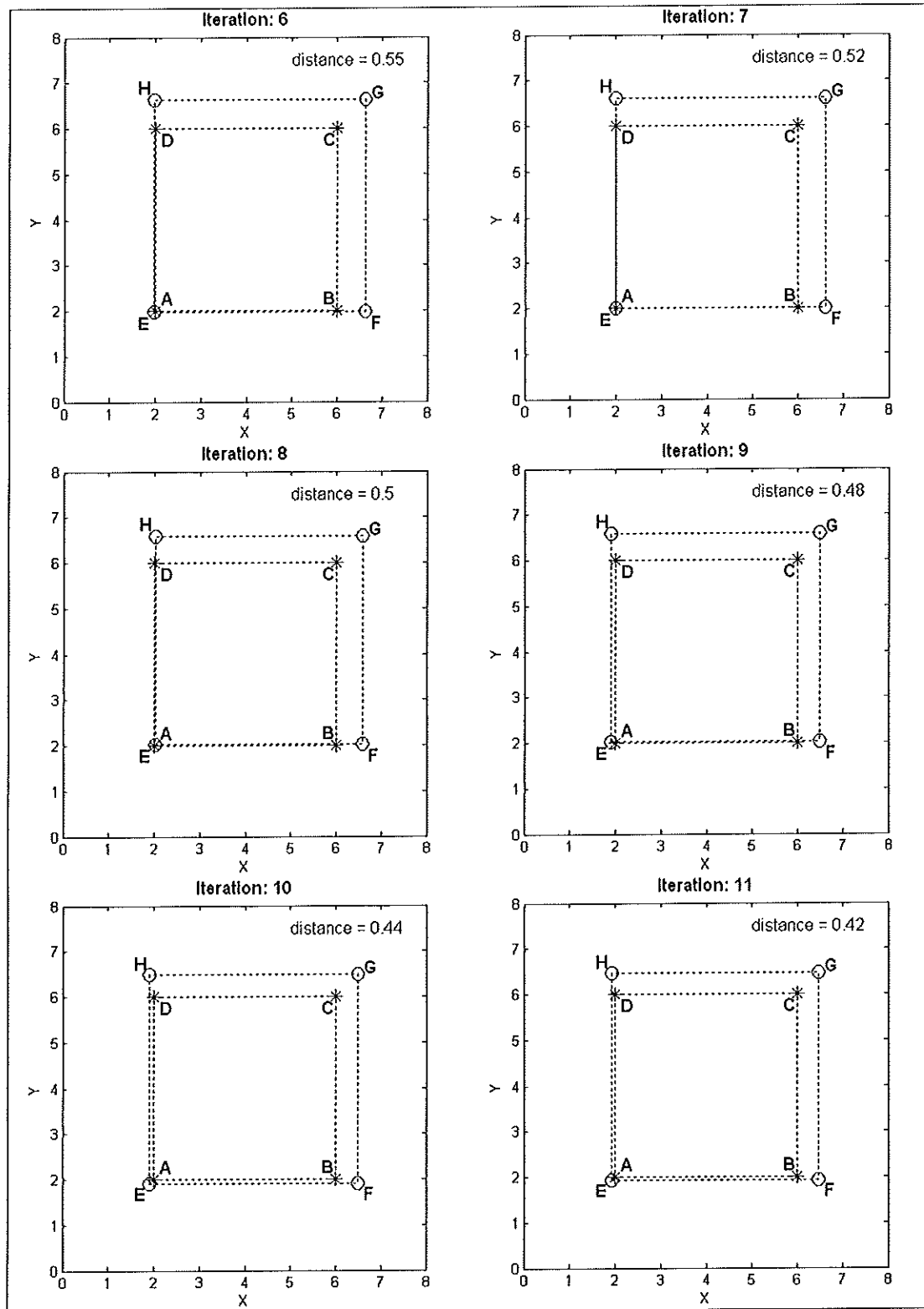


Figure A5 Progression of the ICP Algorithm Implementation from Iteration 0 to 27 (continued)

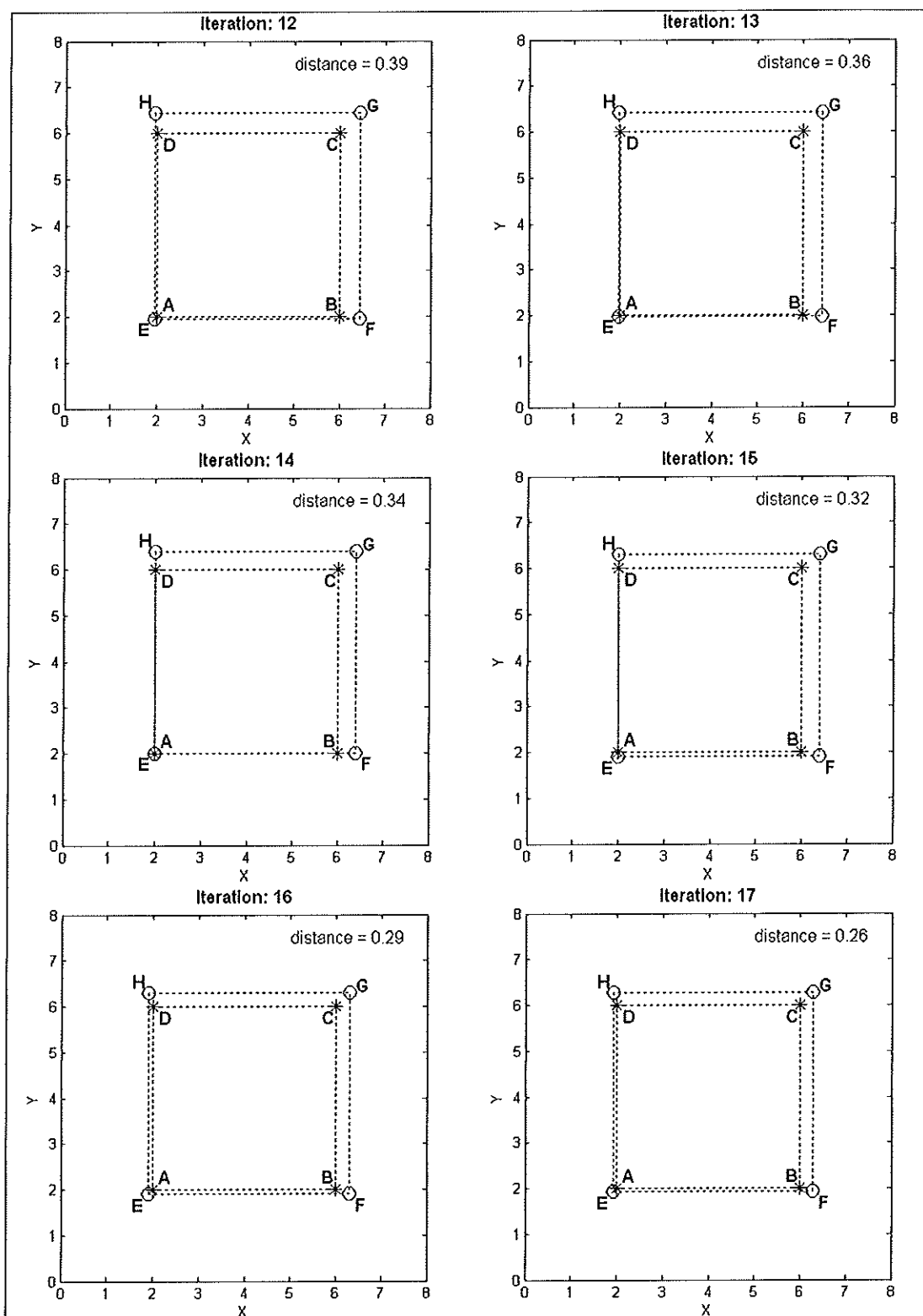


Figure A5 Progression of the ICP Algorithm Implementation from Iteration 0 to 27 (continued)

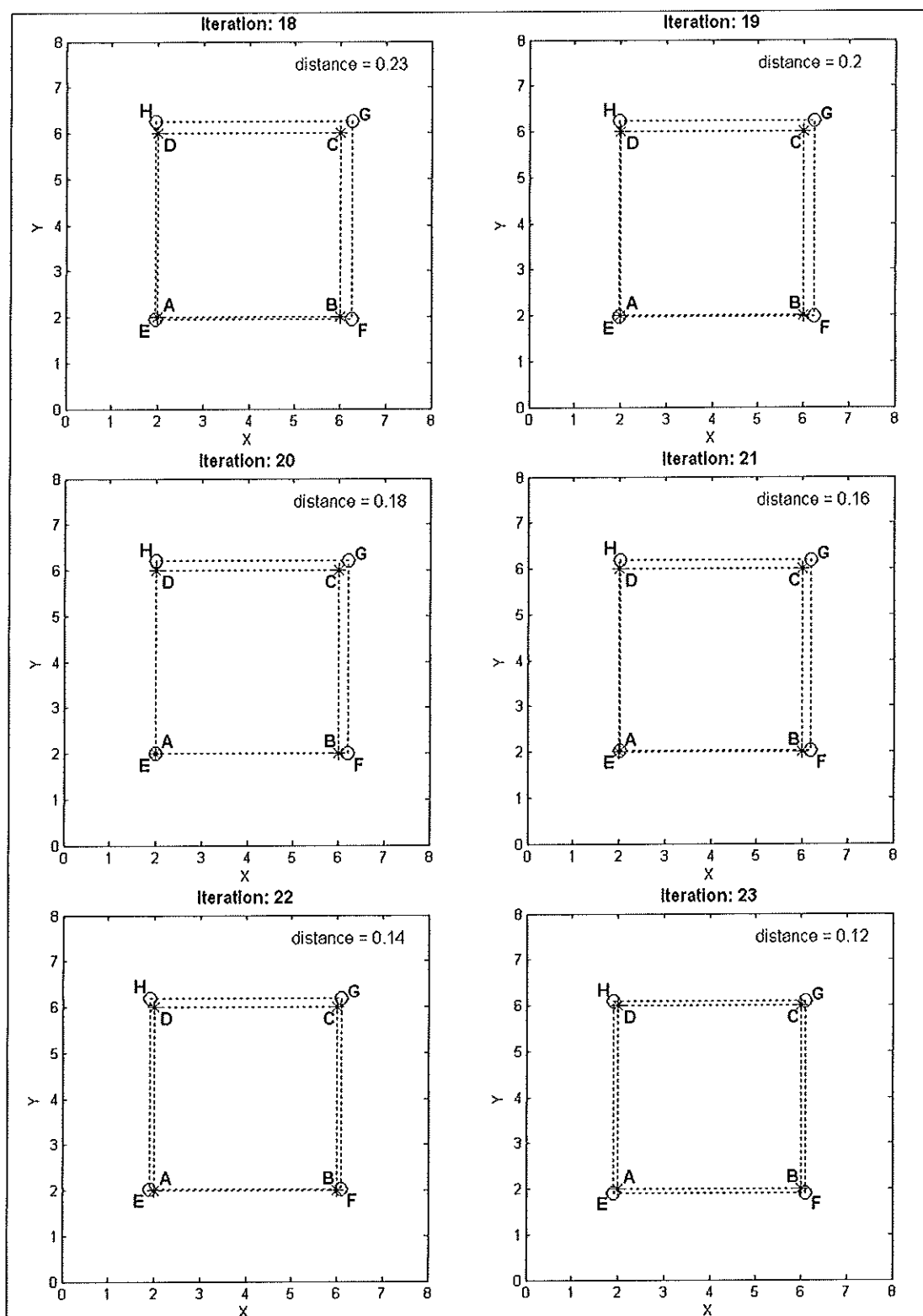


Figure A5 Progression of the ICP Algorithm Implementation from Iteration 0 to 27 (continued)

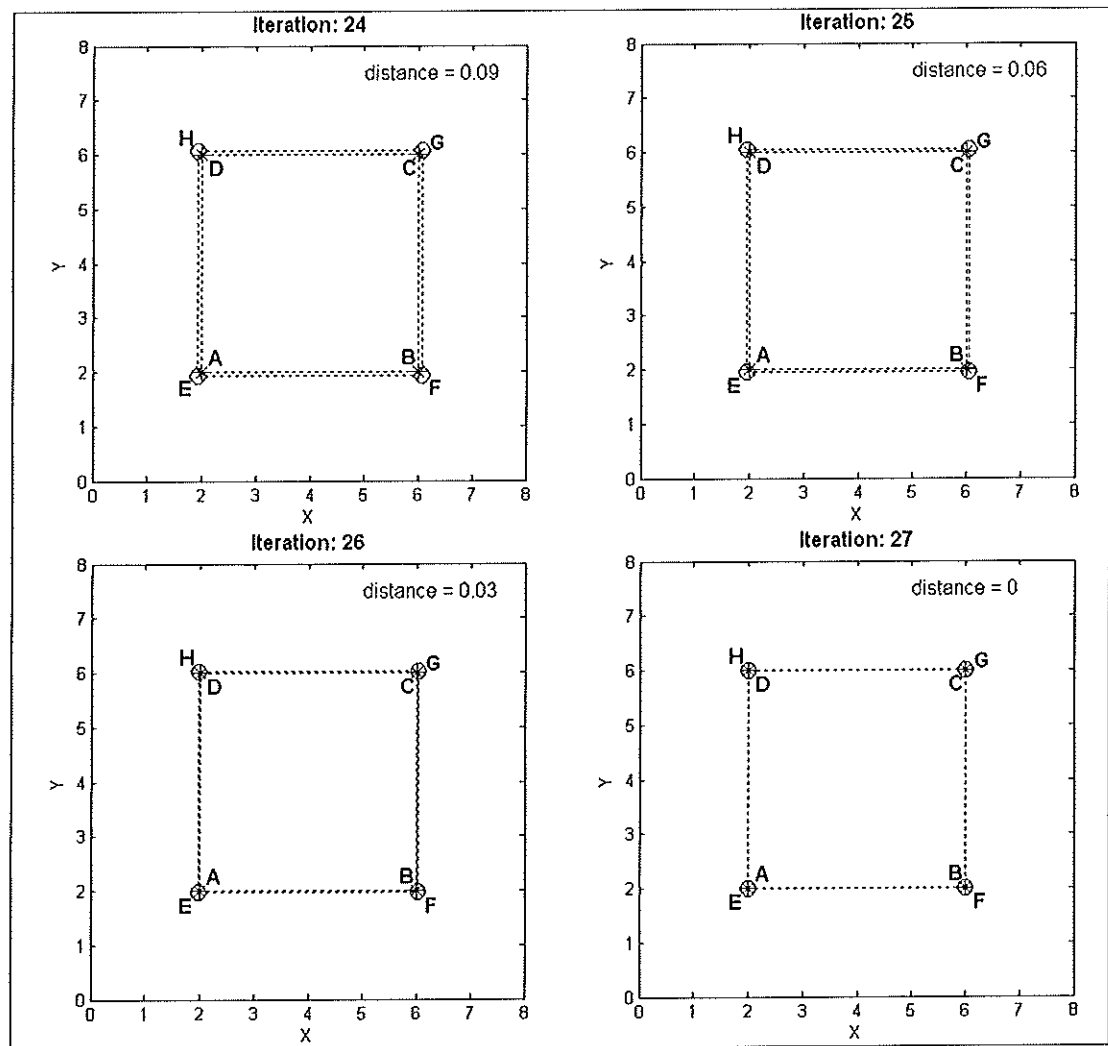


Figure A5 Progression of the ICP Algorithm Implementation from Iteration 0 to 27 (continued)

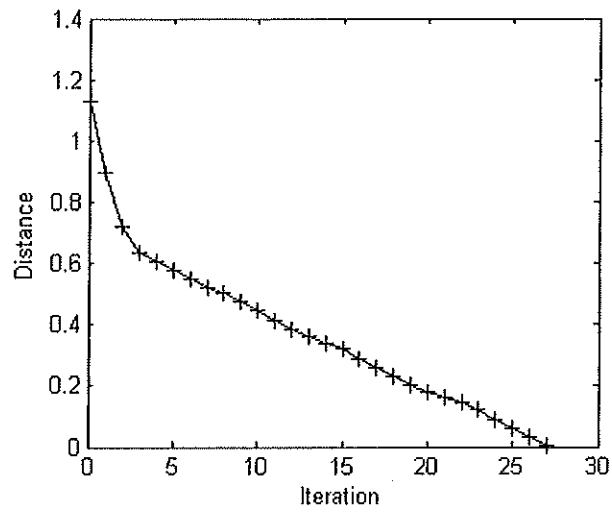


Figure A6 Progression of the ICP Algorithm Implementation from Iteration 0 to 27

Table A1 Progression of the ICP Algorithm Implementation from Iteration 0 to 27

Iteration	Distance	Iteration	Distance
0	1.13	14	0.34
1	0.90	15	0.32
2	0.72	16	0.29
3	0.64	17	0.26
4	0.61	18	0.23
5	0.58	19	0.20
6	0.55	20	0.18
7	0.52	21	0.16
8	0.50	22	0.14
9	0.48	23	0.12
10	0.44	24	0.09
11	0.42	25	0.06
12	0.39	26	0.03
13	0.36	27	0.00

APPENDIX B

FFD FORMULA DERIVATION

Free Form Deformation - FFD introduced by Sederberg and Parry (Sederberg, 2007; Sederberg & Parry, 1986; Song & Yang, 2005) is known to be a powerful shape modification method that has been applied to geometric modeling. This technique deforms an object by embedding it with in a solid defined with a control lattice. A change of the lattice deforms the solid and hence the object. FFD generally involves with 1D, 2D and also 3D data. This chapter presents the derivation of 1D, 2D and 3D FFD accordingly.

1.1 1D FFD

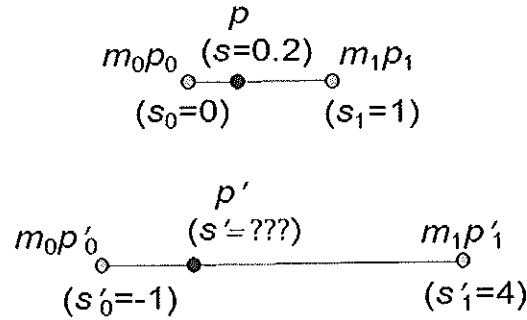


Figure B1 1D FDD, Upper: Before Deformation, Lower: After Deformation

Figure A1 shows the masses system containing two masses m_0 locates at position p_0 and m_1 locates at position p_1 . Before deformation, the position p_0 has 1D position parameter $s_0 = 0$. The position p_1 has 1D position parameter $s_1 = 1$. Let the position p is the center of mass system has 1D position parameter s . This system has to be satisfied with the center of mass equation (B.1).

$$p = (m_0 p_0 + m_1 p_1) / (m_0 + m_1) \quad (\text{B.1})$$

From (B.1), since there is only one position parameter we can rewrite (B.1) to (B.2) this way:

$$s = (m_0 s_0 + m_1 s_1) / (m_0 + m_1) \quad (\text{B.2})$$

Let the sum of masses in the system is equal to one as follow:

$$m_0 + m_1 = 1 \quad (\text{B.3})$$

Hence $s_0 = 0$ and $s_1 = 1$, solving (B.2) from (B.3) gives the solutions

$$m_0 = 1 - s$$

$$m_1 = s$$

The deformation makes two control points move, p_0 moves to p'_0 and p_1 moves to p'_1 . We have to find the new position p' for old position p after the deformation of control point. The mass system has to be satisfied with (B.4) after the deformation.

$$p' = (m_0 p'_0 + m_1 p'_1) / (m_0 + m_1) \quad (\text{B.4})$$

From (B.4), since there is only one position parameter we can rewrite (B.4) to (B.5) this way:

$$s' = (m_0 s'_0 + m_1 s'_1) / (m_0 + m_1) \quad (\text{B.5})$$

Hence $m_0 = 1 - s$ and $m_1 = s$, solving (B.5) gives the solution

$$s' = (1 - s)s'_0 + ss'_1 \quad (\text{B.6})$$

Equation (B.6) is the formula of 1D FFD. The example computation of position p' locates at s' after the deformation in Figure B.1 using 1D FFD formula is as follow:

$$\begin{aligned} s' &= (1 - 0.2)(-1) + (0.2)(4) \\ &= (-0.8) + (0.8) \\ &= 0 \end{aligned}$$

1.2 2D FFD

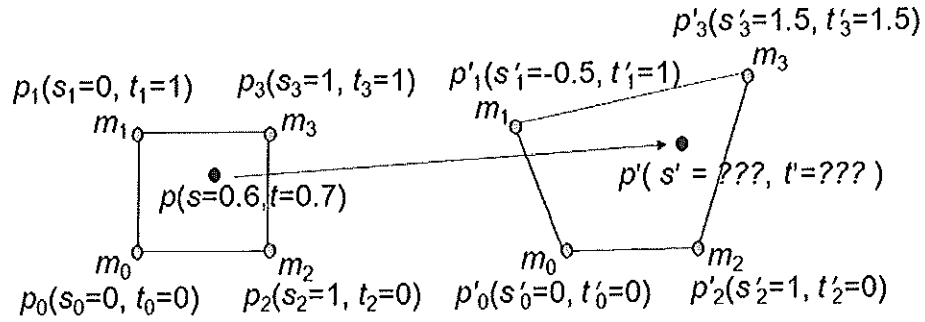


Figure B2 2D FFD, left column: before deformation, right column: after deformation

Figure B2 shows the masses system containing four masses m_0 , m_1 , m_2 and m_3 locate at position p_0 , p_1 , p_2 and p_3 accordingly. Let the position p is the center of masses system has 2D position parameter s and t . This system has to be satisfied with the center of mass equation in two dimensions (see Equation (B.7) and Equation (B.8)).

$$s = (m_0 s_0 + m_1 s_1 + m_2 s_2 + m_3 s_3) / (m_0 + m_1 + m_2 + m_3) \quad (\text{B.7})$$

$$t = (m_0 t_0 + m_1 t_1 + m_2 t_2 + m_3 t_3) / (m_0 + m_1 + m_2 + m_3) \quad (\text{B.8})$$

Let the sum of masses in the system is equal to one as follow:

$$m_0 + m_1 + m_2 + m_3 = 1 \quad (\text{B.9})$$

Let (B.10) presents the relation between four masses. This equation also called mass balance equation.

$$m_0 m_3 = m_1 m_2 \quad (\text{B.10})$$

Hence $s_0 = 0$, $s_1 = 0$, $s_2 = 1$ and $s_3 = 1$ solving (B.7) from (B.9) gives the solution

$$s = m_2 + m_3 \quad (\text{B.11})$$

Hence $t_0 = 0$, $t_1 = 1$, $t_2 = 0$ and $t_3 = 1$ solving (B.8) from (B.9) gives the solution

$$t = m_1 + m_3 \quad (\text{B.12})$$

In this step we substitute (B.11) in (B.9), we thus obtain

$$1 - s = m_0 + m_1 \quad (\text{B.13})$$

In this step we substitute (B.12) in (B.9), we thus obtain

$$1 - t = m_0 + m_2 \quad (\text{B.14})$$

Then multiply (B.13) with (B.14) gives the solution

$$\begin{aligned} (m_0 + m_1)(m_0 + m_2) &= (1 - s)(1 - t) \\ m_0m_0 + m_0m_2 + m_0m_1 + m_1m_2 &= (1 - s)(1 - t) \end{aligned}$$

Consider (B.10) we obtain

$$\begin{aligned} m_0m_0 + m_0m_2 + m_0m_1 + m_0m_3 &= (1 - s)(1 - t) \\ m_0(m_0 + m_1 + m_2 + m_3) &= (1 - s)(1 - t) \end{aligned}$$

Consider (B.9) we obtain

$$m_0 = (1 - s)(1 - t)$$

We can find m_1 in the same manner. Starting from multiplication (B.12) and (B.13)

$$\begin{aligned} (m_0 + m_1)(m_1 + m_3) &= (1 - s)t \\ m_0m_1 + m_0m_3 + m_1m_1 + m_1m_3 &= (1 - s)t \\ m_0m_1 + m_1m_2 + m_1m_1 + m_1m_3 &= (1 - s)t \\ m_1(m_0 + m_1 + m_2 + m_3) &= (1 - s)t \\ m_1 &= (1 - s)t \end{aligned}$$

We can find m_2 in the same manner. Starting from multiplication (B.11) and (B.14)

$$\begin{aligned}
(m_2 + m_3)(m_0 + m_2) &= s(1 - t) \\
m_0m_2 + m_2m_2 + m_0m_3 + m_2m_3 &= s(1 - t) \\
m_0m_2 + m_2m_2 + m_1m_2 + m_2m_3 &= s(1 - t) \\
m_2(m_0 + m_1 + m_2 + m_3) &= s(1 - t) \\
m_2 &= s(1 - t)
\end{aligned}$$

We can find m_3 in the same manner. Starting from multiplication (B.11) and (B.12)

$$\begin{aligned}
(m_2 + m_3)(m_1 + m_3) &= st \\
m_1m_2 + m_2m_3 + m_1m_3 + m_3m_3 &= st \\
m_0m_3 + m_2m_3 + m_1m_3 + m_3m_3 &= st \\
m_3(m_0 + m_1 + m_2 + m_3) &= st \\
m_3 &= st
\end{aligned}$$

Finally, we have all masses in form of s and t as follows:

$$\begin{aligned}
m_0 &= (1 - s)(1 - t) \\
m_1 &= (1 - s)t \\
m_2 &= s(1 - t) \\
m_3 &= st
\end{aligned}$$

After deformation, the masses system are satisfied with center of masses equation

$$\begin{aligned}
s' &= (m_0s'_0 + m_1s'_1 + m_2s'_2 + m_3s'_3) / (m_0 + m_1 + m_2 + m_3) \\
t' &= (m_0t'_0 + m_1t'_1 + m_2t'_2 + m_3t'_3) / (m_0 + m_1 + m_2 + m_3)
\end{aligned}$$

Hence the sum of all masses is equal to one, so we obtain

$$\begin{aligned}
s' &= m_0s'_0 + m_1s'_1 + m_2s'_2 + m_3s'_3 \\
t' &= m_0t'_0 + m_1t'_1 + m_2t'_2 + m_3t'_3
\end{aligned}$$

The two equations above are the formula of 2D FFD. The example computation of position p' locates at (s', t') after the deformation in Figure B2 using 2D FFD formula is as follow:

$$s' = m_0 s'_0 + m_1 s'_1 + m_2 s'_2 + m_3 s'_3$$

$$s' = (1-s)(1-t)s'_0 + (1-s)ts'_1 + s(1-t)s'_2 + sts'_3$$

$$s' = (0) + (1-0.6)(0.7)(-0.5) + (0.6)(1-0.7)(1) + (0.6)(0.7)(1.5)$$

$$s' = 0.67$$

$$t' = m_0 t'_0 + m_1 t'_1 + m_2 t'_2 + m_3 t'_3$$

$$t' = (1-s)(1-t)t'_0 + (1-s)tt'_1 + s(1-t)t'_2 + stt'_3$$

$$t' = (0) + (1-0.6)(0.7)(1) + (0.6)(1-0.7)(0) + (0.6)(0.7)(1.5)$$

$$t' = 0.91$$

1.3 3D FFD

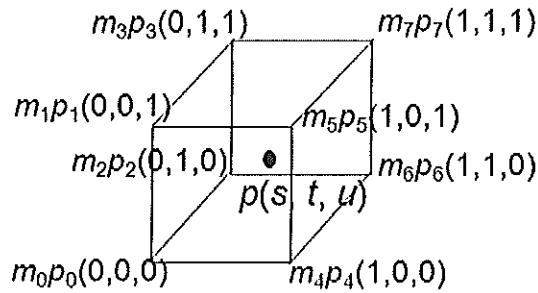


Figure B3 3D Masses System

Figure B3 shows the masses system containing eight masses m_0 through m_7 locates at position p_0 through p_7 accordingly. Let the position p is the center of mass system has 3D position parameter s , t and u . The control points p_i locate at coordinate (s_i, t_i, u_i) . This system has to be satisfied with the center of mass equation as follow:

$$p = \frac{\sum_{i=0}^7 m_i p_i}{\sum_{i=0}^7 m_i} \quad (\text{B.15})$$

Let the summation of all masses is equal to one and split (B.15) into three equations in three directions obtain

$$m_0 + m_1 + m_2 + m_3 + m_4 + m_5 + m_6 + m_7 = 1 \quad (\text{B.16})$$

$$s = \sum_{i=0}^7 m_i s_i \quad (\text{B.17})$$

$$t = \sum_{i=0}^7 m_i t_i \quad (\text{B.18})$$

$$u = \sum_{i=0}^7 m_i u_i \quad (\text{B.19})$$

Substituting s_i , t_i and u_i from Figure A3 into (B.17), (B.18) and (B.19) accordingly gives

$$m_4 + m_5 + m_6 + m_7 = s \quad (\text{B.20})$$

$$m_2 + m_3 + m_6 + m_7 = t \quad (\text{B.21})$$

$$m_1 + m_3 + m_5 + m_7 = u \quad (\text{B.22})$$

Substituting (B.20) into (B.16) gives

$$m_0 + m_1 + m_2 + m_3 = 1 - s \quad (\text{B.23})$$

Substituting (B.21) into (B.16) gives

$$m_0 + m_1 + m_4 + m_5 = 1 - t \quad (\text{B.24})$$

Substituting (B.22) into (B.16) gives

$$m_0 + m_2 + m_4 + m_6 = 1 - u \quad (\text{B.25})$$

At this step, there are the mass balance equations as follows:

$$m_0 m_3 = m_1 m_2, m_0 m_5 = m_1 m_4, m_0 m_6 = m_2 m_4,$$

$$m_2 m_7 = m_3 m_6, m_1 m_7 = m_3 m_5, m_4 m_7 = m_5 m_6,$$

$$m_0 m_7 = m_1 m_6 = m_2 m_5 = m_3 m_4$$

Multiplying (B.23) \times (B.24) \times (B.25) gives

$$(1-s)(1-t)(1-u) = (m_0+m_1+m_2+m_3)(m_0+m_1+m_4+m_5)(m_0+m_2+m_4+m_6) \quad (\text{B.26})$$

Expanding the multiplication and consider the masses balance equation gives

$$\begin{aligned}
(1-s)(1-t)(1-u) = & m_0(m_0 + m_1 + m_2 + m_3 + m_4 + m_5 + m_6 + m_7) + \\
& m_1(m_0 + m_1 + m_2 + m_3 + m_4 + m_5 + m_6 + m_7) + \\
& m_2(m_0 + m_1 + m_2 + m_3 + m_4 + m_5 + m_6 + m_7) + \\
& m_3(m_0 + m_1 + m_2 + m_3 + m_4 + m_5 + m_6 + m_7) + \\
& m_4(m_0 + m_1 + m_2 + m_3 + m_4 + m_5 + m_6 + m_7) + \\
& m_5(m_0 + m_1 + m_2 + m_3 + m_4 + m_5 + m_6 + m_7) + \\
& m_6(m_0 + m_1 + m_2 + m_3 + m_4 + m_5 + m_6 + m_7) + \\
& m_7(m_0 + m_1 + m_2 + m_3 + m_4 + m_5 + m_6 + m_7)
\end{aligned}$$

Consider (B.16) we have

$$m_0 = (1-s)(1-t)(1-u)$$

At this step, we can find m_1 through m_7 in the same manner, finally we have

$$m_1 = (1-s)(1-t)u$$

$$m_2 = (1-s)t(1-u)$$

$$m_3 = (1-s)tu$$

$$m_4 = s(1-t)(1-u)$$

$$m_5 = s(1-t)u$$

$$m_6 = st(1-u)$$

$$m_7 = stu$$

After the deformation the masses system has to be satisfied with center of masses equation

$$p' = \frac{\sum_{i=0}^7 m_i p'_i}{\sum_{i=0}^7 m_i} \quad (\text{B.27})$$

Hence the summation of all masses is equal to one and all point has three dimensional coordinate, splitting (B.27) into three equations and using value of m_0 through m_7 gives the 3D FFD formula as follows:

$$s' = (1-s)(1-t)(1-u)s'_0 + (1-s)(1-t)us'_1 + (1-s)t(1-u)s'_2 + \\ (1-s)tus'_3 + s(1-t)(1-u)s'_4 + s(1-t)us'_5 + st(1-u)s'_6 + stus'_7$$

$$t' = (1-s)(1-t)(1-u)t'_0 + (1-s)(1-t)ut'_1 + (1-s)t(1-u)t'_2 + \\ (1-s)tut'_3 + s(1-t)(1-u)t'_4 + s(1-t)ut'_5 + st(1-u)t'_6 + stut'_7$$

$$u' = (1-s)(1-t)(1-u)u'_0 + (1-s)(1-t)uu'_1 + (1-s)t(1-u)u'_2 + \\ (1-s)tuu'_3 + s(1-t)(1-u)u'_4 + s(1-t)uu'_5 + st(1-u)u'_6 + stuu'_7$$

These above three equations are the 3D FFD formula to find the new position p' at coordinate (s', t', u') from old position p at coordinate (s, t, u) due to the relocation of all control points from old positions p_0 at coordinate (s_0, t_0, u_0) through p_7 at coordinate (s_7, t_7, u_7) to new positions p'_0 at coordinate (s'_0, t'_0, u'_0) through p'_7 at coordinate (s'_7, t'_7, u'_7) .

APPENDIX C

DEMONSTRATION OF ABSOLUTE ERROR CALCULATION BETWEEN TWO CYLINDRICAL PROJECTION SURFACES

As mentioned in Chapter 3, in order to compare skull and face, the 3D head models have to be transformed onto the plane using a cylindrical projection. The advantage of cylindrical projection is the convenient to compute absolute error between two 3D surfaces which can be directly computed from the different of the intensity from each corresponded pixel. Figure C1 shows the absolute errors of cylindrical projection surfaces. In Figure C1, upper row shows the comparison between two skulls, lower row shows the comparison between two faces.

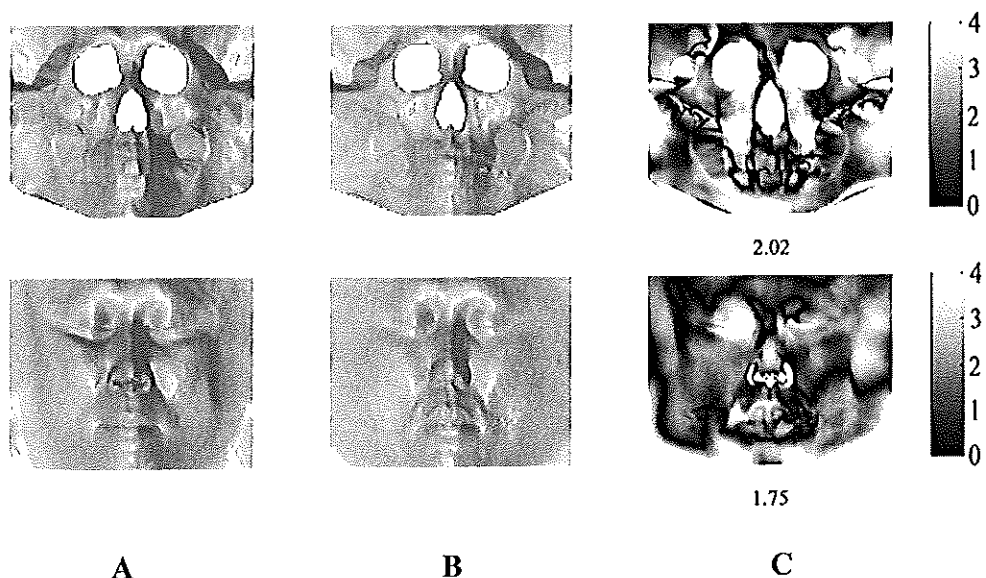


Figure C1 Absolute Errors of Cylindrical Projection Surfaces Upper Row: The Comparison Between Two Skulls, Lower Row: The Comparison Between Two Faces (A) Target Head (B) Reference Head (C) Absolute Errors Surface when Compare Reference Head to Target Head. Errors are Measured in mm.

The calculation of absolute errors of cylindrical projection surfaces is presented in Figure C2. Figure C2A is the target skull. Figure C2B is the reference skull. Figure C2C is the absolute errors surface when compare target skull to reference skull. The pixel value in the white rectangle areas are presented in the left column. Absolute error between two surfaces can be directly computed from the different of the pixel value from each corresponded pixel as presented in Equation C1

$$C_{ij} = |A_{ij} - B_{ij}| \quad (C.1)$$

Where C_{ij} is the pixel value of image C at row i column j which is the absolute value of different between image A and image B at row i column j . In this case, A is the target head and B is the reference head.

The averaging of absolute error gives the idea of how much different between two surfaces. The calculation of this value is presented in Equation C.2.

$$C = \frac{\sum_{i=1}^M \sum_{j=1}^N C_{ij}}{M*N} \quad (C.2)$$

Where M is the number of row of image C and N is the number of column of image C .

From Figure C2C, the darker pixels indicate the lower errors and the brighter pixels indicate the higher errors. Presenting this way gives the idea of where and how different between two surfaces. The value 2.02 is the average value of all absolute errors giving the overall difference information.

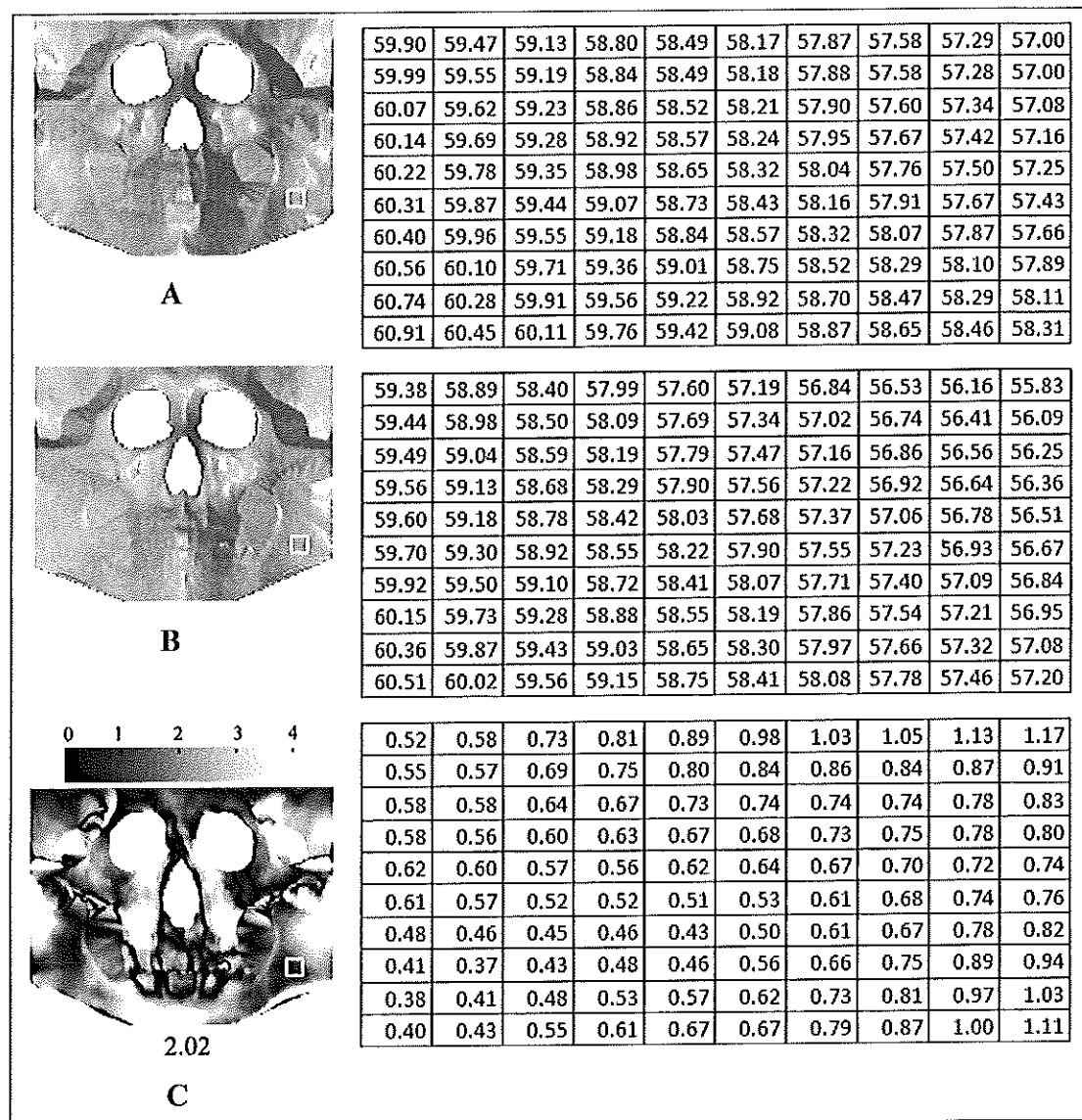


Figure C2 Calculation of Absolute Errors of Cylindrical Projection Surfaces. (A) Target Skull (B) Reference Skull (C) Absolute Errors Surface when Compare Target Skull to Reference Skull. Errors are Measured in mm.

APPENDIX D

THE EVALUATION OF NOSE PROFILE ESTIMATION FROM NASAL APERTURE FOR THAI PEOPLE

In Chapter 3, we mentioned about nose profile estimation from nasal aperture in order to compare the two cylindrical projection surfaces of skull at the nasal part. Because there is less information from nasal aperture, so we have to estimate the nose profile to provide more information for comparing purpose. Figure D1 shows the nose profile estimation method used in this work which was based on the work of Prokobec and Ubelaker (2002). From Figure D1, line A dissects the nasion and prosthion. Line B is parallel to line A and intersects the foremost point on the nasal bone. For each point of nasal aperture, the distance d from line B to the nasal aperture are calculated and mirrored to form the nasal profile estimation.

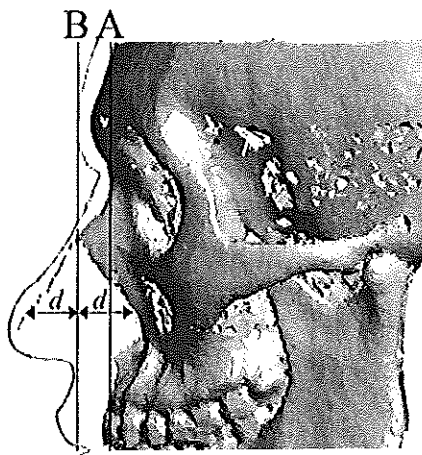


Figure D1 Nose Profile Estimation from Nasal Aperture. Line A Dissects the Nasion and Prosthion. Line B is Parallel to Line A and Intersects the Foremost Point on the Nasal Bone. For Each Point of Nasal Aperture, the Distance From Line B to the Nasal Aperture are Calculated and Mirrored to form the Nasal Profile Estimation.

Because the purpose of this work is to reconstruct the face of Thai people but this method was originally designed for Caucasoid people, so we have to know whether this method can be used for Thai people. Therefore, the error and the result of this method should be inspected before accepted to be used in this work. Measurement of nose profile estimation error is shown in Figure D2. The rectangle region in the left column was magnified and detail added to the right column to be clearly seen. The line with cross marked indicates the estimation line. The line with circle marked indicates the expected line. The cross and the circle are marked every vertical step of 1 mm. The error of estimation is the average value of distance between all pair of cross and circle. The results and the errors of nose profile estimation for Thai people in the head database are shown in Figure D3 to D5. The summary of all estimation errors is shown in Table D1.

As seen in Figure D3, the estimations of subject 1 and 4 were considered as good estimation both for visual inspection and for achieving estimation errors of 1.33 mm and 2.18 mm accordingly. The estimation of subject 2 was considered as slightly too high for visual inspection corresponding to the error of 2.71 mm. The estimation of subject 3 was considered as slightly too low corresponding to the error of 3.04 mm. From Figure D4, the estimation of subject 8 was considered as best estimation both for visual inspection and achieving error of 2.41 mm. The estimations of subject 5 and subject 7 were considered as slightly too low corresponding to the errors of 3.93 mm and 4.54 mm. The estimation of subject 6 was considered as slightly too high corresponding to the error of 3.45 mm. From Figure D5, the estimations of subject 9, 10, and 11 were considered as slightly too low with the errors of 4.39 mm, 7.03, and 5.09 mm accordingly. Except for the estimation of subject 10 which was the worst estimation from this experiment, others result provided acceptable nose profile estimation. Although all the results did not much accurate estimation, it anyway can give the preliminary idea of how nose of the subject should be.

In conclusion, we are pleased with nose profile estimation results from this method because the purpose of nose profile estimation here is to provide more information about nose to be compared with other skulls, not to produce exactly the same nose profile of real subject. At this point, we considered that the results from this method was met the purpose of providing additional information apart from nasal aperture. So, we accepted to use this method in this work for the nose profile estimation phase.

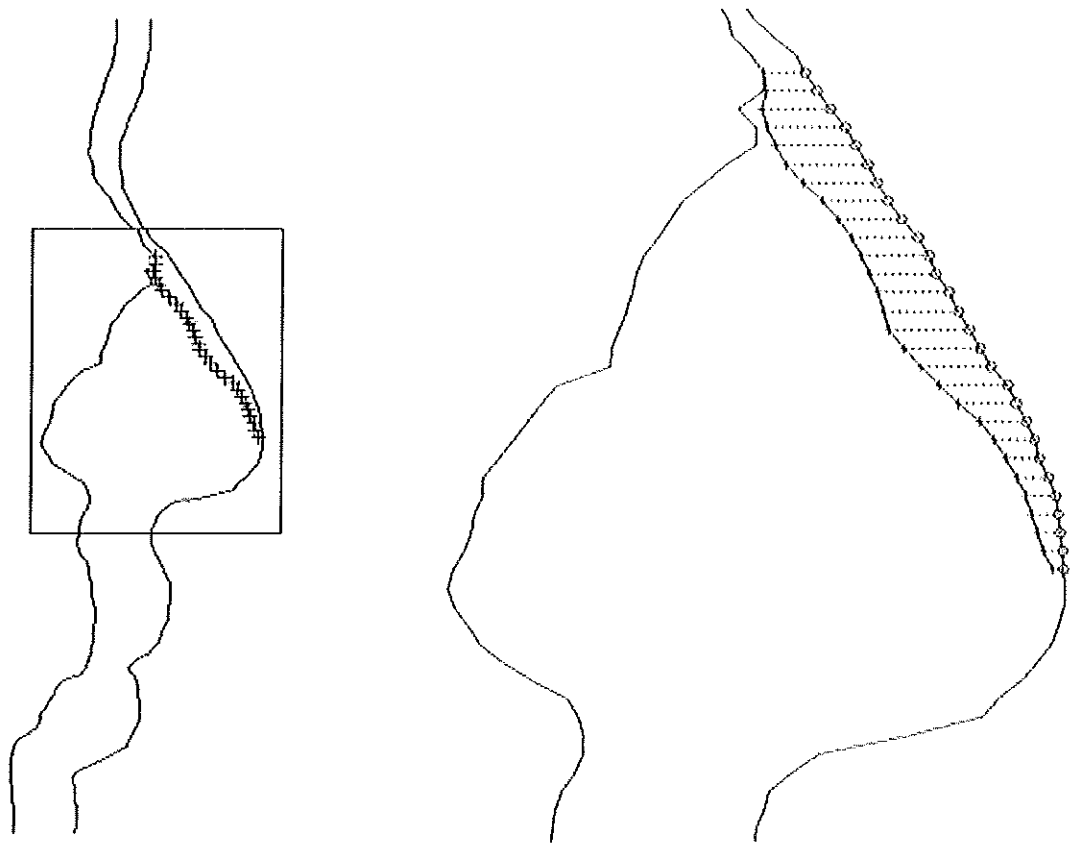


Figure D2 Measurement of Nose profile Estimation Error. The Rectangle Region in the Left Column was Magnified and Detail Added to the Right Column to be Clearly Seen. The Line with Cross Marked Indicates the Estimation Line. The Line with Circle Marked Indicates the Expected Line. The Cross and the Circle are Marked Every Vertical Step of 1 mm. The Error of Estimation is the Average Value of Distance Between all Pair of Cross and Circle.

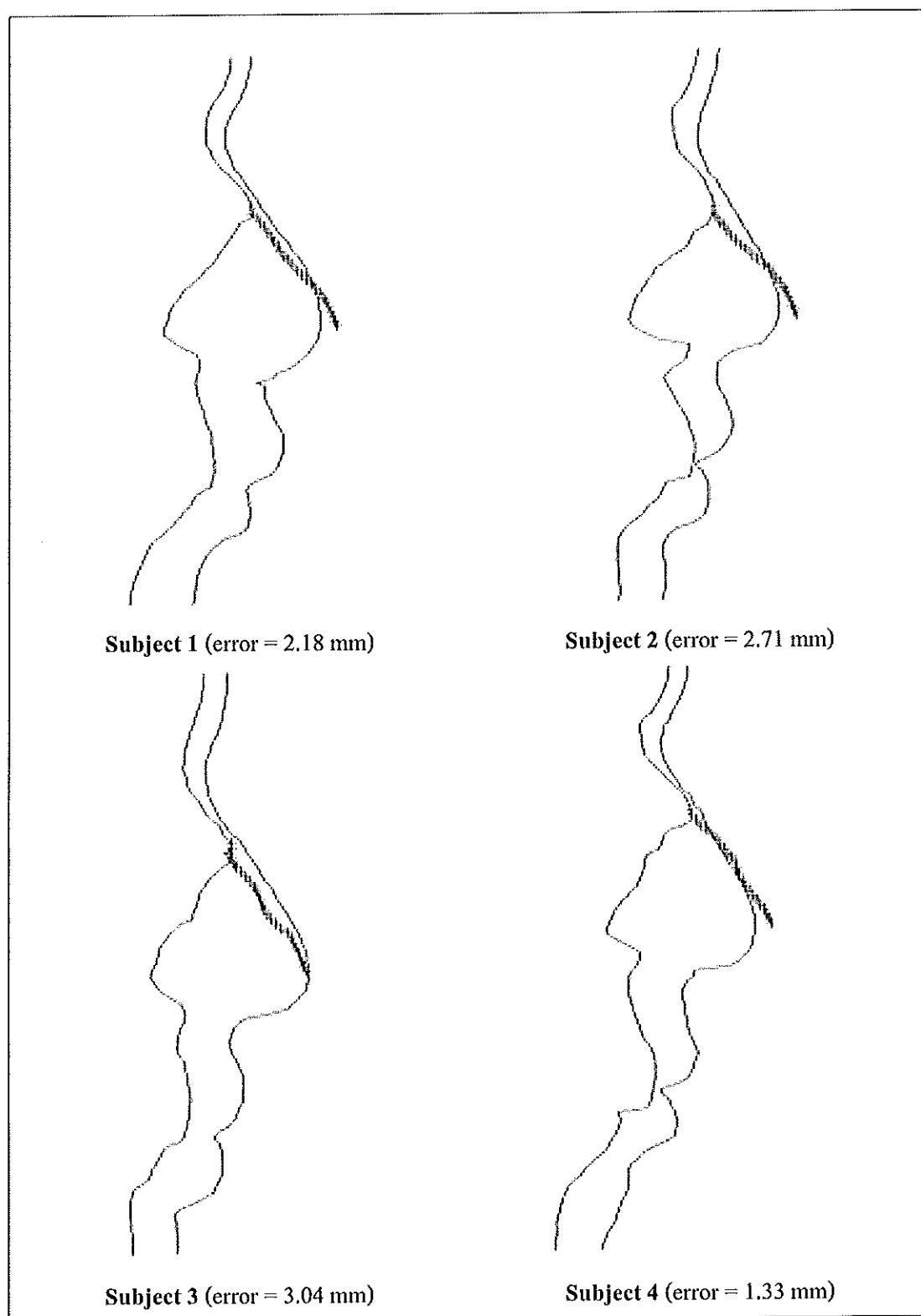


Figure D3 Nose Profile Estimation Results and Errors of Subject 1 to 4

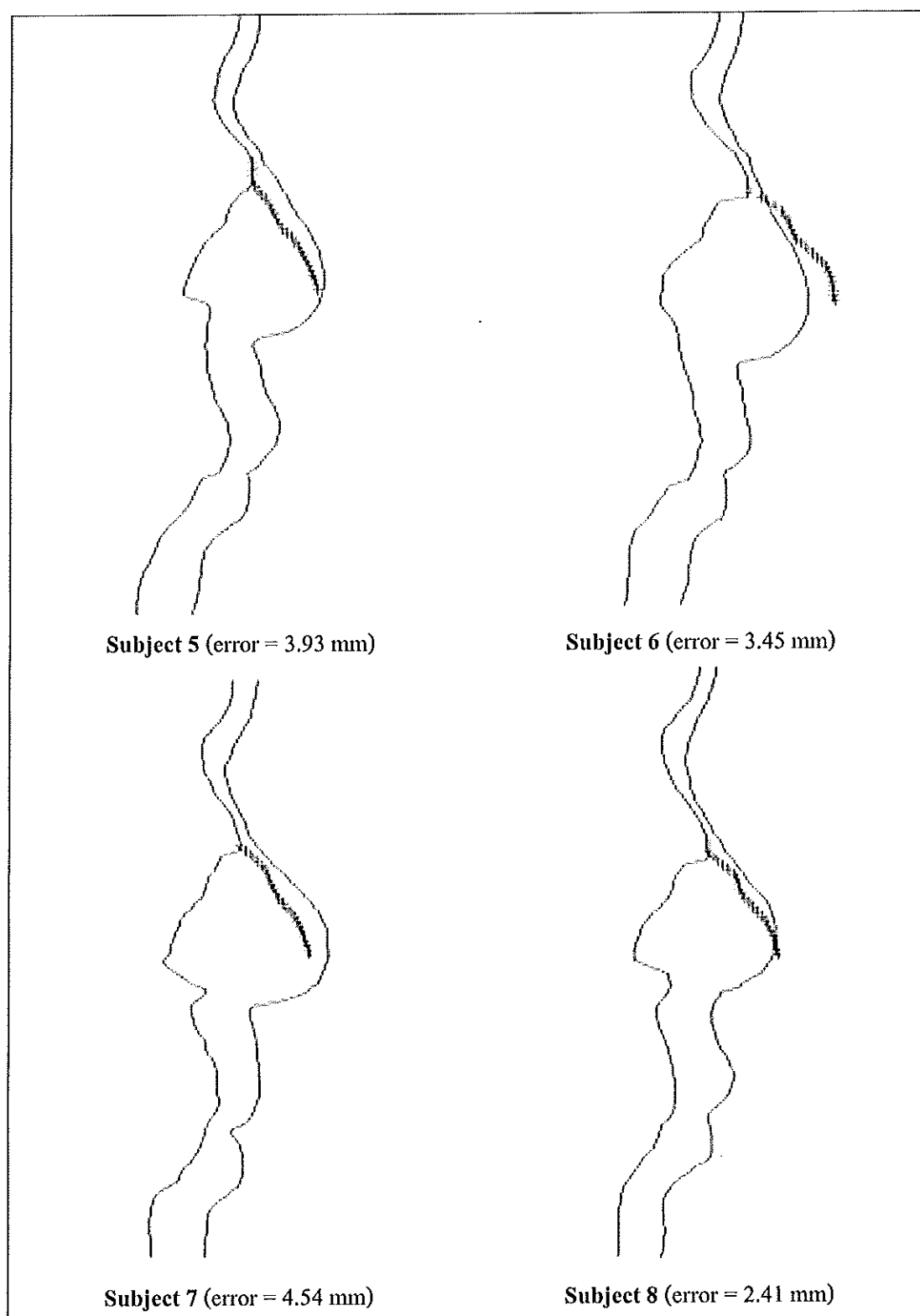


Figure D4 Nose Profile Estimation Results and Errors of Subject 5 to 8

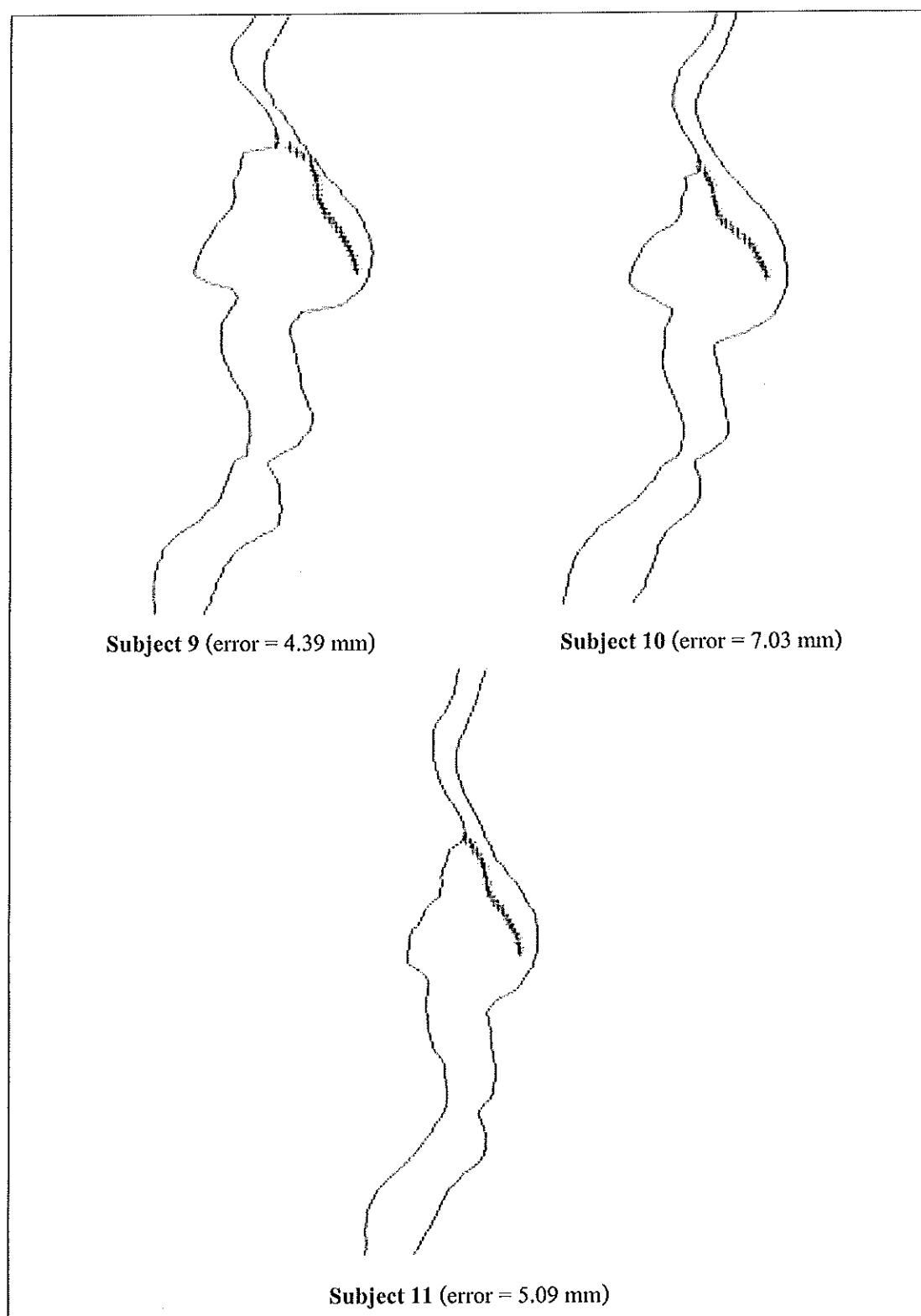


Figure D5 Nose Profile Estimation Results and Errors of Subject 9 to 11

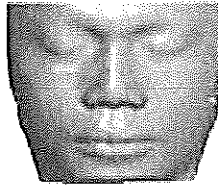
Table B1 Errors of Nose profile Estimation for Subject 1 to Subject 11

Subject	Error of nose profile estimation (mm)
1	2.18
2	2.71
3	3.04
4	1.33
5	3.93
6	3.45
7	4.54
8	2.41
9	4.39
10	7.03
11	5.09
Mean	3.64
Maximum	7.03
Minimum	1.33
Standard deviation	1.59

APPENDIX E

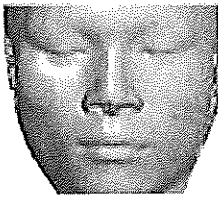
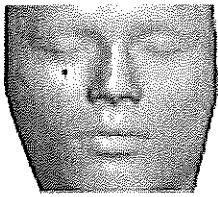
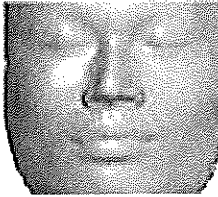
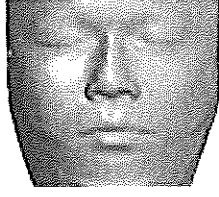
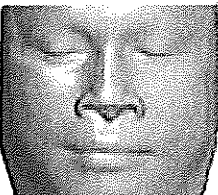
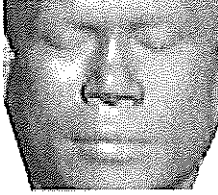
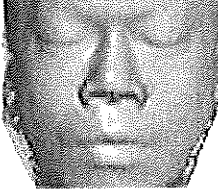
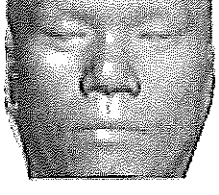
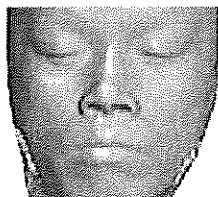
FULL SET OF FACE POOL TEST FORM

In Chapter 4, the quantitative evaluation of facial reconstruction was performed using cylindrical projection approach. However, the goal of facial reconstruction is not reconstruction accuracy but rather recognition or identification success. As mentioned in the review of Claes and coworker (2010), a more realistic and human subjective, identification process can be simulated by generating face pool test. The full set of face pool test is presented in this section. There are 11 pages in the set according to the number of the head in the head database. Top image is the reconstructed face to be identified with the faces from the face pool. The reconstructed faces in the face pool test were from Scheme II reconstruction. Face pool are a set of faces from the face database. The reference faces in the reconstruction process of the reconstructed face were excluded from the face pool. So, the number of faces in the face pool for each test face is varied between 7 and 9 faces. For example, if the number of faces in the face pool is 7 then it means that the reconstructed face uses 4 faces as reference faces for the reconstruction process. If the number of faces in the face pool is 9 then it means that the reconstructed face uses 2 faces as reference faces for the reconstruction process. There are no face pool containing 10 faces because there are no reconstructed faces that use only one face for reference face. The check mark under the face in the face pool presents the target face. The numbers of assessors who decided the faces in the face pool to be the best three matches are presented under the face in the face pool. In this case, the best match is presented by R1, the second best match is presented by R2, and the third best match is presented by R3.



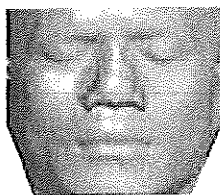
Test Face 1

Face Pool

			
√ R1(11), R2(4), R3(2)	R1(0), R2(1), R3(3)	R1(1), R2(0), R3(0)	R1(0), R2(2), R3(2)
			
R1(1), R2(1), R3(2)	R1(4), R2(5), R3(3)	R1(1), R2(2), R3(1)	R1(1), R2(4), R3(4)
			
R1(0), R2(0), R3(2)			

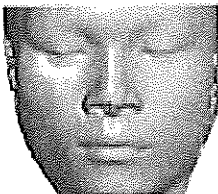
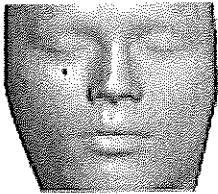
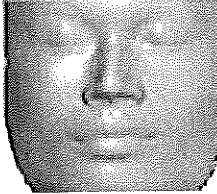
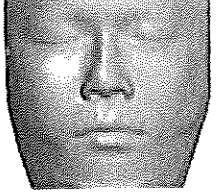
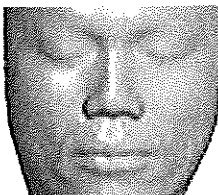

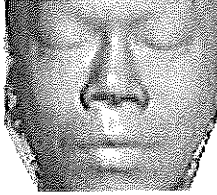
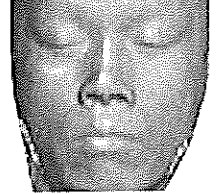
Instruction

Please look at the Test Face and then consider the faces from Face Pool. Please select the best three match faces from the Face Pool. Please indicate the rank of the match by the number 1, 2, and 3 under the face in the Face Pool.



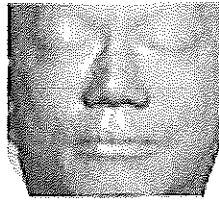
Test Face 2

Face Pool

			
R1(4), R2(4), R3(1)	$\sqrt{R1(2), R2(2), R3(3)}$	R1(0), R2(2), R3(2)	R1(0), R2(4), R3(5)
			
R1(1), R2(0), R3(5)	R1(5), R2(0), R3(2)	R1(7), R2(3), R3(0)	R1(0), R2(4), R3(1)

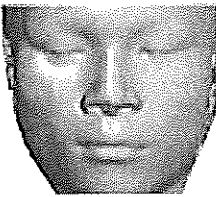
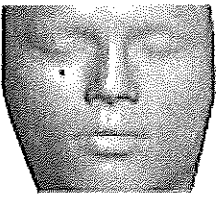
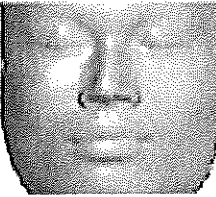
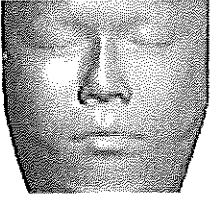
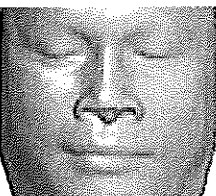
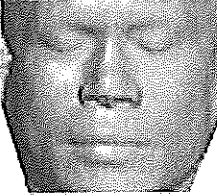
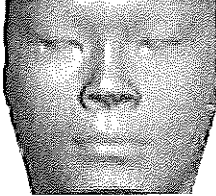
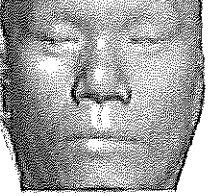
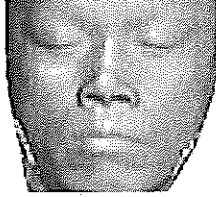
Instruction

Please look at the Test Face and then consider the faces from Face Pool. Please select the best three match faces from the Face Pool. Please indicate the rank of the match by the number 1, 2, and 3 under the face in the Face Pool.



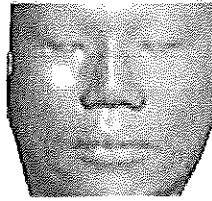
Test Face 3

Face Pool

			
R1(0), R2(0), R3(8)	R1(0), R2(0), R3(0)	$\sqrt{R1(3), R2(2), R3(2)}$	R1(6), R2(1), R3(1)
			
R1(5), R2(5), R3(2)	R1(2), R2(7), R3(2)	R1(0), R2(0), R3(0)	R1(3), R2(4), R3(4)
			
R1(0), R2(0), R3(0)			

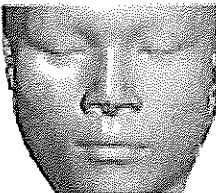
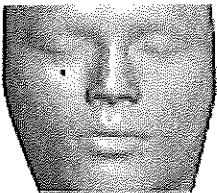

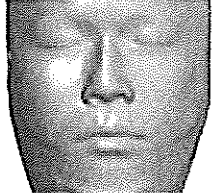
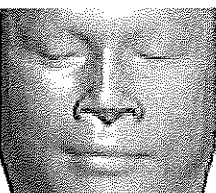
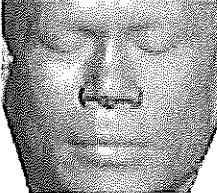

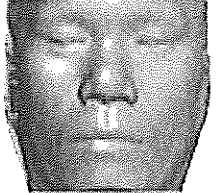
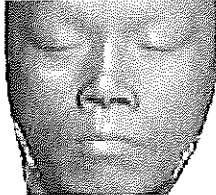
Instruction

Please look at the Test Face and then consider the faces from Face Pool. Please select the best three match faces from the Face Pool. Please indicate the rank of the match by the number 1, 2, and 3 under the face in the Face Pool.



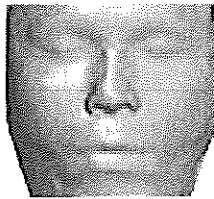
Test Face 4

Face Pool

			
R1(1), R2(4), R3(2)	R1(0), R2(1), R3(1)	R1(0), R2(1), R3(1)	✓ R1(3), R2(7), R3(4)
			
R1(0), R2(2), R3(1)	R1(4), R2(0), R3(5)	R1(0), R2(0), R3(1)	R1(10), R2(2), R3(1)
			
R1(1), R2(2), R3(3)			

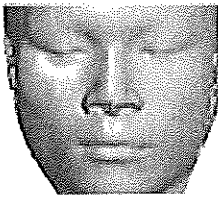
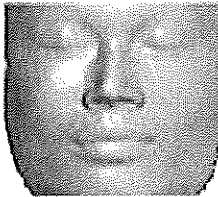
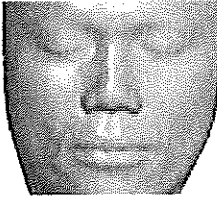
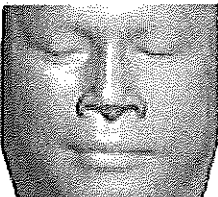
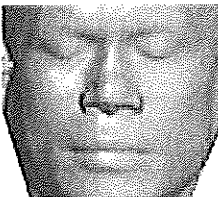
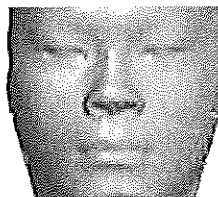
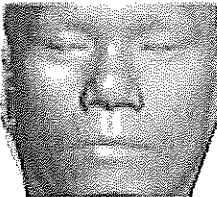
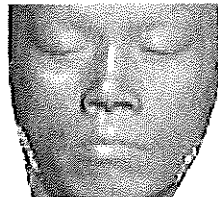
Instruction

Please look at the Test Face and then consider the faces from Face Pool. Please select the best three match faces from the Face Pool. Please indicate the rank of the match by the number 1, 2, and 3 under the face in the Face Pool.



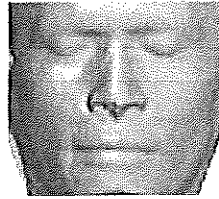
Test Face 5

Face Pool

			
R1(5), R2(3), R3(3)	R1(0), R2(0), R3(1)	✓ R1(7), R2(3), R3(3)	R1(1), R2(1), R3(0)
			
R1(0), R2(3), R3(1)	R1(2), R2(4), R3(5)	R1(3), R2(3), R3(1)	R1(1), R2(2), R3(5)

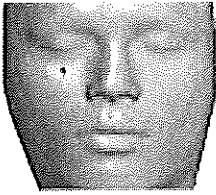
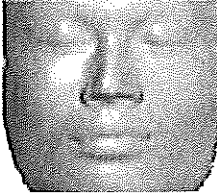
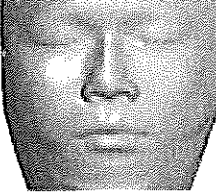
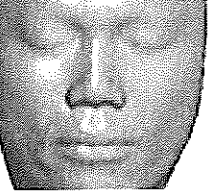
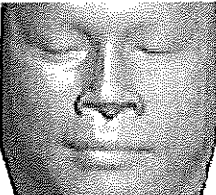
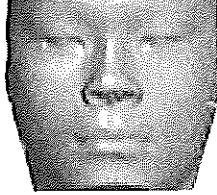
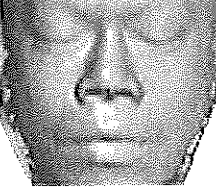
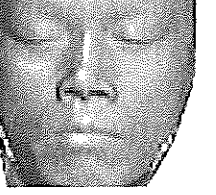
Instruction

Please look at the Test Face and then consider the faces from Face Pool. Please select the best three match faces from the Face Pool. Please indicate the rank of the match by the number 1, 2, and 3 under the face in the Face Pool.



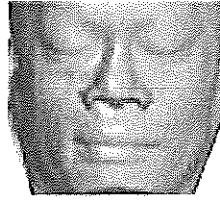
Test Face 6

Face Pool

			
R1(0), R2(1), R3(2)	R1(0), R2(1), R3(0)	R1(3), R2(5), R3(4)	R1(4), R2(5), R3(5)
			
✓ R1(2), R2(2), R3(2)	R1(0), R2(0), R3(3)	R1(10), R2(4), R3(0)	R1(0), R2(1), R3(3)

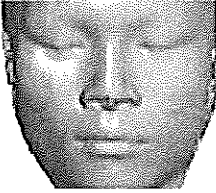
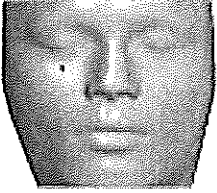

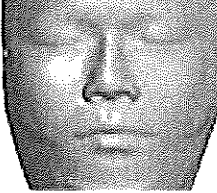
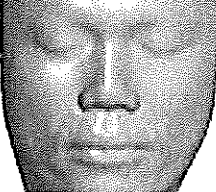
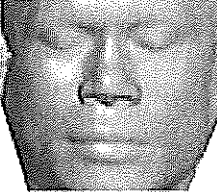

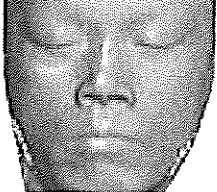
Instruction

Please look at the Test Face and then consider the faces from Face Pool. Please select the best three match faces from the Face Pool. Please indicate the rank of the match by the number 1, 2, and 3 under the face in the Face Pool.



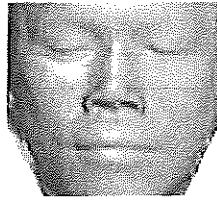
Test Face 7

Face Pool

			
R1(5), R2(5), R3(3)	R1(1), R2(0), R3(0)	R1(0), R2(0), R3(5)	R1(2), R2(4), R3(0)
			
R1(3), R2(5), R3(4)	✓ R1(7), R2(4), R3(4)	R1(0), R2(0), R3(0)	R1(1), R2(1), R3(3)

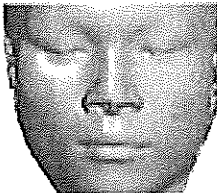
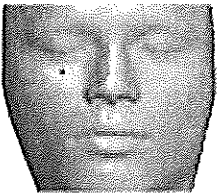
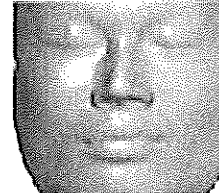
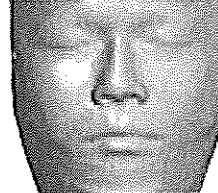
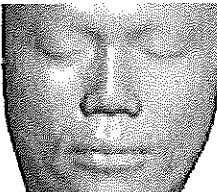
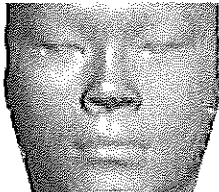

Instruction

Please look at the Test Face and then consider the faces from Face Pool. Please select the best three match faces from the Face Pool. Please indicate the rank of the match by the number 1, 2, and 3 under the face in the Face Pool.



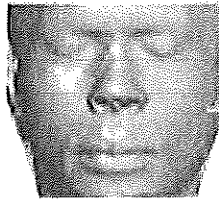
Test Face 8

Face Pool

			
R1(9), R2(1), R3(2)	R1(1), R2(1), R3(1)	R1(0), R2(0), R3(3)	R1(0), R2(4), R3(5)
			
R1(2), R2(4), R3(5)	✓ R1(2), R2(3), R3(0)	R1(5), R2(6), R3(3)	

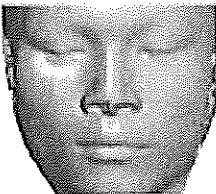
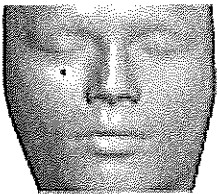

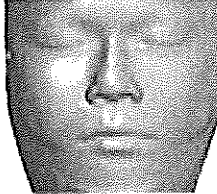

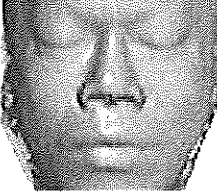
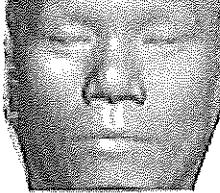
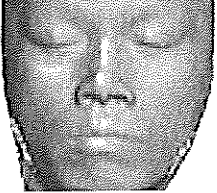
Instruction

Please look at the Test Face and then consider the faces from Face Pool. Please select the best three match faces from the Face Pool. Please indicate the rank of the match by the number 1, 2, and 3 under the face in the Face Pool.



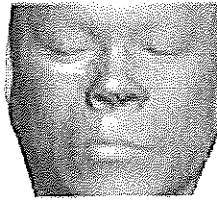
Test Face 9

Face Pool

			
R1(2), R2(2), R3(8)	R1(0), R2(0), R3(1)	R1(0), R2(0), R3(0)	R1(0), R2(4), R3(2)
			
R1(0), R2(1), R3(2)	$\sqrt{R1(14), R2(2), R3(2)}$	R1(1), R2(0), R3(2)	R1(2), R2(10), R3(2)

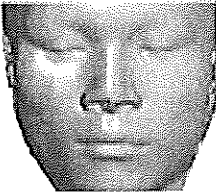
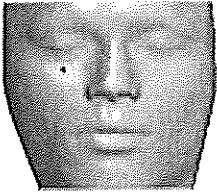
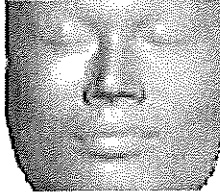
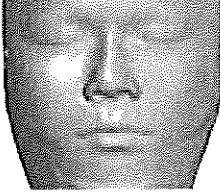
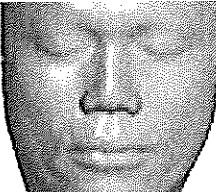

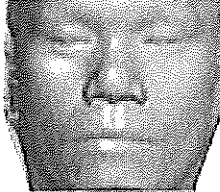
Instruction

Please look at the Test Face and then consider the faces from Face Pool. Please select the best three match faces from the Face Pool. Please indicate the rank of the match by the number 1, 2, and 3 under the face in the Face Pool.



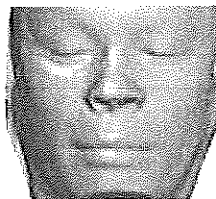
Test Face 10

Face Pool

			
R1(2), R2(1), R3(4)	R1(0), R2(0), R3(0)	R1(0), R2(0), R3(3)	R1(2), R2(7), R3(2)
			
R1(0), R2(2), R3(2)	R1(12), R2(4), R3(2)	✓ R1(3), R2(5), R3(6)	

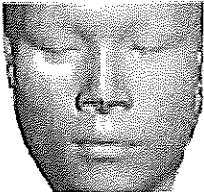
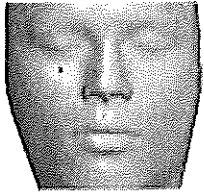
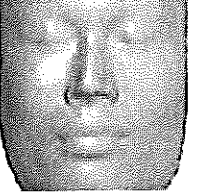
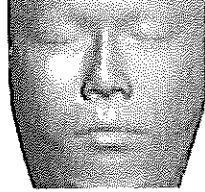
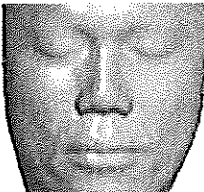
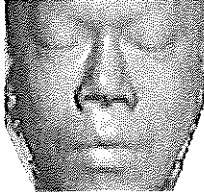
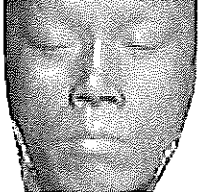
Instruction

Please look at the Test Face and then consider the faces from Face Pool. Please select the best three match faces from the Face Pool. Please indicate the rank of the match by the number 1, 2, and 3 under the face in the Face Pool.



Test Face 11

Face Pool

			
R1(3), R2(3), R3(4)	R1(0), R2(1), R3(2)	R1(0), R2(1), R3(0)	R1(3), R2(3), R3(5)
			
R1(3), R2(1), R3(3)	R1(7), R2(4), R3(4)	✓ R1(3), R2(6), R3(1)	

Instruction

Please look at the Test Face and then consider the faces from Face Pool. Please select the best three match faces from the Face Pool. Please indicate the rank of the match by the number 1, 2, and 3 under the face in the Face Pool.

APPENDIX F

PUBLICATIONS

The following list contains three publications that have resulted from the development of the Facial Reconstruction from Skull Using Free Form Deformation presented in this dissertation.

Facial Reconstruction from Skull

A. Namvong^c and R. Nilthong

School of Science, Mah Fah Luang University,

333, Moo 1, Tasud, Muang, Chiang Rai, 57100, Thailand

^cE-mail: ariyanamvong@gmail.com; Fax: 053-916776; Tel. 053-916775

ABSTRACT

The purpose of facial reconstruction is to estimate the facial outlook from skeleton remains and to aid in human identification. The reconstruction is obtained by deformation the craniometric landmarks of known skull into unknown skull. Forcing soft tissue of the known skull to the unknown skull with the same deformation gives the desired shape of the soft tissue for the unknown skull. This research uses 39 craniometric landmarks editing from five references [1,2,3,4,5]. For the deformation process, the application of Free-form deformation (FFD) is used. The 3D head model is acquired by using computed tomography (CT) with 1 mm resolution. This experiment attempts to deform the skull and skin of one 48 years old woman into another 42 years old woman. The preliminary visual result shows that it is possible to use this scheme for forensic facial reconstruction. Future development of this research will try to collect more reference head models and use the average skin deformation from various head models.

Keywords: Facial Reconstruction, Free-form Deformation.

1. INTRODUCTION

If the usual methods are impossible to identify the skeleton remains, then the possibility of facial reconstruction from the skull is considered. It is true that there are many ways in which soft tissue may cover the same skull leading to different facial outlook. So, the purpose of facial reconstruction is not to produce an accurate likeness of the person during life but the task is successful if it provides a positive effect to human identification from skeleton remains. With the assumption that the underlying skeleton affects directly the overall aspect of facial outlook, we consider that facial reconstruction is possible.

The successful of manual clay sculpting depends on combination of the ability, anatomical and anthropological knowledge of the artist, while the successful of computer-aided reconstruction depends on the number of head database and also the skill of craniometric landmarks localization of user. The facial reconstruction is obtained by deformation the craniometric landmarks of known skull into unknown skull or target skull. Forcing soft tissue of the known skull to the unknown skull with the same deformation gives the desired shape of the soft tissue for the unknown skull.

In this paper we try to develop a novel method for facial reconstruction through the use of volume deformation. Current volume deformation computer-based facial reconstruction methods differ mainly by the selection of landmarks points on the skull or craniometric landmarks, methods used for registration and deformation the model towards a given target skull.

Our procedure can be summarized as follows. For each head model we manually locate 39 craniometric landmarks taken from five references [1,2,3,4,5] then roughly register using Frankfort horizontal plane, then fine register using Iterative Closest Point (ICP). Finally we

deform craniometric landmarks of known skull into target skull using Free-Form Deformation (FFD).

The remainder of this paper is organized as follows. In Section 2 we review theory of Free-Form Deformation. In Section 3 we describe our facial reconstruction method. Section 4 shows the results of our experiment. The paper conclusion and directions for future research are in Section 5.

2. FREE-FORM DEFORMATION (FFD)

Free-form deformation introduced by Sederberg and Parry [6, 7, 8] is known to be a powerful shape modification method that has been applied to geometric modeling. This technique deforms an object by embedding it with in a solid defined with a control lattice. A change of the lattice deforms the solid and hence the object as seen in Figure 1. FFD generally involves with 1D, 2D and also 3D data. We can compute a new location P' from an old location P after deforming control point from P_{ijk} to P'_{ijk} as follows:

$$\text{1D FFD:} \quad P' = \sum_{i=0}^l B_i^l(t) P'_i \quad (1)$$

$$\text{2D FFD:} \quad P' = \sum_{i=0}^l \sum_{j=0}^m B_i^l(s) B_j^m(t) P'_{ij} \quad (2)$$

$$\text{3D FFD:} \quad P' = \sum_{i=0}^l \sum_{j=0}^m \sum_{k=0}^n B_i^l(s) B_j^m(t) B_k^n(u) P'_{ijk} \quad (3)$$

$$\text{Bernstein Polynomials: } B_i^n(t) = \frac{n!}{(n-i)!i!} t^i (1-t)^{n-i} \quad (4)$$

where point P' is a new location at (s', t', u') of an old point P at (s, t, u) after deforming control point P_{ijk} to P'_{ijk} , and l, m, n are the number of control points minus 1 in x, y, z axis. ($0 \leq s, t, u, s', t', u' \leq 1$)

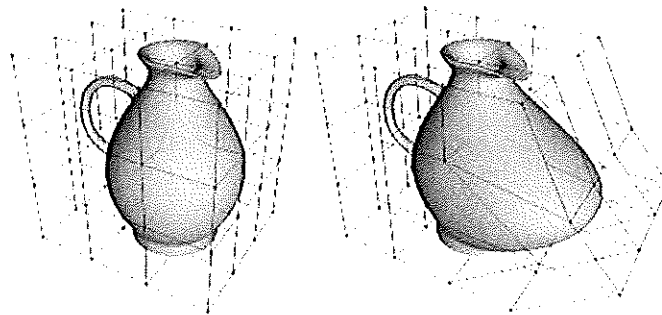


Figure 1 Example of FFD [9]

3. METHODOLOGY

Figure 2 shows the main step of our procedure. First step, we manually locate landmarks on both unknown skull or target and known skull or reference. Second step, we align two skulls into common position. This stage contains two processes, rough alignment and fine alignment. Rough alignment is to make two skulls into the same orientation called Frankfort horizontal plane, for supporting the performance of next process. Next process, fine alignment uses ICP algorithm. Finally, we deform craniometric landmarks of known skull into target skull using Free-Form Deformation.

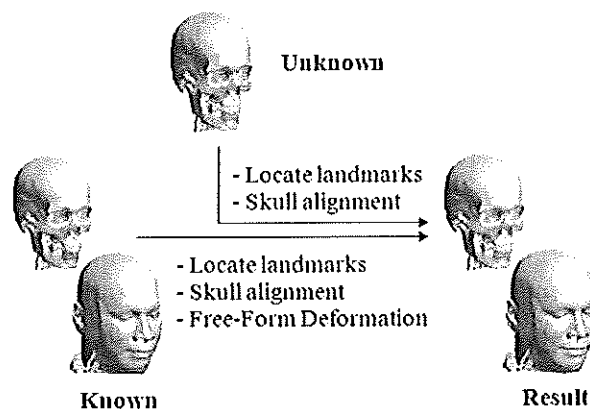


Figure 2 Methodology

3.1 Craniometric Landmarks

Figure 3 and Table 1 show the 39 craniometric landmarks used in this paper. There are two types of landmarks, central landmarks and lateral landmarks. Central landmarks laid on the central of the skull and lateral landmarks laid on left and right side of the skull.

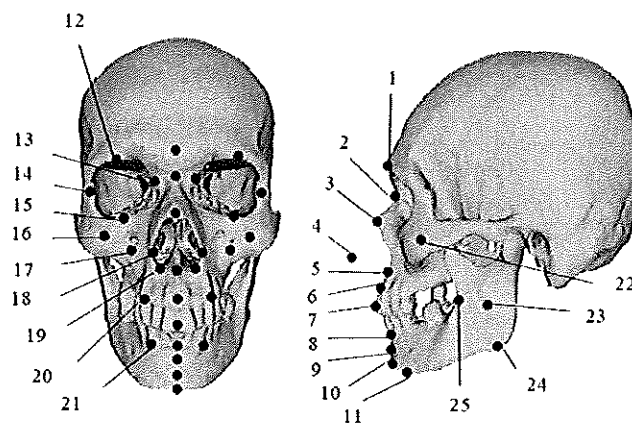


Figure 3. Craniometric landmarks

Table 1 Craniometric Landmarks

#	Central Landmarks	#	Lateral Landmarks
1	Glabella	12	Supracorbital
2	Nasal	13	Inner orbital
3	End of nasal	14	Outer orbital
4	Nose tip estimation	15	Suborbital
5	Mid-philtrum	16	Zygoma
6	Upper lip margin	17	Inferior malar
7	Incisor	18	Outer nasal
8	Lower lip margin	19	Lower nasal
9	Chin-lip fold	20	Supracanine
10	Mental eminence	21	Subcanine
11	Beneath chin	22	Outer Zygoma
		23	Mid-mandible
		24	Gonion
		25	Occlusion line

3.2 Skull Alignment

This stage contains two processes, rough alignment and fine alignment. First process is to make two skulls have the same orientation called Frankfort horizontal plane. The position of Frankfort horizontal Plane is like someone looking straight ahead. The technical explanation of positioning the skull this way is to have the lowest point on the lower margin of the orbit aligning horizontally with the top edge of the external auditory meatus (the ear hole) [1]. See Figure 4 for an illustration of this position.

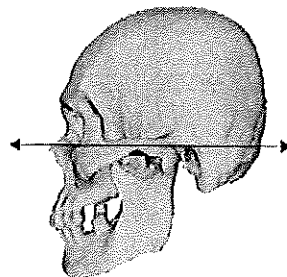


Figure 4 Frankfort horizontal plane

Second process, fine alignment uses the result from first step as an initial alignment. The method used in this process is called Iterative Closest Point or ICP. ICP is a straightforward method to align two free-form surfaces [10, 11]. The algorithms of ICP to align surface X and surface P are as follows:

The Iterative Closest Point Algorithm

- Initial transformation
- Iterative procedure to converge to local minima
 1. $\forall p \in P$ find closest point $x \in X$
 2. Transform $P_k \rightarrow P_{k+1}$ to minimize distances between each p and x
 3. Terminate when change in the error falls below a preset threshold

3.3 Free-Form Deformation

From Section 2 we mention FFD in the manner called global deformation; in this research we use FFD in the manner of local deformation. As seen in Figure 5, it demonstrates the use of local FFD; the middle column shows original skull and face; the left column shows the result of pushing the skull at the upper lip margin point (point 6 from Table 1) inside resulting in deforming of the shape of face. In the right column shows the result of push this point outside.

Reach to this step, two skulls have the same orientation and have the closest distance between reference skull and target skull. Now it is ready to deform all craniometric landmarks point by point from reference skull to target skull to reconstruct the face of the target skull. The reference skull, reference face, target skull, and also result from our facial reconstruction are shown in Section 4.

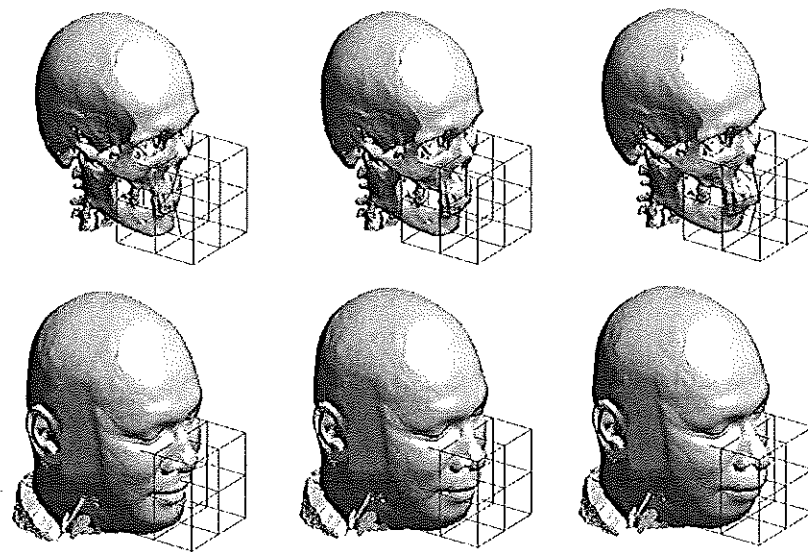


Figure 5 Demonstration of local FFD, original head (middle column), pushing the upper lip margin inside (left column) and pushing outside (right column)

4. EXPERIMENTAL RESULTS

In this experiment, the 3D head model of reference head and target head are acquired by using computed tomography with 1 mm resolution. We attempt to deform the skull and face of one 48 years old woman into another 42 years old woman. In Figure 6 show reference skull, reference face, target skull and also target face derived from our procedure. Reference face and reference skull are in the left column. The results derived from facial reconstruction are in the middle column and real faces of target are in the right column. We can see that the result is still bias to reference face. The result face looks more like reference face than target face. However, when observing the result we can see that it is possible to use this procedure to reconstruct a face from skeleton remains.

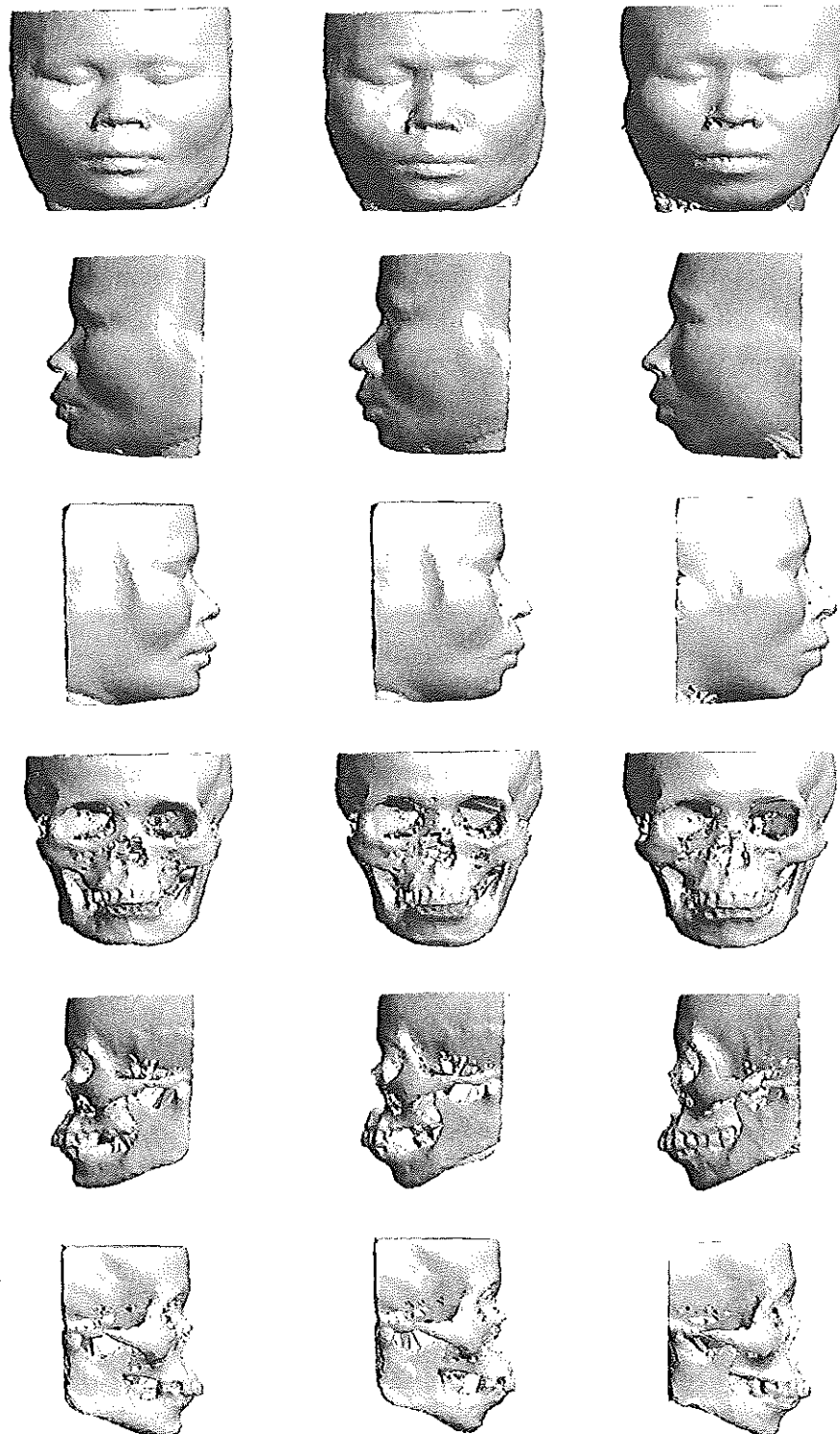


Figure 6 Experimental results, reference head (left column), result from the approach (middle column) and target head (right column).

**ANSCSE14 Mae Fah Luang University, Chiang Rai, Thailand
March 23-26, 2010**

5. CONCLUSION

In this experiment, for each head model we manually locate 39 craniometric landmarks then do rough registration using Frankfort horizontal plane, after that do fine registration using Iterative Closest Point, and finally we deform craniometric landmarks of known skull into target skull using Free-Form Deformation. From the results, we cannot claim that this research successfully because the results cannot be quite the same as the target face. In this experiment we have the limitation of number of head database, therefore only a few head models are produced. Nevertheless, the preliminary visual result shows that it is possible to use this scheme for forensic facial reconstruction. Future development of this research we will try to collect more reference head models for facial reconstructions, and we will use the average skin deformation from various reference head models to reduce the reference bias.

REFERENCES

1. L. Gibson, Forensic Art Essentials: A Manual for Law Enforcement Artists, 1st edition, Academic Press, London, 2008, 266-269, 303-305.
2. C. Wilkinson, Forensic Facial Reconstruction, 1st edition, Cambridge University Press, Cambridge, 2004, 71-73.
3. K.T. Taylor, Forensic Art and Illustration, 1st edition, CRC Press LLC, Washington D.C., 2001, 348-359.
4. P. Claes, D. Vandermeulen, S.D. Greef, G. Willems and P. Suetens, Statistically Deformable Faces Models for Cranio-Facial Reconstruction, Journal of Computing and Information Technology – CIT 14, 2006(1), 21-30.
5. A.F. Abate, M. Nappi, S. Ricciardi and G. Tortora, FACES: 3D Facial reconstruction from ancient Skulls using content based image retrieval, Journal of Visual Languages & Computing, 2004(15), 373-389.
6. T.W. Sederberg, Computer Aided Geometric Design Course Notes, Department of Computer Science, Brigham Young University, Utah, 2007, 133-135.
7. T.W. Sederberg and S.R. Parry, Free-form Deformation of Solid Geometric Models, Computer Graphics, 1986, 20(4), 151-160.
8. W. Song and X. Yang. Free-Form Deformation with weighted T-spline. The Journal of Visual Computer, 2005, 21(3), 139-151.
9. R. Barzel. Computer Graphics Animation Course Notes, Ecole Polytechnique, France. 2003, na.
10. P.J. Besl and N.D. McKay. A Method for Registration of 3-D Shapes, IEEE Transactions on Analysis and Machine Intelligence, 1992, 14(2), 239-255.
11. K. Bae. Automated Registration of Unorganised Point Clouds from Terrestrial Laser Scanners, Ph.D. Dissertation, Department of Spatial Sciences, Curtin University of Technology. Bentley, W.A, Australia. 2006, 1-9.

ACKNOWLEDGMENTS

We would like to thank Mr.Sorawee Thanawong, chief of X-Ray Department, Overbrook Hospital, Chiang Rai, Thailand, for his precious help in the head computer tomography data acquisition phase and also thank to the volunteers that makes this research possible.

ANSCSE14 Mae Fah Luang University, Chiang Rai, Thailand
March 23-26, 2010

A. Namvong^c and R. Nilthong
*School of Science, Mah Fah Luang University,
 333, Moo 1, Tasud, Muang, Chiang Rai, 57100, Thailand*
^cE-mail: ariyanamvong@gmail.com; Fax: 053-916776; Tel. 053-916775

ABSTRACT

The purpose of facial reconstruction is to estimate the facial outlook from skeleton remains and to aid in human identification. The reconstruction is obtained by deforming the craniometric landmarks of known skull into unknown skull. Forcing soft tissue of the known skull to the unknown skull with the corresponded deformation gives the desired shape of the soft tissue for the unknown skull. This work uses 71 craniometric landmarks edited from five references [1,2,3,4,5]. For the deformation process, the application of Free Form deformation (FFD) is used. The 3D head models are acquired by computed tomography (CT) scanner with 1 mm resolution. The questioned head is from 35 years old man. The reference heads are from 31, 38 and 24 years old men. These reference heads are chosen from the most three resembling skulls to the questioned skull. These reference skulls are deformed into questioned skull and then the reference faces are forced to deform correspondingly. Finally these deformed faces are averaged to reconstruct the desired face. The resulting face from this scheme shows promise for forensic facial reconstruction.

Keywords: Facial Reconstruction, Free Form Deformation.

1. INTRODUCTION

If the usual methods are impossible to identify the skeleton remains, then the possibility of facial reconstruction from the skull is considered. It is true that there are many ways in which soft tissue may cover the same skull leading to different facial outlook. So, the purpose of facial reconstruction is not to produce an accurate likeness of the person during life but the task is successful if it provides a positive effect to human identification from skeleton remains. With the assumption that the underlying skeleton affects directly the overall aspect of facial outlook, we consider that facial reconstruction is possible.

The successful of manual clay sculpting depends on combination of the ability, anatomical and anthropological knowledge of the artist, while the successful of computer-aided reconstruction depends on the number of head database and also the skill of craniometric landmarks localization of user. The facial reconstruction is obtained by deformation the craniometric landmarks of known skull into unknown skull or target skull. Forcing soft tissue of the known skull to the unknown skull with the same deformation gives the desired shape of the soft tissue for the unknown skull.

In this paper we try to develop a novel method for facial reconstruction through the use of volume deformation. Current volume deformation computer-based facial reconstruction methods differ mainly by the selection of landmarks points on the skull or craniometric landmarks, methods used for registration and deformation the model towards a given target skull.

ANSCSE15 Bangkok University, Thailand
 March 30-April 2, 2011

Our procedure can be summarized as follows. For each head model we manually locate 71 craniometric landmarks taken from five references [1,2,3,4,5] then coarsely register using Frankfort plane, then fine register using Iterative Closest Point algorithm. Finally we deform craniometric landmarks of known skull into target skull using Free Form Deformation.

The remainder of this paper is organized as follows. In Section 2 we review theory of Free-Form Deformation. In Section 3 we describe our facial reconstruction method. Section 4 shows the results of our experiment. The paper conclusion and discussion are in Section 5.

2. FREE FORM DEFORMATION

Free Form Deformation (FFD) was introduced by Sederberg and Parry [6, 7, 8] is known to be a powerful shape modification method that has been applied to geometric modeling. This technique deforms an object by embedding it with in a solid defined with a control lattice. A change of the lattice deforms the solid and hence the object as seen in Figure 1. FFD generally involves with 1D, 2D and also 3D data. We can compute a new location P' from an old location P after deforming control point from P_{ijk} to P'_{ijk} as follows:

$$\text{1D FFD:} \quad P' = \sum_{i=0}^l B_i^l(t) P_i' \quad (1)$$

$$\text{2D FFD:} \quad P' = \sum_{i=0}^l \sum_{j=0}^m B_i^l(s) B_j^m(t) P_{ij}' \quad (2)$$

$$\text{3D FFD:} \quad P' = \sum_{i=0}^l \sum_{j=0}^m \sum_{k=0}^n B_i^l(s) B_j^m(t) B_k^n(u) P_{ijk}' \quad (3)$$

$$\text{Bernstein Polynomials: } B_i^n(t) = \frac{n!}{(n-i)! i!} t^i (1-t)^{n-i} \quad (4)$$

where point P' is a new location at (s',t',u') of an old point P at (s,t,u) after deforming control point P_{ijk} to P'_{ijk} , and l, m, n are the number of control points minus 1 in x, y, z axis. ($0 \leq s, t, u, s', t', u' \leq 1$)

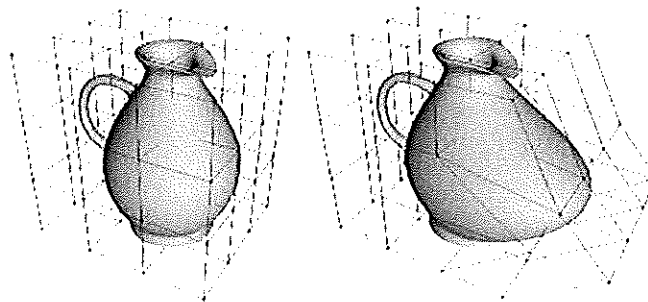


Figure 1. Demonstration of FFD [9]

3. METHODOLOGY

Figure 2 shows the workflow of our proposed method. The questioned skull is compared to skulls in head database. The similarity is defined by average distance between corresponded craniometric landmarks of two skulls. The craniometric landmarks used in this work are displayed in Figure 3. The N most resembling skulls are selected as references. In this work we try $N = 1, 2$ and 3 . Then deform craniometric landmarks of reference skulls into questioned skull using FFD. Forcing soft tissue of the reference skulls to the questioned skull with the corresponded deformation gives the desired facial shape of the soft tissue for the questioned skull. Finally these N deformed faces are averaged to reconstruct the desired face.

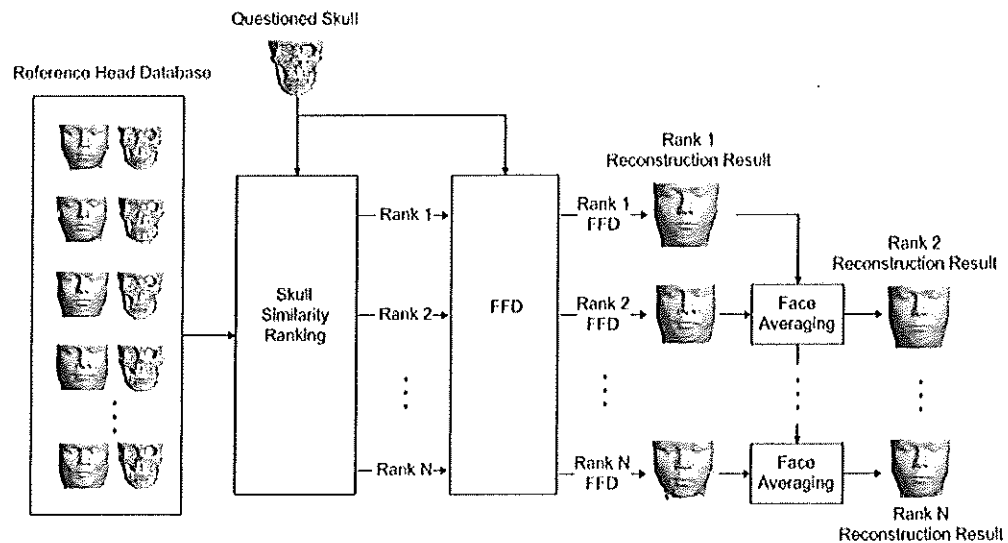


Figure 2. Facial reconstruction workflow

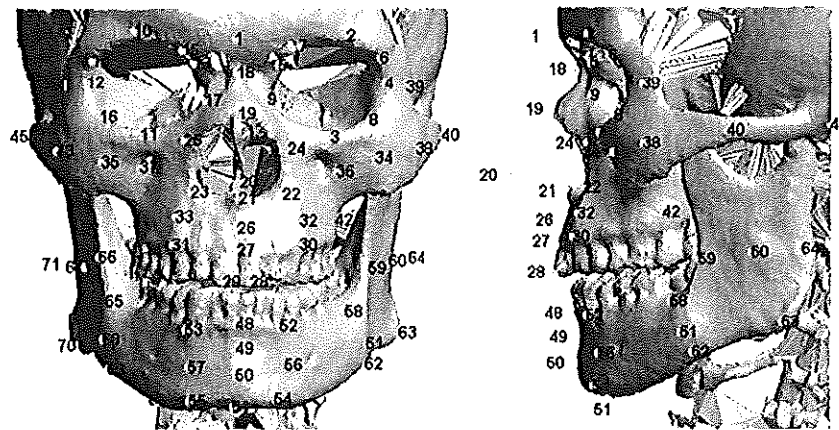
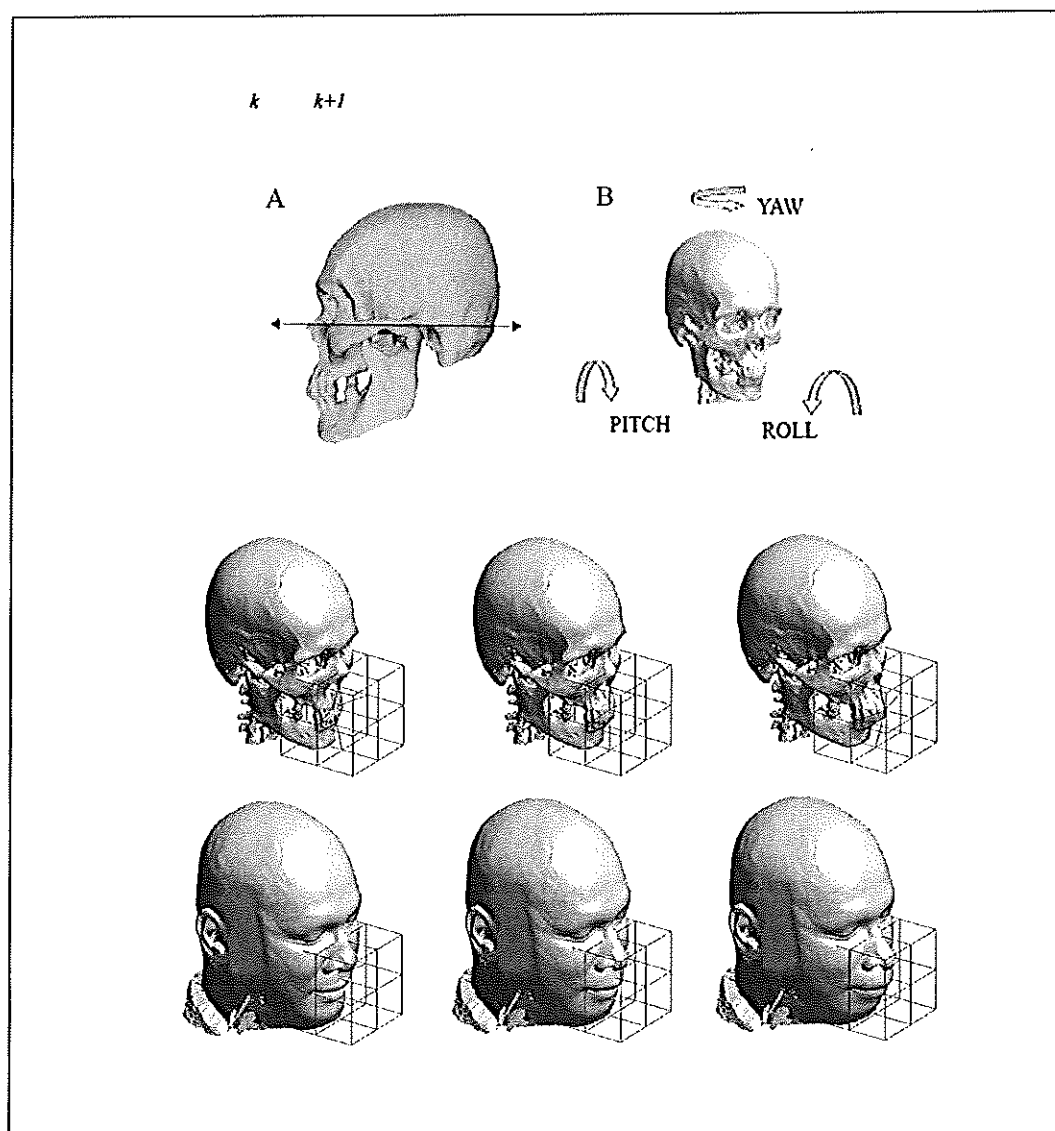


Figure 3. Craniometric landmarks



3.2 Free Form Deformation for Facial Reconstruction

From Section 2 we mention FFD in the global deformation manner. In this work we use FFD in the manner of local deformation by applying the local lattice to the craniometric landmarks. Figure 5 shows the local FFD demonstration of pushing the incisor inside and outside.

At this step, two skulls have the same orientation and have the closest distance between reference skull and target skull. Now it is ready to deform all craniometric landmarks point by point from reference skull to target skull to reconstruct the face of the target skull.

4. EXPERIMENTAL RESULTS

In this experiment, the 3D head database containing six heads are acquired by using CT scanner. The heads with craniometric landmarks are displayed in Figure 6. The label M indicated male gender and number indicated age at scanned date. All skulls in head database are paired up and then the distance between paired skulls are calculated as seen in Table 1. The similarity rank for each skull is displayed in Table 2. For the experiment, M35 is picked out from the reference database to be assumed as questioned skull or so called target skull. From Table 2, we can see that the most three resembling to target skull are M31, M38 and M24 accordingly. From Figure 7, the R1 result is reconstructed from M31 only, the R2 result is reconstructed from M31 and M38, the R3 result is constructed from M31, M38 and M24. From visual evaluation, R3 result shows promise for forensic facial reconstruction.

Table 1. Distance between skulls (mm.)

Head	M24	M29	M31	M35	M38	M55
M24	X	5.49	4.52	4.70	5.80	5.69
M29	5.49	X	4.94	5.62	4.91	3.77
M31	4.52	4.94	X	4.05	5.01	4.79
M35	4.70	5.62	4.05	X	4.18	5.36
M38	5.80	4.91	5.01	4.18	X	5.05
M55	5.69	3.77	4.79	5.36	5.05	X

Table 2. Similarity rank

Head	Rank				
	1	2	3	4	5
M24	M31	M35	M29	M55	M38
M29	M55	M38	M31	M24	M35
M31	M35	M24	M55	M29	M38
M35	M31	M38	M24	M55	M29
M38	M35	M29	M31	M55	M24
M55	M29	M31	M38	M35	M24

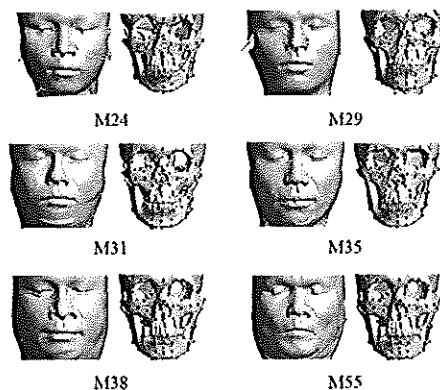


Figure 6. Head database with landmarks

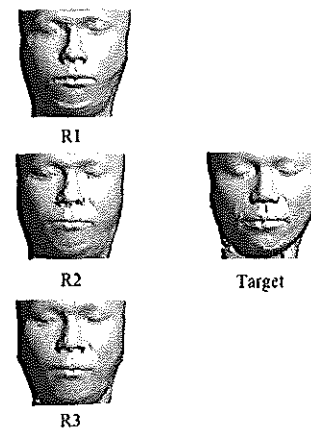


Figure 7. Reconstruction results

5. CONCLUSION AND DISCUSSION

Manual facial reconstruction has a long tradition both in forensic and archaeological fields, but, as long as progressive studies and medical imaging technology leads to the development of alternative computer-based facial reconstruction methods. We have to remark that there is no way to exactly reproduce the face of discovered skull. In stead of using small set of facial soft tissue thickness data and then interpolate the large remaining area, we can use whole facial soft tissue thickness data from 3D head models derived from CT scanner and then approximate questioned face from reference face in face database. The approach presents possibility to use this scheme as a support tool for forensic facial reconstruction.

In this paper, the skull similarity is considered in a whole. In the future, we will try to consider the dissections of skull instead and do the reconstruction from most resembling section. In addition, we will try to consider other factors apart from only skull shape such as age and nutrition condition.

REFERENCES

1. L. Gibson, *Forensic Art Essentials: A Manual for Law Enforcement Artists*, 1st edition, Academic Press, London, 2008, 266-269, 303-305.
2. C. Wilkinson, *Forensic Facial Reconstruction*, 1st edition, Cambridge University Press, Cambridge, 2004, 71-73.
3. K.T. Taylor, *Forensic Art and Illustration*, 1st edition, CRC Press LLC, Washington D.C., 2001, 348-359.
4. P. Claes, D. Vandermeulen, S.D. Greef, G. Willems and P. Suetens, Statistically Deformable Faces Models for Cranio-Facial Reconstruction, *Journal of Computing and Information Technology – CIT* 14, 2006(1), 21-30.
5. A.F. Abate, M. Nappi, S. Ricciardi and G. Tortora, FACES: 3D Facial reconstruction from ancient Skulls using content based image retrieval, *Journal of Visual Languages & Computing*, 2004(15), 373-389.
6. T.W. Sederberg, *Computer Aided Geometric Design Course Notes*, Department of Computer Science, Brigham Young University, Utah, 2007, 133-135.
7. T.W. Sederberg and S.R. Parry, Free-form Deformation of Solid Geometric Models, *Computer Graphics*, 1986, 20(4), 151-160.
8. W. Song and X. Yang. Free-Form Deformation with weighted T-spline. *The Journal of Visual Computer*, 2005, 21(3), 139-151.
9. R. Barzel. *Computer Graphics Animation Course Notes*, Ecole Polytechnique, France. 2003, na.
10. P.J. Besl and N.D. Mckay. A Method for Registration of 3-D Shapes, *IEEE Transactions on Analysis and Machine Intelligence*, 1992, 14(2), 239-255.
11. K. Bae. *Automated Registration of Unorganised Point Clouds from Terrestrial Laser Scanners*, Ph.D. Dissertation, Department of Spatial Sciences, Curtin University of Technology. Bentley, W.A, Australia. 2006, 1-9.

ACKNOWLEDGMENTS

We would like to thank Overbrook Hospital, Kasemrad Sriburin Hospital and Kratumban Hospital for precious help in the head computer tomography data acquisition phase and also thank to the volunteers that make this work possible.

ANSCSE15 Bangkok University, Thailand
March 30-April 2, 2011



FACIAL RECONSTRUCTION FROM SKULL USING FREE FORM DEFORMATION

Arlya NAMVONG, Rungrote NILTHONG

School of Science, Mae Fah Luang University, Chiang Rai, Thailand

Abstract

The purpose of facial reconstruction is to estimate the facial outlook from a discovered skull with the intention to provide a positive effect for deceased identification. In this paper, we tried to develop a novel method for facial reconstruction through the use of Free Form Deformation. The target face was obtained by deforming the craniometric landmarks of known skull into unknown skull. Forcing soft tissue on the known skull to the unknown skull with correspondent deformation gives the desired shape of the soft tissue for the unknown skull. Modified from Rhine's landmarks, the 33 craniometric landmarks were used in this work. For the deformation process, the application of Free Form Deformation was employed. The resulting face from this scheme shows promising forensic facial reconstruction.

Keywords: Facial Reconstruction; Free Form Deformation

Introduction

One of the most complicated tasks for criminal investigation is dealing with unidentified skeleton remains. There are several reasons why identification is essential. For every unidentified deceased person, there might be someone who cared about. Family members should have known what happened to their lover. Most of the time, an unidentified body is found, crime remains unsolved and the murderer may be still walking around. If usual protocols are impossible to identify the skeleton remains, then possibility of facial reconstruction from skull shall be considered. It is true that there are many ways in which soft tissue may cover such the same skull leading to different facial outlook. So, the purpose of facial reconstruction is not to produce an accurate likeness of the person during life but the task is considered successful if it is able to provide a positive effect on deceased identification. With an assumption that the underlying skeleton directly affects the overall aspects of facial

outlook, we considered that facial reconstruction from skull is possible.

Being still in use and constantly evolving, an old technique is a manual clay facial reconstruction also known as sculptural technique (Wilkinson, 2004). This method utilizes average skin thickness data derived from the craniometric landmarks. From tissue thickness of the landmarks, the remaining open spaces are interpolated to form the features of the face. This process is done according to the discretion of the artist resulting in a very subjective and not reproducible face (Taylor, 2001). There are no exact rules for the manual clay facial reconstruction which makes computerization of the process more challenging.

This paper introduces a novel approach to computerize facial reconstruction through the use of Free Form Deformation method. This approach differs from other researches that try to interpolate all face features from small set of tissue thickness data. Stephen et al (2008) stated that the relationships between connective tissue and skull are not completely known at this moment. The assumption behind this novel

approach is the changing in the facial soft tissue responding to the changing in the skull. The reconstruction is obtained by deforming the craniometric landmarks of known skull into unknown skull. Forcing soft tissue on the known skull to the unknown skull with the associated deformation offers a desired shape of the soft tissue for the unknown skull.

The remainders of this paper are organized as follow. Materials and related theories to the method are mentioned in the next section. After that, the methodology workflow is presented. Then, the result and

discussion of this approach are mentioned. The paper conclusion is summarized in the last section.

Materials and Method

Image Acquisition

The 3D data of skull and face used in this paper are acquired from CT scanner (Fig. 1). The Cartesian coordinate is used to represent 3D data in the form of (x, y, z) also known as point cloud. Meshing, shading and shadowing are used for the visualization purpose.

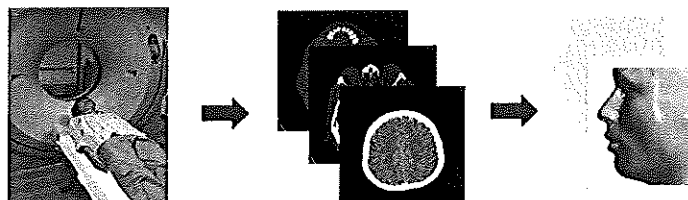


Fig. 1. 3D head data acquisition from CT scanner.

Craniometric Landmarks

Craniometric landmarks are anatomical landmarks on the skull. For manual clay sculpturing method, average skin thickness data table is applied. From tissue thickness at the landmarks, the remaining open spaces are interpolated to form the features

of the face. In this work, the reconstruction is obtained by deforming the craniometric landmarks of known skull into unknown skull giving a desired shape of the soft tissue for the unknown skull. The craniometric landmarks used in this work are modified from Rhine's landmarks (Fig. 2).

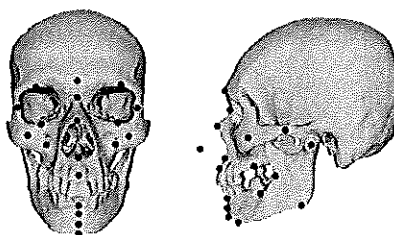


Fig. 2. Craniometric landmarks used in this work.

Frankfort Plane

All heads in the database have to be aligned to the same orientation and position. The favorite standard orientation

of skull used in forensic facial reconstruction is called Frankfort plane. The position of Frankfort plane is like someone looking straight ahead. The



technical explanation of positioning the skull this way is to have the lowest point on the lower margin of the orbit aligning horizontally with the top edge of the ear hole (Gibson, 2008).

Iterative Closest Point

Iterative Closest Point (ICP) is a straight forward method to align two free form surfaces (Besl & McKay, 1992). In this paper, this method is used to align reference skull to questioned skull before doing the facial reconstruction. The algorithms of ICP to align surface X and surface P are as follows:

The Iterative Closest Point Algorithm

- Initial transformation
 - Iterative procedure to minimize the distance
1. $\forall p \in P$ find closest point $x \in X$

2. Transform $P_k \rightarrow P_{k+1}$ to reduce the average distances
3. Terminate when next transformation step does not reduce the average distance

Free Form Deformation

Free Form Deformation (FFD) was introduced by Sederberg and Parry (Sederberg & Parry, 1986) is known as a powerful shape modification method that has been applied to geometric modeling. This technique deforms an object by embedding it with in a solid defined with a control lattice. A change of the lattice deforms the solid and hence the object (Fig. 3). FFD generally involves with 1D, 2D and also 3D data. We can compute a new location P' from an old location P after deforming control point from P_{ijk} to P'_{ijk} as follows:

$$\text{1D FFD:} \quad P' = \sum_{i=0}^l B_i^l(t) P_i' \quad (1)$$

$$\text{2D FFD:} \quad P' = \sum_{i=0}^l \sum_{j=0}^m B_i^l(s) B_j^m(t) P_{ij}' \quad (2)$$

$$\text{3D FFD:} \quad P' = \sum_{i=0}^l \sum_{j=0}^m \sum_{k=0}^n B_i^l(s) B_j^m(t) B_k^n(u) P_{ijk}' \quad (3)$$

$$\text{Bernstein Polynomials:} \quad B_i^n(t) = \frac{n!}{(n-i)! i!} t^i (1-t)^{n-i} \quad (4)$$

where point P' is a new location at (s', t', u') of an old point P at (s, t, u) after deforming control point P_{ijk} to P'_{ijk} , and l, m, n are the

number of control points minus 1 in x, y, z axis.
($0 \leq s, t, u, s', t', u' \leq 1$)

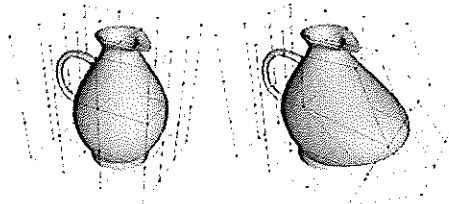


Fig. 3. Demonstration of global FFD (Barzel, 2003).

In this work, we use FFD in the manner of local deformation by applying the local lattice to the craniometric landmarks. Fig.

4 shows the deformation of face according to the deformation of incisor.

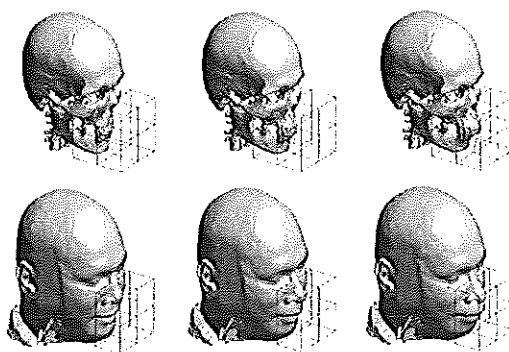


Fig. 4. Demonstration of local FFD. Middle column: original head. Left Column: moving incisor inside. Right column: moving incisor outside.

Cylindrical Projection

In this paper, to compare skull and face, we transform head 3D models onto plane using a cylindrical projection and resample

them with a specified rate. Fig. 5 shows the cylindrical projection of skull and face. Fig. 6 shows the absolute errors of cylindrical projection surfaces of skull and face.



Fig. 5. Cylindrical projection of face and skull

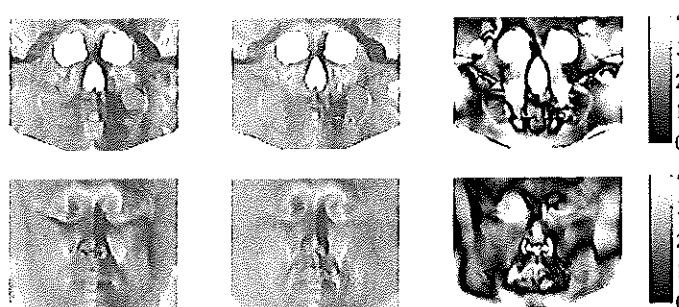


Fig. 6. Absolute errors of cylindrical projection surfaces. Errors are measured in mm.



Nose Profile Estimation

In order to compare the two cylindrical projection surfaces of skull at the nasal part, we have to estimate the nasal profiles due to there are less information from nasal aperture. Fig. 7 shows the nose profile estimation method modified from Prokobe and Ubelaker (2002). Line A dissects the nasion and prosthion. Line B is parallel to line A and intersects the foremost point on the nasal bone. For each point of nasal aperture, the distance from

line B to the nasal aperture are calculated and mirrored to form the nasal profile estimation.

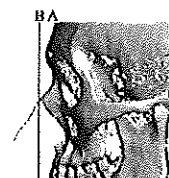


Fig. 7. The nose profile estimation method.

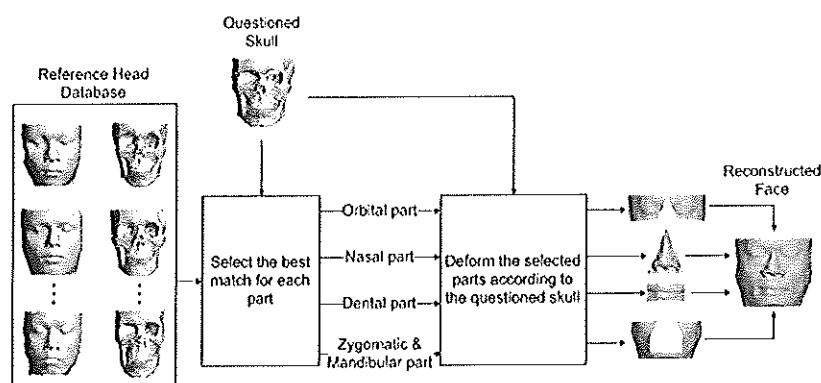


Fig. 8. Facial reconstruction workflow

Methodology

There are 11 three dimensional head models in the head database. Each of them is picked out as questioned skull and the remaining heads are used as reference heads. Fig.8 shows the workflow of the proposed method. First of all, the questioned skull is compared to all skulls in head database each part separately. In this work, the skull is sectioned into 4 parts consisting of orbital part, nasal part, dental part and zygomatic & mandibular part. This work is developed from our previous research which considering zygomatic part and mandibular part separately. In this work, we consider zygomatic part and mandibular part together because these two

bones are linked by masseter muscle. It is one of the major muscles responsible for facial appearance. It is a very large and thick muscle originates at zygomatic bone and terminates at mandibular bone (Fig. 9). The best match for each part is selected as reference part. Then all of the reference parts are deformed according to the questioned skull. Finally, the deformed parts are combined to reconstruct the new face.

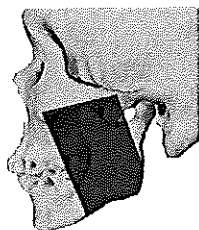


Fig. 9. Masseter muscle

column and second column demonstrate the target faces and reconstructed faces accordingly. These two columns are displayed for visual evaluation. Third column and fourth column present the cylindrical projection of target faces and reconstructed faces accordingly. Then the absolute errors are computed and displayed in fifth column. Although the result shows that we cannot produce exactly the same face as the target face, it still shows a promising forensic facial reconstruction.

Result and discussion

Fig. 10 and 11 present the facial reconstruction of subjects 1 – 11. First

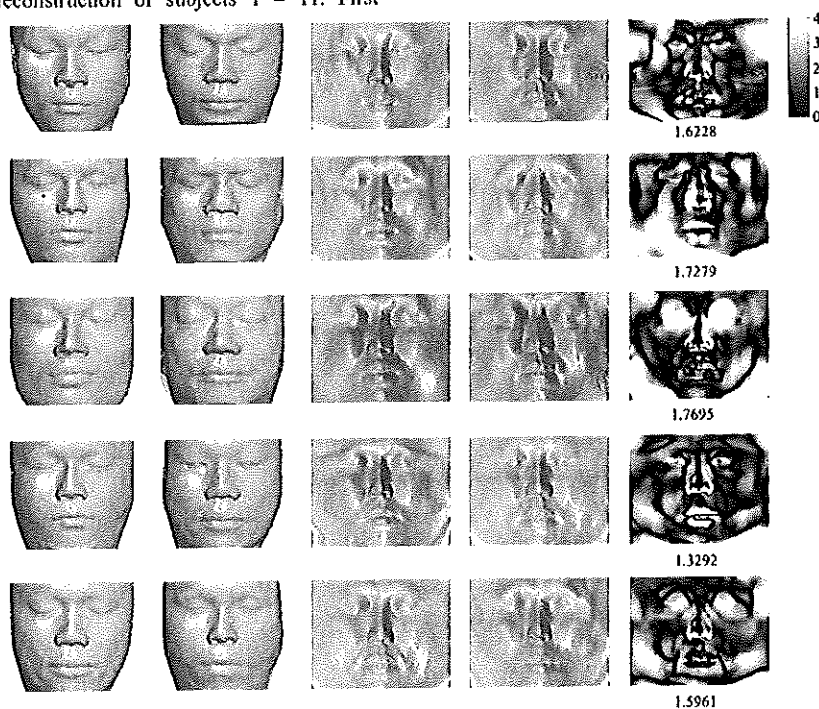


Fig. 10. Facial reconstruction of subjects 1 - 5. First column: target faces. Second column: reconstructed faces. Third column: cylindrical projection of target faces. Fourth column: cylindrical projection of reconstructed faces. Fifth column: absolute reconstruction errors. Errors are measured in mm.

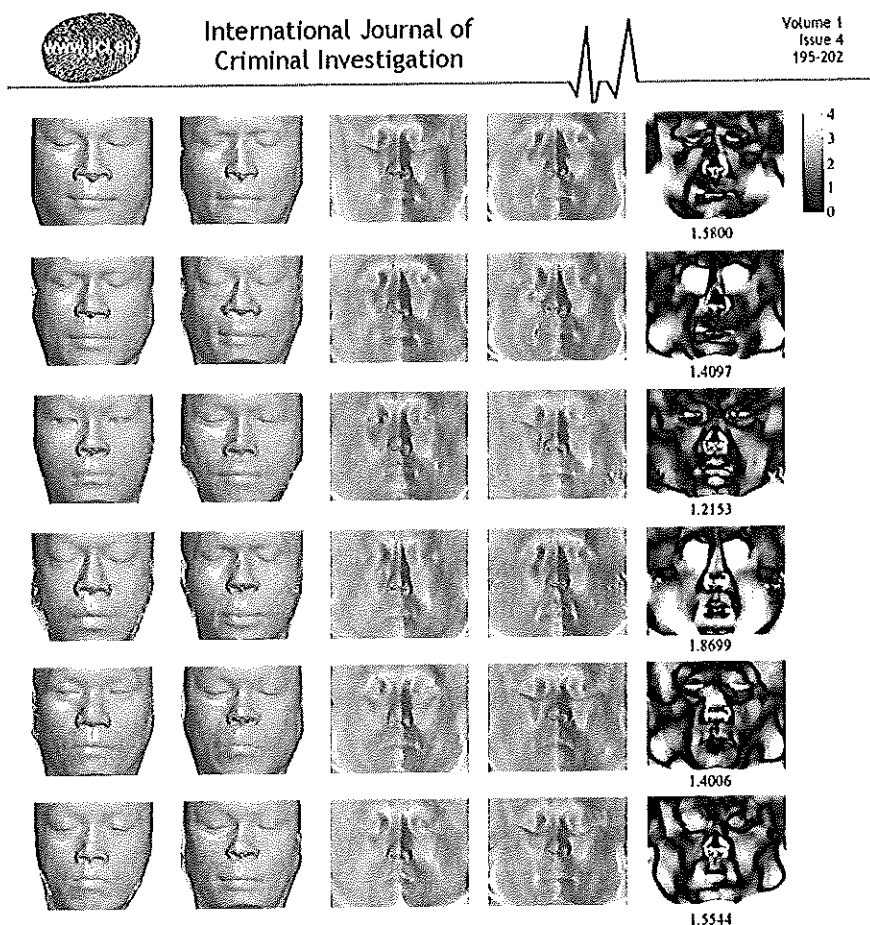


Fig. 11. Facial reconstruction of subjects 6 - 11. First column: target faces. Second column: reconstructed faces. Third column: cylindrical projection of target faces. Fourth column: cylindrical projection of reconstructed faces. Fifth column: absolute reconstruction errors. Errors are measured in mm.

Conclusions

A traditional manual facial reconstruction has been used for a long time in both forensic and archaeological fields. However, the progressive studies and medical imaging technology leads to the development of alternative computer-based facial reconstruction methods. We have to remark that there is no way to reproduce exactly the same face for discovered skull. Instead of using small set of facial soft

tissue thickness data and then interpolate the large remaining area, we can use whole facial soft tissue thickness data from 3D head models derived from CT scanner and then the approximate questioned face from reference faces in face database. The approach presents possibility to use this scheme as a support tool for forensic facial reconstruction.

Acknowledgement

We would like to thank Overbrook Hospital, Kasemrad Sriburin Hospital and

References

- Barzel, R. Computer Graphics Animation Course Notes, Ecole Polytechnique, France. 2003.
- Besl, P.J.; McKay, N.D. A Method for Registration of 3D Shapes, IEEE Transactions on Analysis and Machine Intelligence, 1992, 14(2), 239-255.
- Gibson, L. Forensic Art Essentials: A Manual for Law Enforcement Artist, 1st edition, Academic Press, London, 2008.
- Prokopec, M.; Ubelaker, D.H. Reconstructing the shape of the nose according to the skull, Forensic Science Communications, 2002, 4(1).
- Sederberg, T.W.; Parry, S.R. Free Form Deformation of Solid Geometric Models, Computer Graphics, 1986, 20(4), 151-160.
- Kratumban Hospital for precious help in the head CT data acquisition phase and also thank to the volunteers that make this work possible.
- Stephan, C.N.; Taylor, R.G.; Taylor, J.A. Methods of Facial Approximation and Skull-Face Superimposition, With Special Consideration of Method Development in Australia. In M. Oxenham (Ed.), Forensic Approaches to Death, Disaster and Abuse, Australian Academic Press, Queensland, 2008, 133-147.
- Taylor, K.T. Forensic Art and Illustration, 1st edition, CRC PRESS LLC, Washington D.C., 2001.
- Wilkinson, C. Forensic Facial Reconstruction, 1st edition, Cambridge University Press, Cambridge, 2004.



CURRICULUM VITAE

CURRICULUM VITAE

NAME	Mr. Ariya Namvong
DATE OF BIRTH	30 August 1975
ADDRESS	97 Moo 7 Amphoe Ko Kha, Changwat Lampang 52130 Thailand
EDUCATIONAL BACKGROUND	
2008	Master of Science, Computer Science Khon Kaen University
1997	Bachelor of Science, Computer Science Khon Kaen University
WORK EXPERIENCE	
2011-Present	Lecturer Rajamangala University of Technology Isan
2008-2011	Research assistant and teacher assistant Mae Fah Luang University
2006-2008	Research assistant and teacher assistant Khon Kaen University
2003-2005	Programmer Winward Co., Ltd.
2001-2002	Programmer E-Web Solution Co., Ltd.
1999-2001	Programmer Loxley Information Co., Ltd.
1997-1998	Lecturer Rajamangala University of Technology Isan Khon Kaen Campus